



UNIVERSITA' DEGLI STUDI DI FIRENZE

SCUOLA DI DOTTORATO DI RICERCA UBALDO MONTELATI

DOTTORATO IN BIOTECNOLOGIE MICROBICHE AGRARIE
CICLO XXIII

Dipartimento di Biotecnologie Agrarie – Sez. Microbiologia agraria
Settore scientifico disciplinare AGR 016

***ENERGETIC AND ECONOMIC ASSESMENT OF A
DISPOSABLE PANEL REACTOR FOR *Nannochloropsis* sp.
BIOMASS PRODUCTION***

Coordinatore del Dottorato: Ch.mo Prof. Paolo Capretti

Tutore : Ch.mo Prof. Mario Tredici

Dottorando : Niccolò Bassi

30 Dicembre 2010

Declaration

I hereby declare that this submission is my own work and that, to the best of my knowledge and belief, it contains no material previously published or written by another person nor material which to a substantial extent has been accepted for the award of any other degree or diploma of the university or other institute of higher learning, except where due acknowledgment has been made in the text.

Niccolò Bassi, 30-12-2010

A copy of the thesis will be available at <http://www.diba.unifi.it/>

Dichiarazione

Con la presente affermo che questa tesi è frutto del mio lavoro e che, per quanto io ne sia a conoscenza, non contiene materiale precedentemente pubblicato o scritto da un'altra persona né materiale che è stato utilizzato per l'ottenimento di qualunque altro titolo o diploma dell'Università o altro istituto di apprendimento, a eccezione del caso in cui ciò venga riconosciuto nel testo.

Niccolò Bassi, 30-12-2010

Una copia della tesi sarà disponibile presso DiBA, sez. Patologia vegetale, <http://www.diba.unifi.it/>

INDEX

1. INTRODUCTION	1
1.1. <u>The microalgae</u>	1
1.1.1. Oxygenic photosynthesis.....	1
1.1.2. Cultivation of microalgae and their actual potential.....	5
1.1.3. Commercial applications of microalgae biomass.....	6
1.2. <u>Microalgal Culture Systems</u>	7
1.2.1. Open systems	9
<i>Natural lakes and depressions</i>	9
<i>Circular ponds</i>	9
<i>Inclined ponds</i>	9
<i>Raceway ponds</i>	10
1.2.2. Photobioreactors: design parameters and classification	11
<i>Tubular photobioreactors</i>	14
<i>Vertical cylinders and sleeves</i>	14
<i>Flat photobioreactors</i>	15
1.3. <u>Microalgae and bio-fuels</u>	17
1.4. <u>The strain Nannochloropsis F&M-M24</u>	19
2. EFFECT of DIFFERENT ARRANGEMENTS OF THE “GREEN WALL PANEL” REACTOR ON SOLAR RADIATION COLLECTED	
2.1. <u>Introduction</u>	21
2.2. <u>Materials and Methods</u>	23
2.2.1. Field solar radiation measurements	23
2.2.2. Hourly solar radiation: <i>isolated</i> GWP	23
<i>The solar constant</i>	23

	<i>The atmospheric transparency index (K_t)</i>	23
	<i>Instantaneous solar parameters for a given day/month</i>	24
2.2.3.	Hourly solar radiation: full-scale GWP	25
	<i>The shading effect</i>	25
	<i>Losses of diffuse and reflected radiation</i>	27
2.2.4.	Solar radiation transmittance through reactor's transparent wall	27
	<i>Reflection of direct and disperse solar radiation</i>	27
	<i>Absorption and light attenuation through transparent materials</i> ...	29
	<i>Field measurements of solar radiation transmittance through GWP's culture chamber</i>	29
2.3.	<u>Result and Discussion</u>	30
2.3.1.	Solar model's validation: numerical simulation vs measured values	30
2.3.2.	Influence of orientation and inclination on annual solar radiation collected: isolated GWP	33
2.3.3.	Influence different arrangements (orientation, inclination and distance) on annual solar radiation collected: full-scale GWP	34
2.3.4.	Solar radiation transmittance through the transparent GWP's culture chamber	39
2.4.	<u>Influence of GWP orientation on Nannochloropsis F&M-M24 areal productivity</u>	43
2.5.	<u>Conclusions</u>	43
2.6.	<u>Nomenclature</u>	45
3.	HYDRODINAMICS CHARACTERIZATION A DISPOSABLE FLAT PANEL REACTOR: THE "GREEN WALL PANEL" (WO 2004/074423)	
3.1.	<u>Introduction</u>	46
3.2.	<u>Materials and Methods</u>	48

3.2.1.	Experimental systems.....	48
3.2.2.	Gas hold-up.....	48
3.2.3.	Bubble dimension and their rise velocity.....	48
3.2.4.	Mixing time.....	49
3.2.5.	Axial dispersion coefficient and dispersion number.....	49
3.2.6.	The overall oxygen volumetric mass transfer coefficient.....	51
3.2.7.	Power supply.....	51
3.3.	<u>Result and Discussion</u>	52
3.3.1.	Gas hold-up.....	52
3.3.2.	Bubble dimensions and their rise velocity.....	53
3.3.3.	Mixing rate and fluid dynamics.....	56
3.3.4.	Gas-liquid mass transfer in GWP reactors.....	60
3.3.5.	Power supply.....	62
3.4.	<u>Conclusions</u>	65
3.5.	<u>Nomenclature</u>	66
4.	INFLUENCE OF THE MIXING RATE ON THE PRODUCTIVITY OF <i>Nannochloropsis</i> sp. GROWN OUTDOORS IN GWP REACTORS	
4.1.	<u>Introduction</u>	67
4.2.	<u>Materials and Methods</u>	70
4.2.1.	Cultivation systems.....	70
	<i>The “Green Wall Panel” (GWPI – patent: WO 2004/074423)</i>	70
	<i>The second generation “Green Wall Panel” (GWPII – patent: 9325 PTWO)</i>	70
4.2.2.	Culture media and analytical procedures.....	70
4.2.3.	Experimental plan and culture conditions.....	71

	<i>Outdoor cultivation of Nannochloropsis F&M-M24 in a vertical GWPI.....</i>	71
	<i>Outdoor cultivation of Nannochloropsis F&M-M24 in inclined GWPII.....</i>	71
4.3.	<u>Results and Discussion</u>	73
5.	ECONOMIC AND ENERGETIC ASSESMENT OF MICROALGAE BIOMASS PRODUCITON IN THE DISPOSABLE “GREEN WALL PANEL” REACTOR	
5.1.	<u>Introduction</u>	80
5.2.	<u>Materials and Methods</u>	82
5.2.1.	System boundaries and the functional unit	83
5.2.2.	The Net Energy Ratio	83
5.2.3.	Input energies	83
	<i>The embodied energy</i>	83
	<i>The operative electrical energy</i>	84
	<i>Nutrients</i>	84
5.2.4.	Output energy	84
5.2.5.	Life span	84
5.2.6.	Data source	85
5.3.	<u>Cultivation System’s Description</u>	85
5.3.1.	Base case	85
5.3.2.	Nitrogen starvation: the “two phase strategy”	87
5.4.	<u>Results and Discussion</u>	93
5.4.1.	Energy balance of Nannochloropsis F&M-M24 biomass production in 1 ha GWP plant	93
	<i>Base case</i>	94
	<i>Nitrogen starvation case: the “two phase strategy”</i>	96

5.4.2. Economic evaluation of Nannochloropsis F&M-M24 biomass production costs in 1 ha GWP plant.....	102
5.5. <u>Conclusions</u>	108
6. SUMMARY.....	112
7. RIASSUNTO.....	117
8. REFERENCES.....	123

LIST OF TABLES

1. INTRODUCTION

Tab.1 - Commercially produced microalgae.....	7
--	---

2. EFFECTS OF DIFFERENT ARRANGEMENTS OF THE “GREEN WALL PANEL” REACTOR ON SOLAR RADIATION COLLECTED

Tab. 1 - Total daily PAR radiation ($\text{MJ m}^{-2} \text{ reactor d}^{-1}$) impinging on <i>isolate</i> and <i>full scale</i> GWP for two different orientations. Reactor distance 1 m for full scale arrangement.....	31
--	----

Tab. 2 – Simulation of total daily global radiation ($\text{MJ m}^{-2} \text{ reactor d}^{-1}$) for <i>isolated</i> GWP.....	34
---	----

Tab. 3 - Annual average daily global radiation ($\text{MJ m}^2\text{ground d}^{-1}$) for vertical and inclined (optimal inclination angle for each latitude) GWP. Three different reactor’s distance considered: 1, 0.5 and 0.1 m.....	38
---	----

Tab. 4 - Monthly average global transmittance through LDPE culture chamber for vertical GWP.....	43
---	----

3. HYDRODYNAMICS CHARACTERIZATION OF A DISPOSABLE FLAT PANEL REACTOR: The “Green Wall Panel” (WO 2004/074423)

Tab. 1 - Typical dispersion number (N_d) for industrial reactors.....	51
--	----

Tab. 2 - Influence of air flow rates on fluid dynamic in a 125 L GWP.....	58
--	----

4. INFLUENCE OF MIXING RATE ON *Nannochloropsis* F&M-M24 PRODUCTIVITY, IN OUTDOOR VERTICAL AND INCLINED DISPOSABLE REACTORS

Tab. 1 - Average volumetric productivity ($\text{g L}^{-1}\text{d}^{-1}$) for different mixing rates in three 20 L vertical GWP (WO 2004/074423).....	73
--	----

Tab. 2 - Influence of different air flow rates and solar radiation on average volumetric productivity ($\text{g L}^{-1}\text{d}^{-1}$) in <i>Nannochloropsis</i> F&M-M24 cultured in isolated N-S facing GWPs (1 m x 1 m).....	77
---	----

5. ECONOMIC AND ENERGETIC ASSESMENT OF MICROALGAE BIOMASS PRODUCTION IN THE DISPOSANEL “GREEN WALL PANEL” REACTOR

Tab. 1 - Design parameters for the “Green Wall Panel” reactor.....88

Tab. 2 - Design parameters of the 1 ha facility. *Base case* and *Nitrogen starvation* trough the “two phase” strategy.....89

Tab. 3 - Biomass composition and culture parameters for *Nannochloropsis* F&M-M24.....90

Tab. 4 - Net Energy Ratio for the production of 1 kg of *Nannochloropsis* F&M-M24 biomass in 1 ha GWP facility. *Base case* and *Nitrogen starvation* trough the “two phase” strategy scenarios.....98

Tab. 5 - Energy inputs (GJ ton⁻¹ biomass yr⁻¹) for the production of 1 tons of *Nannochloropsis* F&M-M24 (dry weight) wet biomass and % of the energy stored into the biomass.....98

Tab. 6 - Capital cost assessment for 1 ha GWP facility for the production of *Nannochloropsis* F&M-M24 biomass.....105

Tab. 7 - Summary of the operating costs for the production of *Nannochloropsis* F&M-M24 biomass in 1 ha GWP facility. Scenarios 1 (purchased nutrients and pure CO₂). Scenario 2 (Nutrients purchased and CO₂ from flue-gas). Scenario 3 (Nutrients from wastewaters and CO₂ from flue-gas).....107

Tab. 8 - *Nannochloropsis* F&M-M24 production cost in 1 ha GWP plant for the *base case* and the “*two-phase*” strategy. Csse 1 (purchased nutrients and pure CO₂). Case 2 (Nutrients purchased and CO₂ from flue-gas). Case 3 (Nutrients from wastewaters and CO₂ from flue-gas.).....109

LIST OF FIGURES

1. INTRODUCTION

Fig. 1 - Schematic representation of photosystems (PSII and PSI). The funnelling of excitation energy through the antenna complex to the reaction centres.....	2
Fig. 2 - Schematic representation of light and dark phase of photosynthesis.	4
Fig. 3 - “Light reactions” and production of ATP in the thylakoid membrane of chloroplast.....	4

2. EFFECT of DIFFERENT ARRANGEMENTS OF THE “GREEN WALL PANEL” REACTOR ON SOLAR RADIATION COLLECTED

Fig. 1 - Schematic representation of the profile angle: γ_2	26
Fig. 2 - Schematic representation of profile angle: γ_1	26
Fig. 3 - View factor for diffuse irradiance in vertical full-scale GWP (d = 1 m).....	27
Fig. 4 - Refraction and reflection of light at the interface between medias with different refractive index.....	28
Fig. 5 - Diurnal variation, for Florence latitude (43°48’N-11°12’E), of daily global irradiance (PAR) for isolated vertical N-S facing GWP. 12 th August 2009.....	30
Fig. 6 - Diurnal variation, for Florence latitude (43°48’N-11°12’E), of daily global irradiance (PAR) for isolated vertical E-W facing GWP. 12 th August 2009.....	31
Fig. 7 – Diurnal variation of transmittance for south facing transparent LDPE film at Florence latitude (Italy). 14 th January 2009.....	32
Fig. 8 - Diurnal variation of transmittance for north facing transparent LDPE film at Florence latitude (Italy). 14 th January 2009.....	32
Fig. 9 - Simulation of total daily global solar radiation (Florence, 43°48’N-12°11’E) impinging on vertical and tilted <i>full scale</i> GWPs. Reactors’ distance d =1m.....	36
Fig. 10 - Simulation of total daily global solar radiation (Florence: 43°48’N-12°11’E) impinging on vertical and tilted full scale GWPs. Reactors’ distance d =0.5 m.....	37

Fig. 11 - Simulation of total daily global solar radiation (Florence: 43°48'N-12°11'E) impinging on vertical and tilted full scale GWPs. Reactors are in a full-scale arrangements, distance $d = 0.1$ m.....	37
Fig. 12 - Average total daily solar radiation, MJ m^{-2} of ground area, for vertical GWPs as function of latitude, orientation and distance between rows.....	38
Fig. 13 - Average daily solar radiation, MJ m^{-2} of occupied area, for tilted (optimal inclination angle for each latitude) GWPs for three different distance.....	39
Fig. 14 - Hourly reflectance (%) of beam solar radiation for a N-S facing vertical GWP (Florence: 43°48'N-12°11'E). Refractive index of LDPE =1.54.....	40
Fig. 15 - Hourly reflectance (%) of beam solar radiation for a E-W facing vertical GWP (Florence: 43°48'N-12°11'E). Refractive index LDPE =1.54.....	41
Fig. 16 - Hourly reflectance (%) of beam solar radiation for an horizontal surface (Florence: 43°48'N-12°11'E). Refractive index water: 1.33.....	41
Fig. 17 – Evolution of hourly transmittance (% of the incident solar radiation) for E-W facing GWP.....	42
Fig. 18 – Evolution of hourly transmittance (% of incident solar radiation) for N-S facing GWP.....	42

3. HYDRODYNAMICS CHARACTERIZATION A DISPOSABLE FLAT PANEL REACTOR: THE “GREEN WALL PANEL” (WO 2004/074423)

Fig. 1 - Gas hold-up as function of superficial gas velocity U_g (m s^{-1}).....	53
Fig. 2 - Bubble dimension (mm) as function of air flow rate ($\text{L L}^{-1}\text{min}^{-1}$) in a 20 L GWP.....	55
Comparison between measured and calculated values by means of eq. 2 and 3.....	56
Fig. 3 - Measured bubbles rise velocities (cm s^{-1}) as function of the air flow rates in a 20 L GWP.....	56
Fig. 4 - Influence of the air flow rate on microeddies length scale in a 20 L GWP.....	57
Fig. 5 - Characteristic mixing time in a 20 L GWP calculated by the pH pulse response method.....	58
Fig. 6 - Dispersion number, N_d , and mixing time, t_m , in a 125 L GWP as a function of air flow rate. 90 L min^{-1} water flow applied.....	60
Fig. 7 - Overall oxygen volumetric mass transfer coefficient for a 20 L GWP. Tap water used.....	61

Fig. 8 - $(K_L a)_{CO_2}$ values calculated by means of eq. 12 for a 20 L GWP (Babcock et al . 2002).....	63
Fig. 9 - Influence of air flow rate on power supply ($W m^{-3}$) in GWP reactor.....	64
Fig. 10 - Energy requirement for mixing to Energy content of biomass. An energy content of $23 MJ kg^{-1}$ ad an average areal productivity of $20 g m^{-2} d^{-1}$ were considered.....	65.
Fig. 11 - Power requirements ($W m^{-2}$ of occupied area) for 1 m spaced GWP as a function of air flow rates.	65

4. INFLUENCE OF MIXING RATE ON *Nannochloropsis* F&M-M24 PRODUCTIVITY, IN OUTDOOR VERTICAL AND INCLINED DISPOSABLE REACTORS

Fig. 1 - 20 L vertical GWPI (WO 2004/074423). Reactors were North-South oriented.....	73
Fig. 2 - 20 L GWPII (9325 PTWO). Reactors were 45° inclined and North-South oriented....	73
Fig. 3 – Liquid velocity as function of the air flow rate in 20 L GWP. Velocity profile was measured as the rate of dispersion of a dye inside the reactor.....	75
Fig. 4 - Volumetric productivity as a function of solar radiation intercepted in vertical GWP. Air flow rate: $0.45 LL^{-1}min^{-1}$	76
Fig. 5 - Volumetric productivity as a function of solar radiation intercepted in vertical GWP. Air flow rate: $0.15 LL^{-1}min^{-1}$	76
Fig. 6 - Volumetric productivity as a function of solar radiation intercepted in vertical GWP. Air flow rate: $0.05 LL^{-1}min^{-1}$	77
Fig. 7 - Evolution of productivity as a function of different air flow rates in a 45° tilted GWPII (9325 PTWO). Average solar irradiance intercepted $22.18 MJ m^{-2}reactor day^{-1}$	79
Fig. 8 - Diurnal variation of dissolved oxygen in <i>Nannochloropsis</i> F&M-M24 cultures growth in isolated vertical GWPI at three different air flow rates. Values measured in a typical sunny day: $19 MJ m^{-2}reactor day$ (January 28 th 2010).....	80

5. ECONOMIC AND ENERGETIC ASSESMENT OF MICROALGAE BIOMASS PRODUCTION IN THE DISPOSANEL “GREEN WALL PANEL” REACTOR

Fig. 1 - <u>Base case</u> : Process chain and mass flows for the production of <i>Nannochloropsis</i> F&M-M24 biomass in a 1 ha facility.....	92
Fig. 2 - <u>Nitrogen starvation through the two phase strategy</u> : Process chain and mass flows for the production of <i>Nannochloropsis</i> F&M-M24 biomass in a one hectare “virtual” facility.....	93

Fig. 3 - Schematic example of a "two-phase" strategy applied to a "virtual" plant consisting of 10,000 m of GWP photobioreactor. The facility, as in the base case, is divided into eight modules of 25 GWP 50 m long.....	94
Fig. 4 - Relative contribution of nutrients, operative energy and embodied energy of materials to the overall energy demand for the production of <i>Nannochloropsis</i> F&M-M24 biomass (dry weight) in 1 ha GWP plant.....	100
Fig. 5 - <u>Base case</u> . Main contributions to the total Embodied Energy of materials ($\text{GJ ha}^{-1}\text{yr}^{-1}$) in 1 ha GWP facility for the production of <i>Nannochloropsis</i> F&M-M24 wet biomass.....	100
Fig. 6 - <u>Nitrogen starvation</u> : total Embodied Energy of materials ($\text{GJ ha}^{-1}\text{yr}^{-1}$) in 1 ha GWP facility for the production of <i>Nannochloropsis</i> F&M-M24 wet biomass.....	101
Fig. 7 - <u>Base case</u> : annual operative electrical energy consumption ($\text{GJ ha}^{-1}\text{yr}^{-1}$) in 1 ha facility for the production of <i>Nannochloropsis</i> F&M-M24 wet biomass.....	101
Fig. 8 - <u>Nitrogen starvation</u> : annual operative electrical energy consumption ($\text{GJ ha}^{-1}\text{yr}^{-1}$) in 1 ha facility for the production of <i>Nannochloropsis</i> F&M-M24 wet biomass.....	102
Fig. 9 - Influence of areal productivity on Net Energy Ratio of <i>Nannochloropsis</i> F&M-M24 biomass production in 1 ha GWP plant. <u>Base case</u> scenario.....	102
Fig. 10 - Influence of areal productivity on Net Energy Ratio of <i>Nannochloropsis</i> F&M-M24 biomass production in 1 ha GWP plant. <u>Nitrogen starvation through the "two phase strategy"</u>	103
Fig. 11 - Relative contribution of operating costs on overall annual production costs for different cases. 1 (purchased nutrients and pure CO_2), 2 (Nutrients purchased and CO_2 from flue-gas) and 3 (Nutrients from wastewaters and CO_2 from flue-gas.).....	110
Fig. 12 - Relative contribution of depreciation on overall annual production costs for different cases. 1 (purchased nutrients and pure CO_2), 2 (nutrients purchased and CO_2 from flue-gas) and 3 (nutrients from wastewaters and CO_2 from flue-gas.).....	111
Fig. 13 - <u>Base case</u> : <i>Nannochloropsis</i> F&M-M24 biomass production as function of labour's cost for different cases. 1 (purchased nutrients and pure CO_2), 2 (Nutrients purchased and CO_2 from flue-gas) and 3 (nutrients from wastewaters and CO_2 from flue-gas.).....	111
Fig. 14 - <u>Nitrogen starvation</u> : <i>Nannochloropsis</i> F&M-M24 biomass production cost as function of labour's costs for different cases: 1 (purchased nutrients and pure CO_2), 2 (nutrients purchased and CO_2 from flue-gas) and 3 (nutrients from wastewaters and CO_2 from flue-gas.).....	112

1 INTRODUCTION

1.1 The Microalgae

Microalgae, including cyanobacteria, are phototrophic organisms (i.e they obtain energy from light). They are usually autotrophic and dominate in both fresh and salty water bodies where they form part of the phytoplankton and phytobenthos. Some species are also capable of mixotrophic and heterotrophic growth on organic substrates (sugars, organic acids, alcohols) in the presence or absence of light (Richmond 2004).

Microalgae and cyanobacteria are directly responsible for about half the photosynthesis on earth representing the first ring of the trophic chain (Tredici 2010c). Main criteria adopted for microalgae systematics are currently based on the type of pigments contained, the chemical nature of storage products and characteristics of the cell wall, even if the system of classification has changed frequently during the last years (Tommaselli 2004).

Currently microalgae are subdivided into 11 taxonomic groups including: green algae (Chlorophyta), diatoms (Bacillariophyta), yellow-green algae (Xanthophyta), golden-brown algae (Chrysophyta), red algae (Rhodophyta), brown-algae (Phaeophyta), dinoflagellates (Dinophyceae), Prymnesiophyta, Eustigmatophyta, Rhabdophyta and the blue-green algae (Cyanophyceae) commonly known as cyanobacteria (Williams and Laurens 2010).

The ability of these microorganisms to grow in different and hostile environments (iper-saline waters, glaciers, arid and semi-arid soils) to many other organisms is due to the exceptional variety of unusual lipids and other compounds that algae are able to synthesize (Guschina and Hardwood, 2006).

In recent years microalgae became famous also because responsible of serious environmental and health problems like eutrophication and toxic blooms.

Commercial exploitation of these microorganisms in dedicated plants is still poorly developed and restricted to a few species of the genera: *Chlorella*, *Dunaliella*, *Haematococcus* and *Arthrospira*.

1.1.1 Oxygenic photosynthesis

As oxygenic photosynthetic microorganisms, microalgae and cyanobacteria use the energy of photons to provide the biochemical reductant NADPH₂ and the chemical energy ATP which are in turn used to metabolize inorganic carbon (CO₂) into organic metabolites, carbohydrates

(CH_2O) as first step, necessary for their growth. Oxygen is instead produced as a by-product (fig. 3).

Photons are absorbed by carotenoid and chlorophyll pigments of two protein-pigment complexes: the antenna complex of PS I (photosystem I) and the antenna complex of PS II (photosystem II) (fig.1).

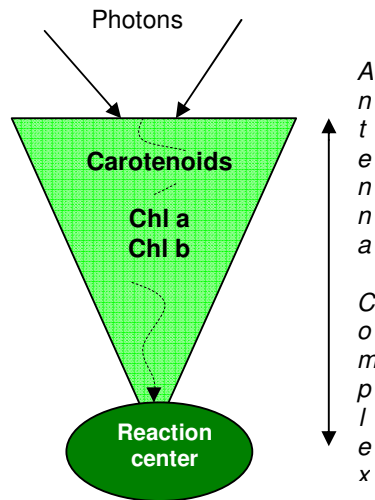


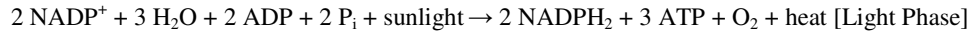
Fig.1 Schematic representation of photosystems (PSII and PSI). The funnelling of excitation energy through the antenna complex to the reaction centres. Adapted from Jansenn (2002).

Absorbed photon's energy by antenna complex is transferred to the two reaction centres, P680 for PSII and P780 for PSI (Masojidek et al. 2004).

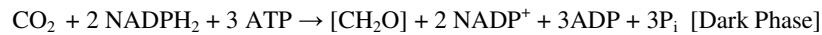
Photosystems work in series together with a chain of electron carriers in the so called "Z" scheme. When photons are absorbed and transferred to the reaction centres, give rise to charge separation and ejections of electrons from water, O_2 is so produced (fig.3). Electrons are so transferred from PSII to PSI through the electron carries by means of reactions that transfer electrons from donors to lower electrical potential (more negative) to acceptors at higher potential (more positive). Energy of photons is so necessary to transfer electrons from the reactor centres of PSII and PSI to their first acceptors characterized of a lower electrical potential. The final acceptor, NAD^+ , is thus reduced to NADH_2 . At the same time a pH gradient, due to transport of protons (H^+) through the tylakoidal membrane, is generated.

It is thanks to this gradient that it is possible the synthesis of ATP through a reaction catalyzed by the protein complex ATP synthase (Tredici 2010c, Masojidek et al. 2004) (fig.3).

This first stage of photosynthesis, called *photophosphorylation* or *light phase*, because it needs light (photons) to be processed, can be so summarized by the following reaction:



ATP and NADPH₂ produced by photophosphorylation are then used in the Calvin-Benson cycle, or *dark reaction* of photosynthesis, to fix CO₂ in CH₂O.



The synthesis of one molecule of glucose requires 6 molecules of CO₂. If each molecule of CO₂ requires 2 NADPH₂ and 3 ATP to be fixed, the synthesis of one molecule of glucose will require a total of 12 ATP and 18 NADPH₂. This means that for every molecule of CO₂ fixed 4 electrons must be transferred through the "Z" scheme, from water to NADP⁺ and at least eight photons must be absorbed by the photosystems: 4 from PSII and 4 from PSI.

Considering an average caloric content of 457 kJ for one fixed mole of CO₂ and assuming an average value of 217 kJ mole of photons (Tredici 2010c), it is evident as the maximum efficiency for conversion of light energy into chemical energy can not be greater than 27.4% of photosynthetically active radiation (PAR) absorbed. As the PAR is on average the 44 % of the overall solar radiation spectrum, the overall maximum photosynthetic efficiency (MPE) of oxygenic photosynthesis can not be greater than 12 % (Tredici 2010c).

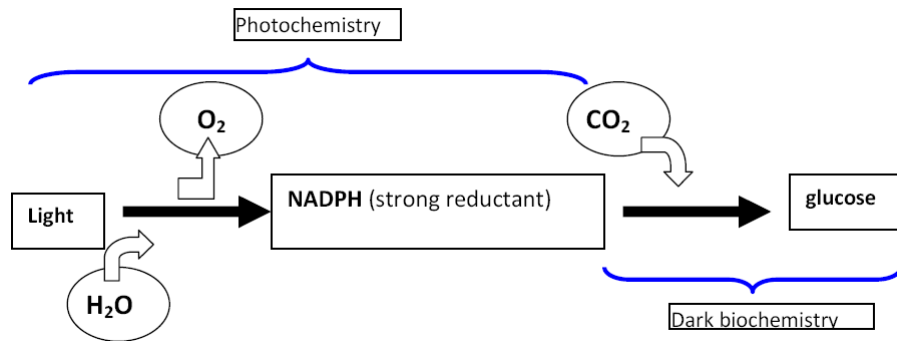


Fig.2 Schematic representation of light and dark phase of photosynthesis. With permission from (Tredici, 2010c).

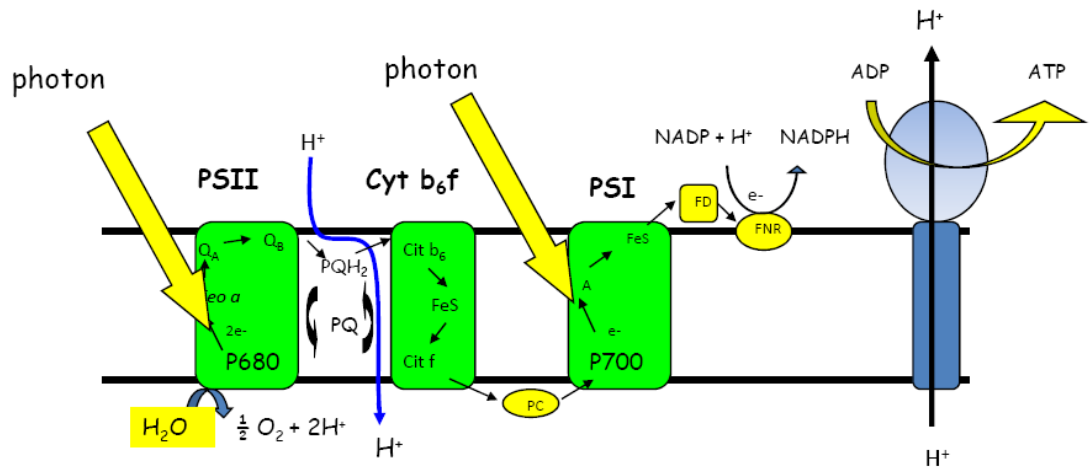


Fig.3 "Light reactions" and production of ATP in the thylakoid membrane of chloroplast. With permission from (Tredici, 2010c).

1.1.2 Cultivation of microalgae and their actual potential

The enormous expectations placed upon microalgae during the last years, mainly as a new source of bio-fuels, generated much confusion and uncertainty about the true productive potential of these microorganisms, even in the scientific community. Their real outdoor photosynthetic efficiency, that together with solar radiation available determine the maximal productivity obtainable, has been often overestimated creating unrealistic expectations (Tredici 2010c).

Their structural simplicity (no complex structures typical of higher plants are present in microalgae), plus the fact that the process of photosynthesis occurs in the aquatic environment, thus the efficiency of the reaction is facilitated by the ease of access to water, carbon dioxide and other nutrients, is so not sufficient to ensure higher PE respect to terrestrial plants under full sunlight. This means that areal productivities, tons of biomass per unit of occupied surface, would not be higher than those of many other plant species.

If the maximum theoretical photosynthetic efficiencies (MPE) would be achieved in outdoor microalgae cultivation systems, the cultivation of microalgae would not have competitors in terms of biomass productivity, reaching areal productivities of hundreds of tons $\text{ha}^{-1} \text{yr}^{-1}$.

Unfortunately the MPE under full sunlight in outdoor mass culture rarely get to 12%, but depending on environmental and cultivation conditions, usually range from 1 to 3% of the incident global radiation (Tredici, 2010c, Richmond, 2004). This is due to the fact that even under low light intensities most of photosynthetic microorganisms intercept too much light than they are able to process (photosaturation and photoinhibition). That part of the absorbed radiation do not used by the photosystems is so disposed as heat or fluorescence (Backer 2008). Photosaturation and photoinhibition are not the only causes that determine a reduction of the theoretical MPE to lower actual values in outdoor microalgae cultures. Reflection, depending on the geometry and the type of material with which the culture system is realized, photorespiration and respiration helps to a further reduction of the photosynthetic efficiency (Tredici 2010c). Actual outdoor biomass productivities are so reduced from 30 to 90 tons $\text{ha}^{-1} \text{y}^{-1}$.*

However, what is the real advantage of microalgae respect to higher plants, is their high natural biodiversity and their metabolic flexibility. It is possible in fact to address the metabolic “behaviour” of these microorganisms to the production of compounds or molecules of commercial interest, subjecting cultures to stress conditions such as nutrient deficiency, excess

* 20 $\text{MJ m}^{-2} \text{d}^{-1}$ average solar radiation considered and PE in the range 1-3%.

of light intensity or suboptimal values of salinity or pH (Rodolfi et al 2009, Guschina & Hardwood, 2006).

If we also consider that there is no a direct connection with the soil fertility and the possibility of using salty or iper-saline waters or wastewaters (industrial, civil and agricultural) as culture medium and flue-gas emissions as CO₂ source, is then easy to understand why a growing attention raised during recent years towards these microorganisms especially as new feedstock for energy use.

1.1.3 Commercial applications of microalgae biomass

The cultivation of microalgae biomass is not new. In some areas of the world (Chad, China, America) species like *Arthrospira* and *Nostoc* (Cyanophyceae) have been used as food for centuries by local people (Abdulqader et al., 2000).

Back in the '40s microalgae biomass production was proposed as a possible solution to meet the increasing demand for proteins for human nutrition (Burlew, 1953). The interest in these microorganisms then took force again in the late '70s with the first great oil crisis. The United States launched in 1978 the Aquatic Species Program (ASP). The program was funded by the United States Department of Energy (USDA), which over the course of two decades (1978-1996) looked into the production of energy using algae. Initially, the funding was to develop renewable transportation for fuel. Later, the program focused on producing bio-diesel from algae. The research program was discontinued in 1996 (Sheehan et al., 1998).

Microalgae, together with cyanobacteria, are currently cultivated for the production of many commercially important products including: bio-pesticides and agricultural fertilizers, food supplements, cosmetics, dyes, preservatives, antioxidants, probiotics for aquaculture (Pulz et al., 2004, Tredici et al., 2009, Richmond 2004). Because microalgae incorporate inorganic carbon (CO₂ and HCO₃⁻) they can be also employed for the production of isotopically labelled ¹³C-compaunds. Others labelled compounds as ²H- or ¹⁵N- can easily obtained from ¹⁵NO₃⁻ and ²H₂O (Apt and Behrens, 1999).

The annual production of algal biomass in the world, mainly used for humans and animals, is estimated to date between 8000 and 10000 tonnes, 90% of which is made in open culture systems like raceway ponds (Leher and Posten, 2009).

Tab.1 Commercially produced microalgae. Adapted from Tredici et. al (2009).

GENUS	ANNUAL PRODUCTION (TONS YR ⁻¹)	CULTURE SYSTEM	APPLICATION	LOCATION
<i>Arthrospira</i>	3000	Raceway ponds	Dietary supplements, cosmetics, phycobiliproteins	Asia, USA
<i>Chlorella</i>	2000	Circular ponds, PBR, fermenters	Aquaculture, dietary supplements, cosmetics	Asia, Germany
<i>Dunaliella</i>	1200	Raceway ponds, lagoons	B-carotene, cosmetics, dietary supplements	Australia, Israel, Asia
<i>Haematococcus</i>	300	Raceway ponds, PBR	Astaxanthin, aquaculture, dietary supplements	USA, Israel
<i>Porphyridium</i>	n.d	PBR	Cosmetics, ω -6 PUFA AA ¹	Israel
<i>Aphanizomenon</i>	500	Natural bloom	Dietary supplement	USA
<i>Nostoc</i>	600	Arid and Semi-arid soils	Health food	Asia, America
<i>Cryptocodinium</i>	240 (oil)	Fermenters	PUFA ω -3 DHA ²	USA
<i>Schyzochytrium</i>	10 (oil)	Fermenters	PUFA ω -3 DHA	USA
<i>Odontella</i>	n.d	Raceway ponds	Dietary supplement	France, Germany

1.2 Microalgal Culture Systems

Different reactor's designs for the cultivation of phototrophic microorganisms have been developed and patented over the years. With the term *reactor* we indicate a generic culture system in which phototrophic organisms carry out their photobiological reactions (Tredici 2010a). Reactors design that have really found a commercial application in large scale facilities, the scaling-up of these systems has always represented one of the main limits to the commercial application of the most of the existing designs, are not numerous (Lehr and Posten 2009, Tredici 2010a).

Culture systems for photosynthetic microorganisms can be divided into two main categories:

¹ AA= arachidonic acid

² DHA= docosahexaenoic acid

- *Open Systems.* 90% of world microalgae biomass production is realized with these systems (Lehr and Posten 2009). Open systems presents low investment and management costs respect to photobioreactors, allowing to produce biomass at lower costs. Average values of areal productivity for an open system can fluctuate between $5 \text{ g m}^{-2} \text{ day}^{-1}$ and $25 \text{ g m}^{-2} \text{ day}^{-1}$, with peaks of $40\text{-}50 \text{ g m}^{-2} \text{ day}^{-1}$ for short periods (Tredici 2010a). The low surface to volume ratio ($5\text{-}10 \text{ m}^{-1}$) typical of such kind of systems, together with a suboptimal light regime, poor mixing and long light paths, does not permit to obtain high volumetric productivities and to support concentrations higher than 1 g L^{-1} (Tredici 2010a). As consequence culture concentration at harvest is one of the main bottlenecks in the scaling up of open systems, where high volumes at low concentrations have to be processed daily with high energy expenditure.

- *Closed Systems.* Properly defined *photobioreactors* (Tredici, 2010a), show investment and management costs higher than open systems, but provide higher volumetric productivity and culture concentrations (Williams & Laurence 2010). In addition to the higher concentrations and productivity, the added value for a photobioreactor is represented by the possibility to control the main cultivation parameters, optimizing by this way the growth conditions. Key factors for the growth such pH, temperature, dissolved oxygen and carbon dioxide are more easily controlled than in open systems. This also allows to minimize culture's contamination due to the presence of bacteria, fungi, protozoa, but also other species of microalgae that over time could replace the strain selected. This is essential both when the biomass is specifically designed for high value markets, where products with the lowest level of contamination are required (aquaculture, food supplements, pharmaceuticals and cosmetics), but also in the production of inoculum for to be use in applications where the bulk production is realized in open systems. Thanks to the lower level of contamination, a greater number of strains that can be cultivated and commercially exploited. Many strains susceptible to contamination by other species would not be stable over the time when grown in open systems.
 The high s/v ratio ($20\text{-}200 \text{ m}^{-1}$) typical of photobioreactors, permit to obtain higher volumetric productivity than those obtainable in open systems. This is translate in higher culture concentration when culture is collected, resulting in lower energy and investment costs for harvesting operations.

1.2.1 Open systems

Open systems include: natural lakes and depressions, circular ponds, inclined ponds and "raceway" type ponds.

Natural lakes and depressions:

In presence of specific environmental conditions such high levels of nitrates and phosphates, pH and temperatures close to the optimum, natural bloom of microalgae or cyanobacteria can occur. At Chad lake (Chad) an abundant population of *Arthrospira* sp. (filamentous cyanobacteria) is regularly collected and consumed by local populations (Abdulqader et al. 2000). In Australia, the Western Biotechnology Ltd., cultivates *Dunaliella salina* in natural ponds for the production of β -carotene (6-10 tons yr⁻¹). The typical extensive approach of these systems results in very low productivities, few grams per square meter per day (Tredici, 2010a).

Circular ponds:

They did not find large-scale commercial applications due to their high construction costs (they are almost entirely made of concrete). Used mainly in Asia for the cultivation of *Chlorella* sp.

Inclined ponds:

In this systems turbulence of the culture is created by gravity. Culture flows down in a thin film layer of about 1 cm thick, or even less, on an inclined plane. The reduced thickness ensure a high s/v ratio and consequently higher volumetric productivity and high levels of biomass concentration. Culture is circulated by means of pumps. The high sedimentation rates, especially in conditions of low turbulence, large evaporation losses, low CO₂ solubilization are the main limitations of these systems (Tredici 2004). There are currently no commercial plants that use this technology. There are however numbers of pilot-scale plants that have made use of this ponds. One of the largest one is that at Roupa (Bulgaria), where areal productivity of 18 and 25 g m⁻² day⁻¹ with *Arthrospira* and *Scenedesmus* have been obtained. A 0.5 ha sloping pond was used to produce *Chlorella* in Western Australia. The system attained an average areal productivity of 25 g m⁻¹d⁻¹ operating semi-continuously (Tredici 2010a).

Raceway ponds:

Currently most of the worldwide production of algal biomass is obtained using this type of culture systems. Raceway ponds are a consolidated and acquired technology (Benemann & Oswald 1996, Weissman and Goebel 1987). Ponds are elliptically shaped and construction materials with which they are made depends on the level of investment to be performed. The hydraulic level of the culture is maintained at 15-30 cm and culture is continuously mixed by means of a paddlewheel. This last, must be designed in order to keep a well homogenized culture and ensure flow rates that should never be under 15 cm s^{-1} (Weissman & Goebel 1987).

The main advantage of raceway ponds, if compared to other culture designs both open and closed systems, is the ease with which they can be realized. A simple trench covered with a waterproof liner, HDPE or PVC liners are generally used, which costs $5\text{-}10 \text{ € m}^{-2}$ and a paddlewheels are already sufficient to realize a raceway ponds and to start to culture. The ability to use materials available locally and their relative low costs allows the realization of these culture systems also in developing areas, where high levels of technology skills are difficult to find. However in large facilities, Cyanotech Corporation (USA) or Earthrise® (USA), the structural complexity increase and careful design is required. In addition to the simplicity in structure and design, another positive aspect offered by raceway ponds, is given by the reduced energy required for culture mixing. Weissman & Goebel (1987) reported a detailed design and costs characterization for large scale open raceway ponds. For 8 hectares ponds, no commercial ponds exists of this size, they computed a total unit power of 0.1 W m^{-2} with a culture depth of 20 cm and a channel flow velocity of 20 cm s^{-1} . The same authors, working on smaller ponds of 100 m^2 calculated an energy consumption for mixing equal to 0.22 W m^{-2} , with the same velocity and culture depth.

This type of system is anyway not free from drawbacks, many of which are common to all open systems:

- Culture is in direct contact with the external environment and contamination can results very high. Competitors like other species of algae, protozoa and bacteria can seriously reduce culture productivity.
- Low productivity per unit of volume, due to the low s/v ratio ($5\text{-}10 \text{ m}^{-1}$). The low concentrations, usually not greater than 1 g L^{-1} , contribute to making the culture more susceptible to contamination.
- Temperature control is difficult to achieve and is not applied in any large-scale plants. This further contributes to the reduction of daily production.

- Evaporation. In areas characterized by high solar radiation, $20 \text{ MJ m}^{-2} \text{ d}^{-1}$ as annual average, and dry weather, the amount of water lost by evaporation can be considerable: 1 cm per day. Where availability of fresh water is scarce this can represent a serious problem. Evaporated water can be replenished with seawater, but this leads to an increase in the salinity of the culture medium. The greater is the salinity of the water used and lower the rate of dilution applied greater will be the increase in medium salinity.

1.2.2 Photobioreactors: design parameters and classification

To overcome some of the problems mentioned above, since the '50s different research groups around the world have focused their researches in the development and optimization of culture systems alternative to the classic ponds. Closed systems or photobioreactors (PBR) can be defined as "*culture system for phototrophs in which a great proportion of the light (> 90%) does not impinge directly on the culture surface, but has to pass through the transparent reactor's walls to reach the cultivated cells*" (Tredici 2010a). Over the years, many different designs of PBR have been developed and tested. Although each model has its own peculiarities here we summarized features common to all:

- High s/v ratio ($20\text{-}200 \text{ m}^{-1}$) compared to open systems.
- High volumetric productivity ($\text{g L}^{-1} \text{ day}^{-1}$) due to the high s/v ratio. Increasing the s/v ratio means to increase the amount of photons available per unit of culture volume and for the single cell. This together with an optimized mixing rate leads to higher concentrations and so high light intensity can be more efficiently used. This means that high levels of solar radiation, far beyond the threshold of photosaturation and photoinhibition, can be used effectively by ensuring high productivity (Richmond 2004).
- Opportunities to control and to maintain near optimal values important culture parameters such as temperature, pH, $p\text{O}_2$ and $p\text{CO}_2$.
- Being closed systems, well isolated from the outside, there is less possibility of contamination by both other species of microalgae, but also by protozoa. This affects in a very positive effect on productivity and stability of the crop.

Drawback are however presents:

- The high investment and operative costs, that make biomass produced in photobioreactors still too expensive, especially for the production of biomass for low-value markets.
- High auxiliary energy consumptions. In the event that the biomass has a low added value and is destined for processing into bio-fuels (biogas, bio-ethanol or bio-diesel), the net energy balance of the entire production process is essential to the viability and efficiency of the process itself. If we take in consideration also the energy content of materials and components needed for the construction of the reactor, the so called *Embodied Energy of Materials*, we understand how the use of photobioreactors today represents a non-sustainable energy technology for biomass production for energy use. (Rodolfi et al. 2009, Burges and Fernandez-Velasco 2007, Jorquera et al 2009, Lehar and Posten 2009).

A classification of the existing PBR can be made taking into account the following three parameters: design, operation mode and construction materials (Tredici 2010a):

According to the design we have:

- tubular or flat plate photobioreactors,
- horizontal, vertical, inclined or spiral photobioreactors,
- manifolds photobioreactors,
- helical (bio-coil) photobioreactors.

An operational classification includes (Asenjo and Merchuk, 1994):

- pneumatically or mechanically stirred photobioreactors,
- single phase reactors in which gas exchange and photostage are usually shared in to distinct portions.

- two-phase reactors. In which the gas and liquid phase are presents simultaneously and gas exchange takes place continuously. This category includes: bubble columns and air-lift reactors (Asenjo and Merchuk 1994).

A further classification can be made according to the materials used for the culture chamber. Materials like glass or plastics (PVC, polyethylene, Plexiglas®, polycarbonate) can be used.

The design of a photobioreactor include a series of decisions on matters ranging from basic microbiology and biochemistry to process engineering (Asenjo and Merchuk 1994). Main parameters which should be taken into account in the design and implementation of a photobioreactor can be summarized in:

- surface to volume ratio (s/v),
- gas-liquid mass transfer,
- optimization of solar exposure in order to maximize solar radiation capture,
- mixing rate, in order to ensure an optimal light regime to individual cells and therefore the highest photosynthetic efficiency.

As the s/v ratio affects volumetric productivity and concentration was already discussed above and a detailed literature exist about this matter (Richmond 2004, Richmond & Wu 2000, Hu et al. 1996). The obsessive research for the maximization of this parameter, however, was also one of the reasons to the failure of commercial facilities (Tredici 2010a).

Inclination and orientation are two other fundamental aspects determining overall area productivity in photobioreactor. For an open system like a pond is not possible, except within certain limits, to arrange the system other than the horizontal. Solar radiation intercepted is so defined by the season and the latitude of the place considered. Flat panel reactors, and to a lesser extent also tubular reactors, may be arranged in different configurations. This allows to vary the amount of radiation intercepted depending on season and latitude considered. Doing so we can ensure an optimal radiation on annual base and to improve the photosynthetic efficiency and productivity (Lee and Low 1991, Tredici and Chini Zittelli 1997, Perez & Seals 1995, Hu et al. 1996b).

Mixing degree at which photosynthetic microorganism are subjected strongly influence the photosynthetic efficiency and the optimal concentration of cultures, determining the light regime at which single cells are subjected (Richmond 2004). Each type of photobioreactor is in fact characterized by its typical light regime, function of reactor's geometry and biomass concentration maintained. This makes microalgae cultures continuously exposed to a complex highly fluctuating light field (Tredici 2010c). Due to the exponential light attenuation that

occurs in dense algal cultures a light profile is created along the light path. The "photic zone" and the "dark zone" are so created and cells are moved through "layers" with different light intensity. At the reactor surface they will be exposed to light intensities well above the saturation, while further away from the surface mutual shading condition prevails.

High light intensities can so be used efficiently by the cells if these are induced to move between the "photic zone" and the "dark zone" at high frequency (Tredici 2010c, Richmond 2004, Janssen 2002, Molina Grima et al. 1996). Turbulence is so a fundamental parameter determining the efficient use of available radiation both in photobioreactors and open systems.

Tubular photobioreactors:

These systems can be either vertical or horizontal and can be divided in:

- *Serpentine photobioreactors:* the first models were used for the cultivation of *Chlorella* in the early '50s at the Massachusetts Institute of Technology (MIT-USA). Usually the crop is circulated a speed of 20-30 cm s⁻¹ using pumps or an air lift systems (Molina et al. 2001). Many types of serpentine reactors have been developed over the years. A detailed overview was made by Tredici (2004b).
- *Manifold photobioreactors:* parallel tubes are connected at the ends, one for distribution and the other one for culture collection. In comparison with serpentine reactors shows lower head losses due to the absence of bends. A lower power input is so required for culture circulation. Productivity of 1.26 g L⁻¹d⁻¹ (28 g m⁻²d⁻¹) and 0.8 g L⁻¹d⁻¹ were obtained with *Arthrospira platensis* and *Nannochloropsis* sp. respectively in the so called NHRT manifold reactor, developed at University of Florence
- *Helical photobioreactor:* consists of tubes of small diameter (2.5-5 cm) usually in plastic materials, coiled on cylindrical vertical supports. Culture is circulated through pumps or an air-lift system.

Vertical cylinders and sleeves:

Low density polyethylene sleeves, usually made of LDPE, are the easiest and cheapest way to build a photobioreactor. The bags are hung on metal structures and the culture is agitated by blowing compressed air enriched with CO₂. The main limitation of this design is the low s/v

ratio, the difficulty in scaling-up and high levels of *bio-fouling*. These systems are widely used in hatcheries for the production of phytoplankton. Currently NOVA green GmbH (Vechta-Langförden, Germany) is using LDPE sleeves for the cultivation of microalgae for food, pharmaceutical and cosmetic market (Tredici 2004a). In Israel (Kibbutz Keturah, Eilat), a small pilot plant uses this technology for the cultivation of *Phorphyridium*.

The vertical columns, usually made of fiberglass or Plexiglas[®], developed by Cook at Stanford University in the '40s, are widely used for the cultivation of microalgae. Columns are usually 2 m high with a diameter of several tens of cm. Low *s/v* ratio are characteristic of this kind of PBR, but despite this vertical columns are commonly used in hatcheries.

To overcome the low *s/v* ratio and to effectively use the amount of incident photons, Plexiglas[®], annular columns were design. The culture is placed in the annular culture chamber, 3-5 cm thick and 6 to 120 L in volume, formed by two cylinders of different diameters placed one inside the other. In almost all the vertical columns mixing is provided by bubbling air enriched of CO₂. Annular columns can operate both with artificial and natural light.

The potential of annular columns in addition to the high productivity achievable, 38 g m⁻² day⁻¹ were obtained in a full-scale simulation with *Tetraselmis suecica* (Chini Zittelli et al., 2006), is given by the high photosynthetic efficiency achievable due to their vertical arrangement able to dilute the incident light. However, the limited size of the unit (volume 230 L max) and their relatively high cost makes these systems difficult to be scaled up.

Flat photobioreactors:

This type of reactors, unlike tubular reactors, can be tilted and oriented in such a way to optimize the radiation intercepted.

The types of flat panel reactors that have been developed during the years can be summarized in the following categories:

- *Alveolar panels*: developed since the early '80s are made of PVC, polyethylene or other plastic materials, having small internal narrow channels, called *alveoli*. Channels can be parallel to the ground or vertically to it. In the first case the agitation of the culture is carried out by means of pumps, while in the second case by blowing compressed air from the bottom of the panel. Pilot plants inspired by this type of reactors have been developed by Prof. Pulz dell'IGV-Institut für Getreideverarbeitung (Bergholz-Rehbrücke, Germany) and are currently commercialized by Braun Biotech International GmbH (recently incorporated in

Sartorius Biotechnology Division) in modules from 10 to 2,000 L (Tredici et al., 2004 a).

- *Glass plates*: Developed since the '90s by the Prof. Richmond (Ben-Gurion University, Israel), are made of glass plates assembled to form a PBR of reduced thickness. They can be constructed of the desired thickness (reactors were tested with a thickness ranging between 1.3 and 10 cm) (Wu et al. 2001). Good productivity was obtained with species such as *A. platensis* (50 g day⁻¹ per m² of illuminated surface) and *Nannochloropsis* (12 g m⁻² illuminated surface d⁻¹), in a reactor of 500 L (Richmond & Wu 2000). These kind of reactors are easy to clean, highly transparent and have greater inertia than Plexiglas[®] respect to weather.
- *Disposable panels*: the development of this new design originated simultaneously by two distinct groups: the Department of Agricultural Biotechnology (University of Florence) and the Ben-Gurion University in Israel, but with two different motivations. The Italian group aimed at a low-cost system for large scale applications, instead the Israeli researchers needed a clean and disposable culture chamber for the cultivation of those microalgae which suffer from contamination (Tredici et al., 2004b). Disposable panels are essentially flat panel reactors consisting of a transparent plastic culture chamber (transmittance > 80%) enclosed in a rectangular metal frame or cage. Mixing is provided by means of a perforated pipe placed on the bottom of the reactor in which compressed air is blown. Temperature control is achieved by water spraying on the outer reactor's surface or by means of an internal heat exchanger. Systems are extremely easy to assemble and allow easy scaling-up to industrial plants. The "Green Wall Panel"(patent WO 2004/074423), as the Italian version was called, has been extensively employed in outdoor condition to grow several marine microalgae strains (Rodolfi et al., 2009). The potential of the marine eustigmatophyte, *Nannochloropsis* sp. as a source of oil for biodiesel production has been investigated by Rodolfi et al. (2009). In a two-phase cultivation process (a nutrient sufficient phase to produce the inoculum followed by a nitrogen deprived phase to boost lipid synthesis) the lipid content of the biomass was increased up to 60% and a potential lipid productivity of 20 t ha⁻¹ in the Mediterranean climate was attained (Rodolfi et al., 2009). Reactor's design has been recently improved in order to reduce its cost (Tredici et al., 2010b). The improved design allows to use a much lighter metal frame decreasing construction costs to about € 15 per meter. Research pilot plants employing GWP

reactors are currently operating at ENI S.p.A. refinery of Gela (Italy), at ENEL Ingegneria e Innovazione S.p.A. (Brindisi, Italy), at Bioscan S.A. (Antofagasta, Chile). Commercial facilities are instead presents at Archimede Ricerche S.r.l. (Camporosso, Italy) and at Necton S.A. (Olhão, Portugal).

1.3 Microalgae and bio-fuels

The enormous expectations placed upon microalgae as a new source of bio-fuels (biodiesel, bio-ethanol but also hydrogen and biogas), have contributed during the last 5 years to the birth of many companies (Singh & Gu 2010). Not all, however, have proven experience in the field and often, data provided by these companies exceed the maximal theoretical values of photosynthetic efficiency and productivity or are a simple extrapolation from laboratory experience never verified experimentally in outdoor mass culture (Tredici 2010c).

Here some of the possible applications of microalgae for energy use are reported (Huesemann & Benemann 2009):

- Direct combustion, gasification and pyrolysis. These processes requires dried biomass. This phase will further increase the cost of production. Only natural drying can be considered an economically viable solution.
- Methane production by anaerobic digestion of algal biomass. CH₄/CO₂ (biogas) production via fermentations of algae slurry is already a proven technology. Production of 0.21 m³ CH₄ kg VS (volatile solids) have been obtained from the biomethanation of the marine algae *Tetraselmis* (Legros et al. 1983). Anaerobic digestion of microalgae biomass is an interesting application when combined with wastewater treatment processes.
- Bio-ethanol production. There are two ways that we can get ethanol from microalgae:
 - Fermentation, provided by yeasts, of storage compounds like starch in microalgae and glycogen in cyanobacteria. Fermentation tests of glycerol, the main storage product of *Dunaliella salina*, hyper-saline microalgae, resulted in ethanol productivity up to 0.49 g ethanol/g of glycerol (Huesemann & Benemann 2009).
 - Endogenous fermentation in anaerobic conditions. Some species, particularly *Chlamydomonas* sp. are capable to ferment the storage starch accumulated

inside the cell without the aid of enzymes produced by yeasts, producing acetate, glycerol, ethanol and in some cases hydrogen.

- Hydrogen (H₂) production. There are three ways by which H₂ can be produced with microorganisms:
 - Self-fermentation of organic acids, glycerol and starch in *Chlamydomonas* sp.
 - Photofermentation. Organic acids produced during the fermentation process described above, can be converted from phototrophic bacteria in H₂. Photosynthetic efficiency of this process are still limited: 5- 8 moles of H₂ per mole of starch (Huesemann & Benemann 2009).
 - Biophotolysis. The ability of microalgae to produce H₂ and O₂ from water through a photosynthetic process has been known for more than 65 years. Most of the studies on biophotolysis in microalgae were carried out with *Chlamydomonas reinhardtii*. The production of H₂ through this process is not common to all microalgae, but is linked to the presence of a particular enzyme, hydrogenase, which allows the reduction of two protons H⁺ to elementary H₂. The process, however, is strongly inhibited by the presence of molecular oxygen that inactivate the synthesis of hydrogenase.

- Biodiesel. The high lipid productivity of microalgae represents the real added value of this kind of biomass respect to traditional energy crops. The average lipid content in microalgae is species specific and so it is extremely wrong to make generalizations. The average lipid content varies from 10 to 30% on dry biomass (Rodolfi et al. 2009). Most lipids are important constituents of the cell membrane or are synthesized and stored as reserve compounds, others plays important roles as cofactors and pigments. Triglycerides (TAG), representing the major class of lipids stored as energy reserve (up to 80% of the total lipid fraction) (Becker 2004) are accumulated in the form of oil droplets within the cytoplasm. Numerous studies and projects have been carried on in order to evaluate the use of these photosynthetic organisms as a new source of oil to process into biodiesel. Worthy of note is the research conducted by National Renewable Energy Laboratory (NREL): the Aquatic Species Program (ASP). The program was funded by the United States Department of Energy (USDA), which over the course of two decades (1978-1996) looked into the production of energy using algae. Initially, the funding was to develop renewable transportation for fuel.

Later, the program focused on producing bio-diesel from algae. Despite the substantial resources invested in the project and the work of several American

research centers, the conclusions of the work have shown that microalgae were a potential oil source, but still not quite competitive with conventional traditional fuels. Of considerable interest is the work of Rodolfi et al. (2009), where a screening of 30 different strains (marine or freshwater) of microalgae was carried out to identify one or more strains with high potential lipid productivity (Rodolfi et al. 2009). Detailed information about this research are given below.

1.4 The strain *Nannochloropsis* F&M-M24

It is a marine unicellular algae belonging to Eustigmatophyceae family, known in the past as “marine Chlorella” (Maruyama et al. 1986).

The genus *Nannochloropsis* is one of the most cultivated and employed in the aquaculture industry, both as feed for live prey and in the “green water” and “pseudo-green water” techniques (Tredici et al., 2009, Chini Zittelli et al., 2003). The strain is characterized by spherical no flagellate cells 2-3 μm in diameter. Commercial interest for this strain raise from its high polyunsaturated fatty acid (PUFA) content representing up to 5.32% of dry biomass. Particular interest is due to the high level of eicosapentaenoic acid (EPA - 20:5 ω 3) about 5 % of the dry biomass and for a 0.68% of arachidonic acid (AA – 20:4 ω 6) (Chini Zittelli *et al.*, 1999).

During the last years the interest in this genera and especially for the strain here examined, has incredibly increased thanks to its relative high lipid content, on average 32% of dw, and also to the fact that TAGs synthesis, the fraction important for biodiesel production, can be modulate by inducing stress condition determining a variation of growth and a total lipid content up to 50% of the biomass. (Rodolfi et al., 2009, Borowitzka 1988, Chisti 2007). *Nannochloropsis* F&M-M24 results in this way a good candidate as “alternative” biomass for oil production.

Commercial interest for this algae makes *Nannochloropsis* one of the most cultured and studied marine algae.

Here as follow we briefly report some of the most interesting studies made by Prof. Tredici research group during the last years where *Nannochloropsis* F&M-M24 was employed.

Different light source and reactor designs have been used to characterized *Nannochloropsis* productivity and to study the influence of growth parameters on biochemical composition of this strain.

In 120 and 140 L annular columns influence of natural, artificial and mixed (artificial-natural) light on productivity was studied (Chini Zittelli et al., 2003). Combined artificial and natural illuminated cultures obtained the best results in terms of volumetric productivity. Also in typical sunny periods (May at Florence latitude) combination of natural and artificial illumination resulted as the best solution to promote strain productivity.

The effect of medium recycling on growth and productivity of *Nannochloropsis* F&M-M24 grown was investigated in 120 L F&M-AC annual columns (Rodolfi et. al 2003). At industrial and commercial scale, characterized by great volumes of water handled every day, the exhausted medium, obtained from culture harvesting operation, can represents a resource as new feedstock water to be reuses for daily reactor's dilution.

Great interest on this strain raised up after a recent paper has been published (Rodolfi et., al 2009). Thirty different strains have been screened for their lipid content and biomass productivity in laboratory condition. After that *Nannochloropsis* F&M-M24 resulted the best strain in terms of lipid synthesis under nitrogen deprivation. Its lipid production potential was so evaluated under outdoor conditions in a 110 L first generation GWP photobioreactors (Tredici & Rodolfi 2004). An average lipid productivity of 204 mg L⁻¹ d⁻¹ was obtained, respect to only 117 mg L⁻¹d⁻¹ of the nutrient sufficient culture. Adopting a so called “two-phase” strategy, where nutrient sufficient phase devoted to inoculum production, is followed by a nitrogen deprived phase to boost lipid synthesis. Potential of high lipid productivity up to 30 ton. ha⁻¹ anno⁻¹ was so proved under outdoor culture condition.

EFFECTS OF DIFFERENT ARRANGEMENTS OF THE “GREEN WALL PANEL” REACTOR ON SOLAR RADIATION COLLECTED

Introduction

One of the biggest challenges in microalgae biotechnology is to increase light harvesting capacity of culture systems and to increase the efficiency with which the collected light (solar radiation or artificial light) is converted into chemical energy by photosynthesis (Tredici, 2010c). If for an open system, like a pond, solar radiation intercepted is only function of season and latitude, photobioreactors, especially flat plate reactors, can be arranged, by varying inclination and orientation, in such a way to maximize the solar radiation intercepted.

When culture parameters as nutrients, dissolved oxygen and carbon dioxide, pH, temperature and cell concentration are optimized and contaminants (biological and chemical) are kept under control, the only factor limiting biomass productivity becomes light (Tredici 2010c, Richmond 2004, Tredici & Chini Zittelli, 1997). If these conditions are realized, the effect of light intensity on algal growth is well described by the so called PI-curve (Masojidek et al., 2004).

In a well mixed dense algal culture the higher is the light collected by the reactor the higher will be the biomass productivity. This is true up to saturating or inhibiting light intensity are reached.

Often confusion is made between the importance of maximizing solar radiation captured for square meter of illuminated reactor's surface and the amount of irradiance intercepted per square meter of occupied plant area. Both of them are important but lead to different results. An increase in total photosynthetic photon flux (PPF, $\mu\text{mol photons. m}^{-2} \text{ s}^{-1}$) intercepted per square meter of illuminated surface causes an increase of the volumetric productivity and so the efficiency with which the unit of reactor's volume is used (Richmond 2004, Zhang et al. 1999). In outdoor cultivation this is usually reached by means of *isolated* reactors or by disposing culture systems in such a way to minimize losses of direct and disperse radiation due to reactor's mutual shading. If the purpose is instead to maximize areal productivity (g m^{-2} of ground d^{-1}), as in the case of land scarcity or where land cost represents an important percentage of plant's investment cost, solar radiation intercepted per m^2 of occupied land, instead of solar radiation per m^2 of illuminated surface, should be maximized.

To obtain high areal biomass productivities, solar radiation impinging on an fixed ground area must be maximized and used efficiently. At this scope culture “lamination“by means of closely packed vertical reactors has been proposed as possible solution to obtain both the goals (Wijffels and Barbosa 2010, Tredici 2010c).

Evaluation of total solar radiation collected by photobioreactors is a fundamental step in the characterization and optimization process for any given system devoted to photosynthetic microorganisms growth.

Commercial tools are available to evaluate global radiation for a generic oriented solar panel, but reactors for microalgae differ from solar collectors for some important aspects related to algae physiology and so these models are not always useful. For this reason, in order to quantify light intercepted by a flat panel reactor like the GWP reactor, a model has been developed and validated. The model, modifying well known formulations used in solar engineering for the calculation of daily and hourly irradiance (Kreith and Kreider, 1978), is able to estimate global, beam, diffuse and reflected radiation received by flat panel reactors for different latitudes, inclinations and orientations. Losses of direct irradiance by mutual shading, diffuse radiation due to the presence of obstacles (parallel reactor’s rows) and reflected irradiance were also considered for *full-scale* arranged reactors.

Numerical simulations and on field measurement were performed, for Florence latitude, both for *isolated* and *full scale* N-S and E-W oriented GWP in order to validate the methodology used.

Besides the quantification of the solar irradiance falling onto the reactor’s walls the characterization of any system employed for photosynthetic microorganisms needs quantification of the real amount of light penetrating inside the reactor. Photon flux losses due to the reflection and absorption by the reactor wall’s material can not be neglected and have been calculated and verified by field measurements.

The model has then been used to obtain annual simulations of the average daily global radiation ($\text{MJ m}^{-2} \text{ ground day}^{-1}$) collected by *full scale* GWPs (vertical or inclined) for different latitudes, in order to investigate the most suitable orientation (N-S vs E-W) directions and reactor spacing.

2.2 Materials and Methods

2.2.1 On field solar radiation measurements

Field measurements, on 12th August 2009 at Florence latitude (43°48' N - 11°12' E), were performed to validate the solar radiation model both for *isolated* and *full scale* configurations, for N-S and E-W facing “Green Wall Panel” (GWP) (patent: WO 2004/074423).

The photosynthetic photo flux density (PPFD) at the reactor surface was measured by a LP 9021 PAR quantum sensor connected to a DO9021 quantum-photo- radiometer (DeltaHom S.r.l, Padova, Italy). PFD was measured at three different height (0-0.5 and 1 m from the ground) on north, south, east and west facing surfaces. Six measurements were so collected every hour for each isolated or *full-scale* arranged GWP. Daily solar radiation intercepted, MJ m⁻² (reactor) day⁻¹, was calculated by integrating the curves obtained from hourly measured values.

2.2.2 Hourly solar radiation: *isolated* GWP

Hourly global solar radiation impinging on a given surface was calculated following the procedure described by Mustacchi (1985), calculating the following parameters:

The solar constant:

It is defined as “ *the intensity of solar radiation beyond the earth’s atmosphere, at the average earth-sun distance, on a surface perpendicular to the sun’s rays* ” (Kreith and Kreider 1978).

$$I_0 = 1365\{1 + a \sin[b(N - c)]\} \quad (1)$$

The atmospheric transparency index (K_t)

It represents the total radiation on the terrestrial surface to that on the corresponding extraterrestrial surface (Kreith and Kreider 1978). Depending from the location considered and climatic conditions, K_t assumes values between 0 and 1. Low values are given by absorption phenomena due to aerosol, clouds, air humidity (water vapour) and ozone, while high value are index of clearness. For this analysis an average transparency index for Italy was calculated as function of the latitude (L) and the month considered (m) (Mustacchi 1985).

$$K_t = [1.232 - 0.0781 \text{abs}(m - 7)] * (0.914 - 0.0106L) \quad (2)$$

Values of K_t , for a set of ground meteorological stations can be also calculated from measured horizontal global radiation G_h and the computed values of clear-sky horizontal global radiation G_{hc} (<http://re.jrc.ec.europa.eu/pvgis/solres/solrespvgis.htm>).

Instantaneous solar parameters for a given day/month:

In order to determine solar incident angle (θ_{beam}) on a arbitrary surface, instantaneous parameters has to be first calculated. Declination (δ) and hour angles (ω), depending by the day of the year and the hour considered, were determined using the following equations:

$$\delta = a' * \text{sen}[b'(N - c')] \quad (3)$$

$$\omega = 15(14.5 - h) \quad (4)$$

Is now possible, for a defined latitude (L), to calculate hourly incident angle on a fixed surface (θ_{beam}):

$$\begin{aligned} \cos \theta_{beam} = & (\text{sen} \delta * \text{sen} L * \cos \beta) - (\text{sen} \delta * \cos L * \text{sen} \beta * \cos \gamma) + (\cos \delta * \cos L * \cos \beta * \cos \omega) \\ & + (\cos \delta * \text{sen} L * \text{sen} \beta * \cos \gamma * \cos \omega) + (\cos \delta * \text{sen} \beta * \text{sen} \gamma * \text{sen} \omega) \end{aligned} \quad (5)$$

The former equation is simplified if solar incident angle on horizontal surface (θ_h) has to be determined:

$$\cos \theta_h = \text{sen} \delta * \text{sen} L + \cos \delta * \cos L * \cos \omega \quad (6)$$

Hourly global radiation impinging on a horizontal surface (W m^{-2}) is then given by K_t , I_0 and θ_h :

$$G_h = K_t * I_0 * \theta_h \quad (7)$$

Using K_t is also possible to calculate the proportion of diffuse to total global radiation (D_h/G_h) on horizontal surface:

$$D_h / G_h = 1.39 - 4.027 * K_t + 5.531 * K_t^2 - 3.108 * K_t^3 \quad (8)$$

The fraction of global solar radiation impinging on a given plane (G) to global solar irradiance on the horizontal plane (G_h), is then given by eq.9:

$$G / G_h = (1 - D_h / G_h) * \cos \theta_{beam} / \cos \theta_h + D_h / G_h * (1 + \cos s) / 2 + \rho(1 - \cos s) / 2 \quad (9)$$

Where ρ is the *albedo* index, representing the ratio of radiation reflected from a surface to that incident on the same surface. It can assume values in the range of 0.1 (low reflection) up to 0.75, typical of snow cover (high reflection). Field measurements, used to confirm model's calculated values, were performed on GWP reactors placed on a basement of white stones basement. Reflection index was however lower than 0.55 (typical albedo index for that kind of material) due to the high level of moisture content of the soil caused by continuous water spraying for cooling the reactors. Surface roughness influence soil albedo as well, other than wet/dry condition (Matthias et al. 2000). A value of 0.3 was so here considered. Is now possible to calculate the value of the hourly global radiation impinging onto given surface combining eq. (8) with eq. (9). Thanks to eq. (9) it is also possible to determine the relative contribution of each solar component (*beam, diffuse and reflected*) impinging onto the surface of interest.

2.2.3 Hourly solar radiation: *full-scale* GWP

The shading effect:

Mutual shading caused by obstacles, as in the case of parallel rows in *full scale* plant, can be computed by determining two defined angles: γ_1 and γ_2 . The first of them represents the difference between solar azimuth (ψ) and the azimuth of the surface (ψ_s). For N-S facing reactors γ_1 is equivalent to the hourly solar azimuth. When γ_1 is known, γ_2 can be determined by the following equation:

$$\text{Tan} \gamma_2 = \text{Tan} h_s / \text{Cos} \gamma_1 \quad (10)$$

where the solar altitude angle (h_s), the angle between the line joining the center of the solar disc to the point of observation at any given instant and the horizon plane through that point of observation, is given by the following formula (Kreith and Kreider 1978):

$$\text{sen}h_s = \cos L * \cos \delta * \cos \omega + \text{sen}L * \text{sen} \delta \quad (11)$$

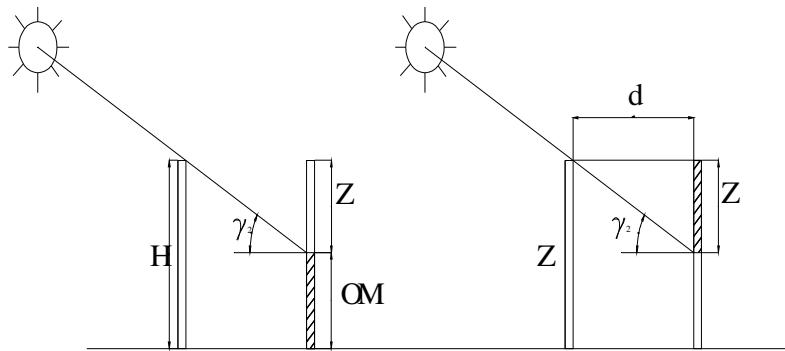


Fig.1 Schematic representation of γ_2

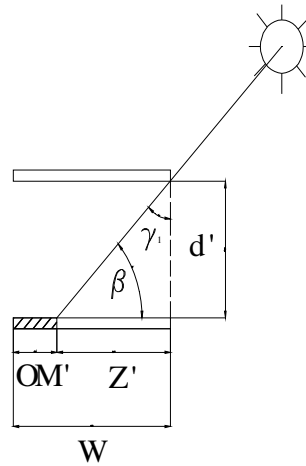


Fig. 2 Schematic representation of γ_1

Beam irradiance for a multi row configuration (*full scale*) is given by eq. 12:

$$G_{beam}^* = G_{beam} (Z * Z') \quad (12)$$

Losses of diffuse and reflected radiation:

Losses of diffuse radiation, with respect to an isolated reactor, were calculated determining the relative reduction of the view factor (the percentage of the sky dome viewed by a surface).

Losses of reflected radiation were determined following the same procedure described above and considering solar radiation isotropically reflected.

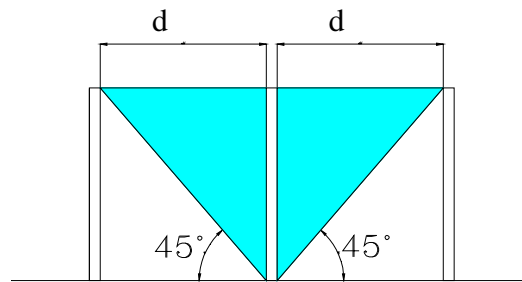


Fig.3 View factor for diffuse irradiance in vertical full-scale GWP ($d = 1 \text{ m}$)

2.2.4 Solar radiation transmittance through the reactor transparent wall

Reflection of direct and disperse solar radiation:

Percentage of the incident light reflected off by low density polyethylene (LDPE) culture chamber of GWP reactor was determined by the Snell and Fresnel's laws. Reflection of beam and disperse component were computed separately.

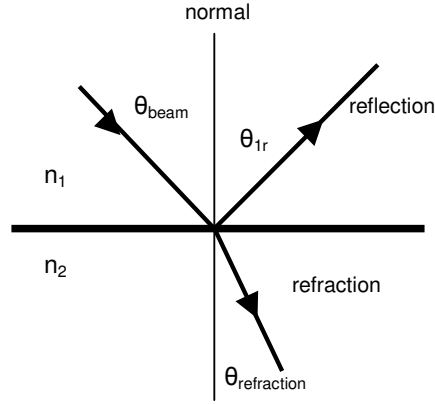


Fig.4 Refraction and reflection of light at the interface between media with different refractive index: $n_2 > n_1$. n_1 represent air and n_2 LDPE.

The incident and refraction angles are related by Snell's law:

$$\frac{\sin \theta_{beam}}{\sin \theta_{refraction}} = \frac{n_1}{n_2} \quad (13)$$

When incident angle of beam radiation is known, refraction angle ($\theta_{refraction}$) can be determined from the former equation, where n_1 and n_2 represents index of refraction for air and reactor's wall material. An average refraction index of 1.52 was here assumed for the LDPE transparent film.

The proportion of reflected irradiance respect to the incident radiation can be calculated with Fresnel law. In the case of solar irradiance (non polarized light) average reflection for the beam component is given by (Zijffers *et al.* 2008):

$$\bar{R}_{beam} = 0.5 * \frac{\tan^2(\theta_{beam} - \theta_{refraction})}{\tan^2(\theta_{beam} + \theta_{refraction})} + 0.5 * \frac{\sin^2(\theta_{beam} - \theta_{refraction})}{\sin^2(\theta_{beam} + \theta_{refraction})} \quad (14)$$

The first and the second terms of eq.(14) represents the two components of reflectance corresponding to the two components of light polarizations: parallel, first term, and perpendicular, the second term, to the plane of incidence (Kreith and Kreider 1978).

Reflection of disperse radiation is a more problematic matter. Light for disperse radiation strikes the reactor surfaces with not a defined incident angle, so disperse radiation is not reflected homogenously. An average reflection coefficient has to be considered. 13% reflectance for disperse radiation was here considered and calculate as follows:

$$R_{diff} = \sum_{N=0}^{90} \frac{R_{beam}}{N} \quad (15)$$

Absorption and light attenuation through transparent materials:

In the case of transparent material of thickness, L, the monochromatic transmittance τ_λ , expressing the relative percentage of incident radiation passing trough the transparent wall, can be determined by Bouger's law (Kreith and Kreider 1978):

$$\tau_\lambda = e^{-K_\lambda L} \quad (16)$$

An average extinction coefficient (K) of 1.65 was here assumed for polyethylene transparent material (Kreith and Kreider, 1978).

In eq. (16) the optical path length is given by (Kreith and Kreider 1978):

$$L = \frac{t}{\cos \theta_{refraction}} \quad (17)$$

Hourly values of transmittance were determined in order to calculate the real amount of solar radiation passing trough the LDPE film.

Field measurements of solar radiation transmittance through GWP's culture chamber:

Outdoor measurements, on a 90° tilted reactor, were performed for *isolated* N-S and E-W oriented GWPs, in order to compare calculated solar radiation transmittance with measured values. Field measurements were performed (Sesto Fiorentino, latitude: 43°48' N, longitude: 11°11' E) at *Fotosintetica & Microbiologia* s.r.l spermental area, on days with high atmospheric transparency ($K_t > 0.5$): e.s 14th January 2010. Ground was covered with a low

albedo liner ($\rho < 0.2$) in order to reduce as much as possible reflectance from the ground and make easier the comparison between predicted and measured values.

A 1 m², 300 μ m LDPE sheet inserted in a standing frame was used to simulate an operating GWP. Measurement of the incident and transmitted irradiance were performed both for north, south, east and west facing surfaces at fixed hours. The horizontal diffuse radiation was also measured. The photosynthetic photo flux density (PPFD) was measured by a DO 9721 cosine quantum sensor (400-700 nm) connected to a DO quantum radiometer/photometer (Delta Ohm, USA).

2.3 Results and Discussions

2.3.1 Solar model validation: numerical simulation vs measured values

Calculated values obtained by means of the methodology described previously were compared with field irradiance measurements in order to evaluate the model.

Fig. 5 and Fig. 6 show measured diurnal variations (12th August 2009) of global solar irradiance for N-S and E-W facing *isolated* GWPs compared with calculated values.

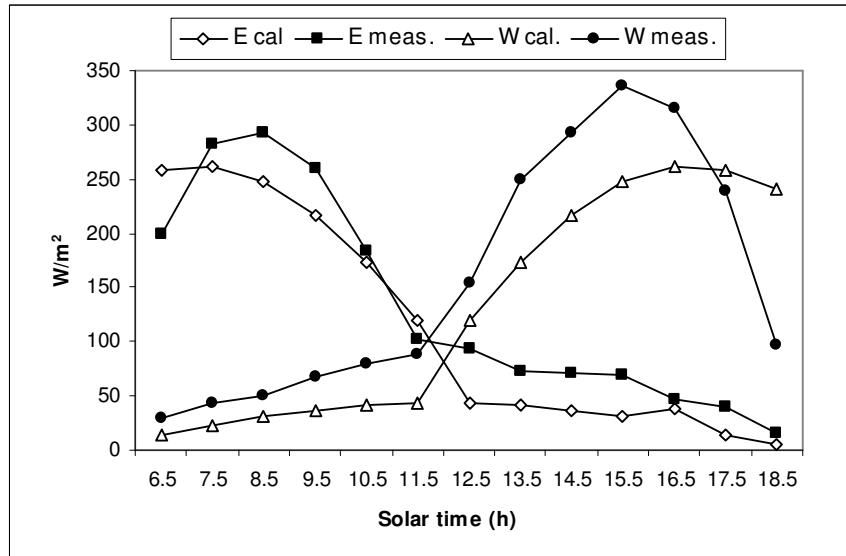


Fig.5 Diurnal variation, for Florence latitude (43°48'N-11°12'E), of daily global irradiance (PAR) for isolated vertical N-S facing GWP. 12th August 2009

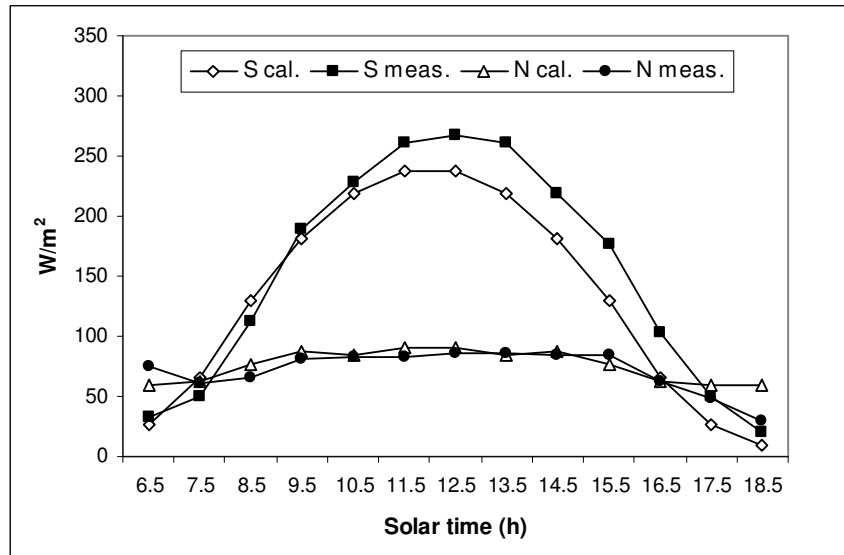


Fig.6 Diurnal variation, for Florence latitude (43°48'N-11°12'E), of daily global irradiance (PAR) for isolated vertical E-W facing GWP.12th August 2009

Good agreement between calculated and experimental measurements has been obtained for both orientations. Difference, between calculated and measured daily solar irradiance, was about 7% for N-S facing reactor (tab.1). E-W facing GWP showed a difference slightly higher than N-S reactors: 18%.

Reliability of the present methodology, for the determination of the amount of solar radiation impinging on an arbitrary surface, was also proved and confirmed for a multi rows (*full scale*) arrangement. Even in this case calculated data fitted well with filed measurements as shown in tab.1:

Tab.1 Total daily PAR radiation ($MJ m^{-2} reactor d^{-1}$) impinging on isolate and full scale GWP for two different orientations. Reactor distance 1 m for full scale arrangement.

	<i>Isolated</i>		<i>Full scale</i>	
	N-S	E-W	N-S	E-W
Calculated ($MJ m^{-2} reactor d^{-1}$)	9.75	11.49	5.41	6.23
Measured ($MJ m^{-2} reactor d^{-1}$)	10.43	13.58	5.73	6.38

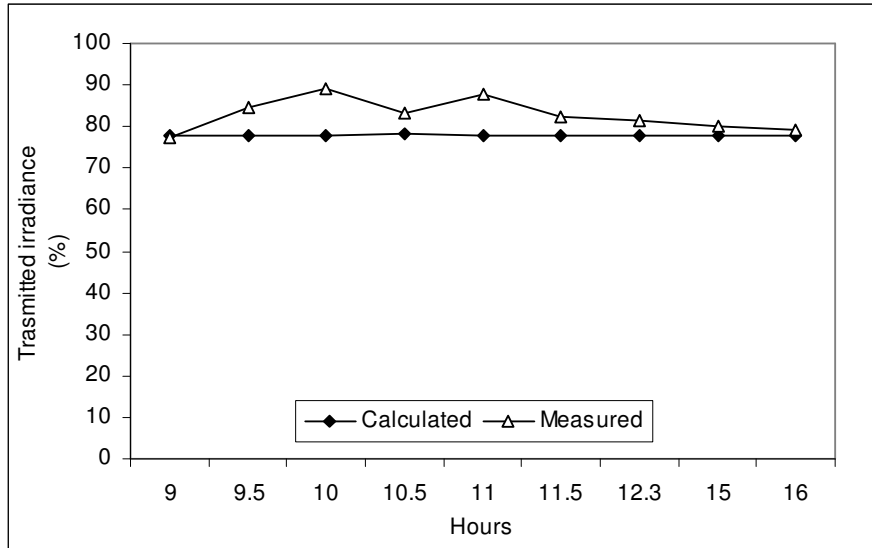


Fig.7 Diurnal variation of transmittance for south facing transparent LDPE film at Florence latitude (Italy) for 14th January 2009

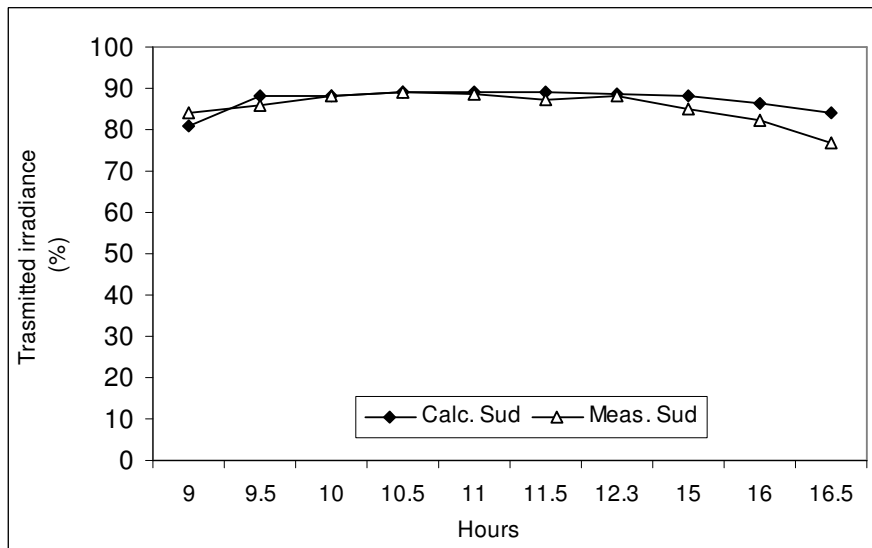


Fig. 8 Diurnal variation of transmittance for north facing transparent LDPE film at Florence latitude (Italy). for 14th January 2009.

Fig.7 and Fig.8 show measured (14th January) diurnal variation of transmittance for Florence latitude (43°48'N) for a N-S oriented GWP compared with calculated values. Transmittance is expressed as % of the impinging global radiation.

North and south surfaces are treated separately because they do not receive the same type of radiation. For the period considered, full winter, only the south facing surface is hit by beam radiation, while only diffuse radiation impinges onto the north exposed face. As shown in Fig.8, calculated transmittance for the north surface is constant during the day. This is consequence of the average reflectance for diffuse radiation (eq. 15) and absorbance for the same component. As explained above these values are constant despite the hour and the period of the year considered.

Despite some differences, calculated and on field measured values, fit well showing an average difference of about 6%.

2.3.2 Influence of orientation and inclination on annual solar radiation collected: *isolated GWP*

As the numerical simulation produced by the solar model resulted in agreement with measured values, daily global radiation ($\text{MJ m}^{-2} \text{ reactor d}^{-1}$) were determined on annual basis for vertical E-W and N-S isolated GWP and for a 43° inclined reactor. Reported values refer to 40 L GWP 1 m high, 1 m long and 4 cm thick plac at Florence latitude.

Tab. 2 Simulation of total daily global radiation ($\text{MJ m}^{-2} \text{ reactor d}^{-1}$) for isolated GWP. $\rho = 0.3$, Latitude ($43^{\circ} 48' \text{ N} - 11^{\circ} 12' \text{ E}$). Reactor dimensions: 1 m high, 1 m wide.

	N-S facing vertical (MJ reactor⁻¹ d¹)	E-W facing vertical (MJ reactor²d⁻¹)	N-S facing 43° inclined (MJ reactor¹d⁻¹)	Horizontal (MJ m⁻² d⁻¹)
Jan	9.39	7.40	8	4.62
Feb	12.34	12.12	11.12	7.41
Mar	14.32	15.76	14	11.12
Apr	16.11	21.93	16.67	15.65
May	18.79	27.41	18.52	19.42
Jun	20.05	29.66	19.82	21.78
Jul	20.69	31.35	20.98	22.15
Aug	17.91	25.31	19.13	17.97
Sep	16.49	18.40	16.51	12.88
Oct	14.86	14.46	13.48	8.49
Nov	11.94	9.12	10.23	5.49
Dec	10.28	7.54	8.56	4.24
Average	15.26	18.37	14.75	12.60

Average total daily global radiation impinging on a vertical isolated GWPs showed totally different annual trends for the two orientations. The E-W oriented reactor showed a typically bell-shaped curve with a maximum in summer of $31.35 \text{ MJ reactor}^{-1} \text{ d}^{-1}$ and a minimum in winter of $7.4 \text{ MJ reactor}^{-1} \text{ d}^{-1}$. Daily global radiation for N-S isolated GWP, shows a more regular distribution along the year, with a maximum of $20.69 \text{ MJ m}^{-2} \text{ reactor d}^{-1}$ in July and a minimum of $9.39 \text{ MJ m}^{-2} \text{ reactor d}^{-1}$ in January. E-W orientation resulted the best collecting configuration with a 46% more radiation captured respect to N-S facing GWP, but also with respect to inclined and horizontal surfaces (tab.2)

2.3.3 Influence of arrangement (orientation, inclination and distance) on annual solar radiation collected: full scale GWP.

Average daily solar radiation for isolated reactors is of limited importance for scale up. Photobioreactor potential must be evaluated by its overall areal productivity (OAP, $\text{g m}^{-2}\text{d}^{-1}$) and this is maximized when solar radiation falling on a defined area is collected as much as possible (Zhang et al., 1999). Since at large scale is it impossible to collect more radiation

than that falling on the horizontal surface, all possible solutions for reactors arrangements lead to lose some of the radiation available (Perez and Seals, 1995, Zhang et al., 1999).

In fig. 9, 10 and 11 simulations of total daily global radiation for Florence latitude (43°48'N-12°11'E) of different arrangements for *full scale* GWP is reported. Differently than for isolated reactors (tab.2), the difference between orientations, in average annual solar radiation intercepted are strongly reduced. E-W vertical GWP, in fact, intercept only from 2 to 3% more radiation respect to N-S orientation, depending on the distance considered (tab.3). Difference between orientations is so reduced from 16 to only 3 % passing from isolated to full scale vertical reactors.

Reducing the relative distance between parallel rows increases the solar radiation collected per unit of occupied land ($\text{MJ m}^{-2} \text{ ground d}^{-1}$) both for vertical and inclined GWP (fig. 9, 10 and 11).

During summer months when the sun is high on the horizon, the difference between radiation falling on horizontal surface and the radiation collected by vertical reactors spaced 1 m, is up to 60% for N-S facing GWP (fig.9). Differences between orientations and inclinations are progressively flattened as distance between reactors is reduced (fig. 9, 10 and 11).

For vertical 1 m spaced GWP, the most usual configuration adopted in pilot and commercial plants (Rodolfi et al., 2010) it is not possible to define the best solution in terms of reactor's orientation, because the differences in solar radiation collected are negligible (tab.3). However the choice is so related to other factors, such as the lower heating of the culture on summer for the E-W orientation respect to N-S facing reactors or the possibility to extend the growing season for a longer period for N-S respect to E-W facing reactors. Different results can be expected changing the site's latitude, as the mutual shading effect can strongly vary. As we can see from tab.3 and fig.12 and 13 considerations made for the center Italy case are also true for other latitudes.

E-W orientation always results as the best arrangements for vertical reactors in terms of solar radiation collected per unit of occupied land (fig.12). Even if the difference with N-S oriented reactors is progressively reduced by setting the panels close.

Inclined reactors, at the optimal inclination angle for each latitude, shows a more regular pattern respect to the vertical one (fig.13). Differences between 1 m spaced GWP and reactors 0.1 m spaced (10 times more "dense"), is in fact much less pronounced than for vertical GWP (fig.12). This means that we can intercept almost the same radiation of the horizontal by reducing 10 times the investment. This is not possible with vertical reactors. If tilted reactor results in an advantage in terms of intercepted radiation, there are nevertheless

some technical problems that often limit the possibility of adopting this arrangement. For example the mixing of the culture (by air bubbling) tends to get worse the more the reactor is tilted, facilitating the sedimentation of cells on the back surface.

Closely packed reactors, as in the case of 0.1 m spaced GWPs, means high illuminated surface per m^2 of occupied land, achieving by this way a sort of light “lamination” or light “dilution”. This has been frequently proposed as an effective method to boost areal productivity (Wijffels and Barbosa, 2010, Carlozzi 2003, ChiniZittelli et al., 2003). If an increase of areal biomass productivity from closely spaced reactors could be obtained, it also true that energetic and economic assessments should be made when numerous reactors are installed per square meter of land. We should therefore assess whether the higher investment and energy costs are compensated by higher productivity.

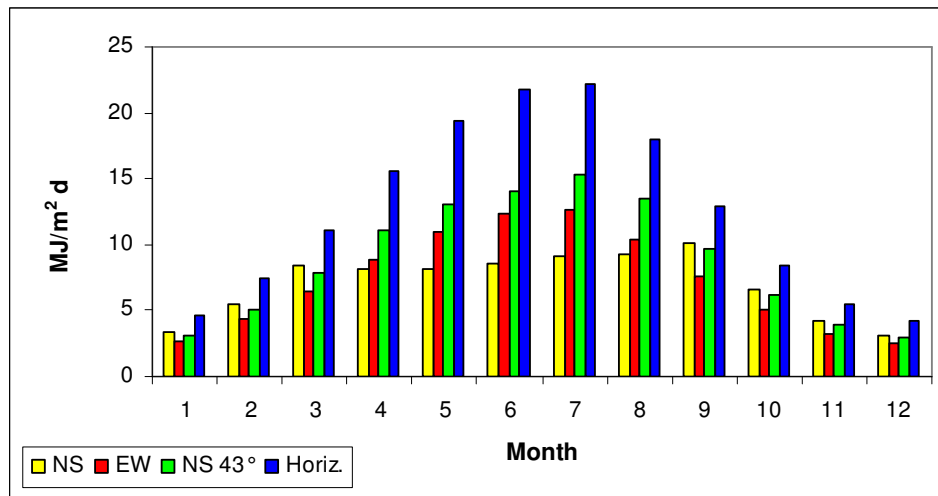


Fig.9 Simulation of total daily global solar radiation (Florence, 43°48'N-12°11'E) impinging on vertical and tilted full scale GWPs. Reactors' distance $d = 1m$.

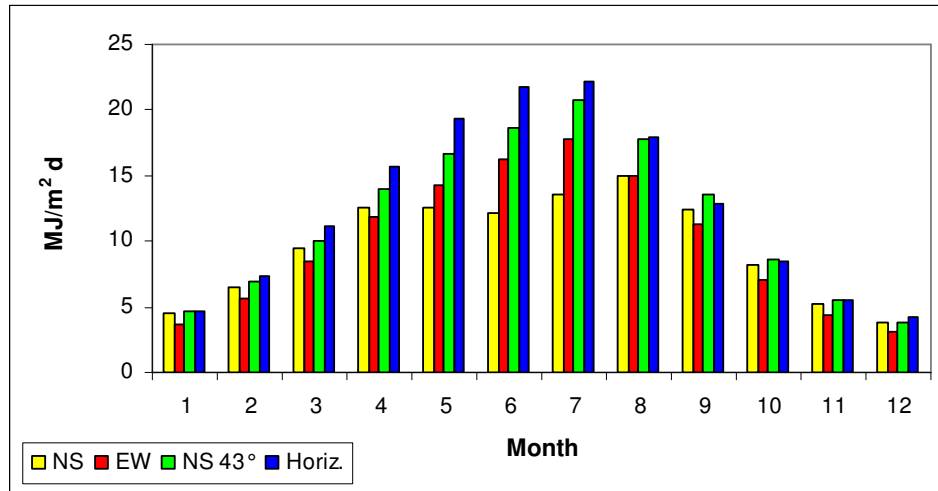


Fig.10 Simulation of total daily global solar radiation for Florence latitude ($43^{\circ}48'N-12^{\circ}11'E$) impinging on vertical and tilted full scale GWPs. Reactors' distance $d = 0.5$ m.

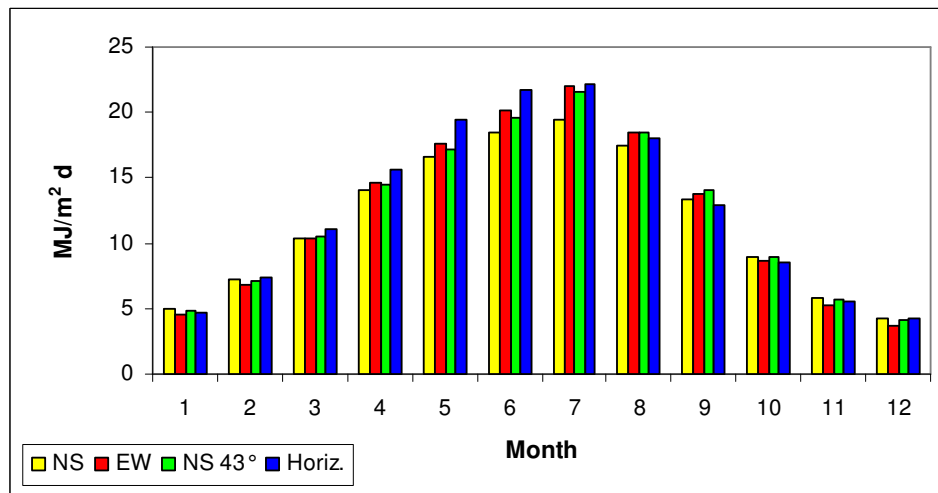


Fig.11 Simulation of total daily global solar radiation (Florence, $43^{\circ}48'N-12^{\circ}11'E$) impinging on vertical and tilted full scale GWPs. Reactor's distance $d = 0.1$ m.

Tab.3 Annual average daily global radiation ($MJ\ m^2\ ground\ d^{-1}$) for vertical and inclined (optimal inclination angle for each latitude) GWP. Three different reactor's distance considered: 1, 0.5 and 0.1 m.

	N-S			E-W			Inclined			Horizontal
	1	0.5	0.1	1	0.5	0.1	1	0.5	0.1	
Nairobi	7.48	11.26	15.30	9.90	13.08	16.40	17.92	18.24	18.2	18.26
Ryad	9.72	13.26	18.00	12.58	16.48	20.60	20.08	21.66	21.9	21.8
Florence	7.06	9.70	11.80	7.27	9.91	12.18	8.82	11.74	12.23	12.6
Stockolm	6.52	8.26	9.3	6.38	7.96	9.6	8.05	9	9.4	9.69

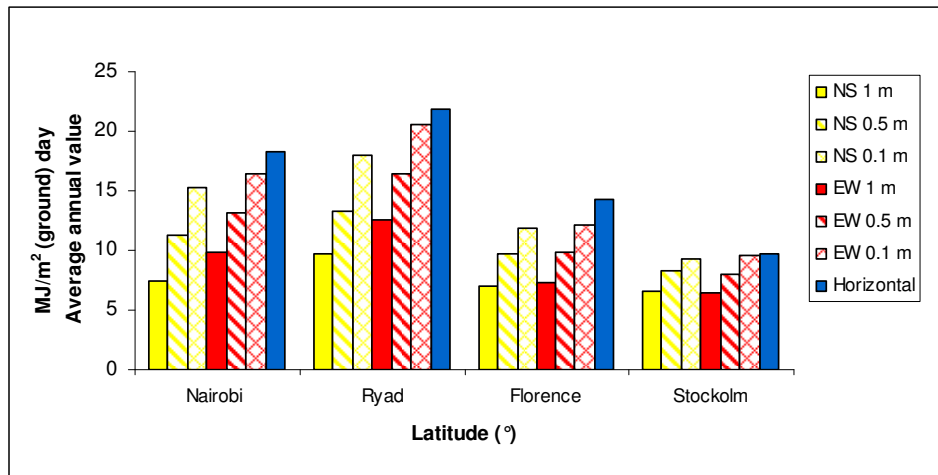


Fig.12 Average total daily global solar radiation, $MJ\ m^{-2}$ of ground area, for vertical GWPs as function of latitude, orientation and distance between rows.

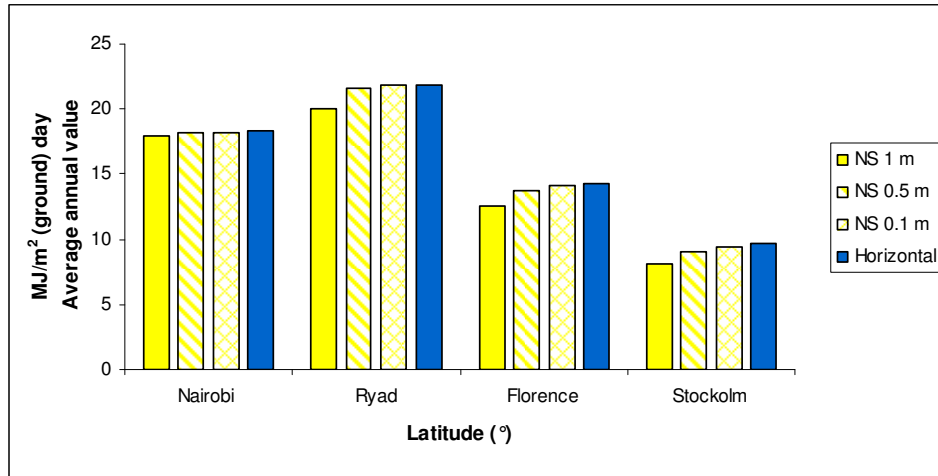


Fig.13 Average daily global solar radiation, $MJ\ m^{-2}$ of occupied area, for tilted (optimal inclination angle for each latitude) GWPs for three different distance. N-S: north-south facing GWP

2.3.4 Solar radiation transmittance through the transparent GWP's culture chamber in vertical GWPs.

The mechanism of transmission of solar radiation through the transparent polyethylene film (LDPE) of GWP's culture chamber is a complex process depending on the wavelength of the radiation considered, the incident angle, the relative refractive index and the extinction coefficient of the transparent material.

In fig. 14 and 15 hourly *reflectance* for beam solar radiation, expressed as % of impinging irradiance, for vertical N-S and E-W facing GWPs is reported for four representative months.

Percentage of beam radiation reflected off by the reactor surface has totally different trend both on annual and a daily base. N-S facing vertical GWP showed a sharp difference between summer/spring and autumn/winter periods, increasing reflectance during summer time when solar rays strike reactor's surface with low angles. For E-W facing GWP no difference on annual trend was revealed, but daily reflectance shows a peak value (100%) at midday when the sun is exactly over the reactor and no beam radiation is striking onto the reactor surface (fig. 15).

By determining reflectivity for beam and disperse irradiance and absorbance for the LDPE films, as a function of hour, inclination, orientation and season, values of trasmissivity

reported in tab.4 were obtained. N-S oriented reactors shows up to 22% of solar radiation lost due to reflection and absorption. E-W facing GWP instead presents a more regular trend with losses never lower than 18%.

Reflectance for disperse (diffuse and reflected) radiation was evaluated to be about a 13% of the impinging disperse irradiance and it was considered for the calculation of global transmittance.

In fig.16 reflectance of beam radiation for an horizontal surface at Florence (Italy) latitude is reported. The surface considered simulate a pond. A refractive index of 1.33, typical of water, was in fact adopted Daily reflectance is similar to that of a vertical N-S oriented GWP (fig. 14), but with a completely inverse annual trend.

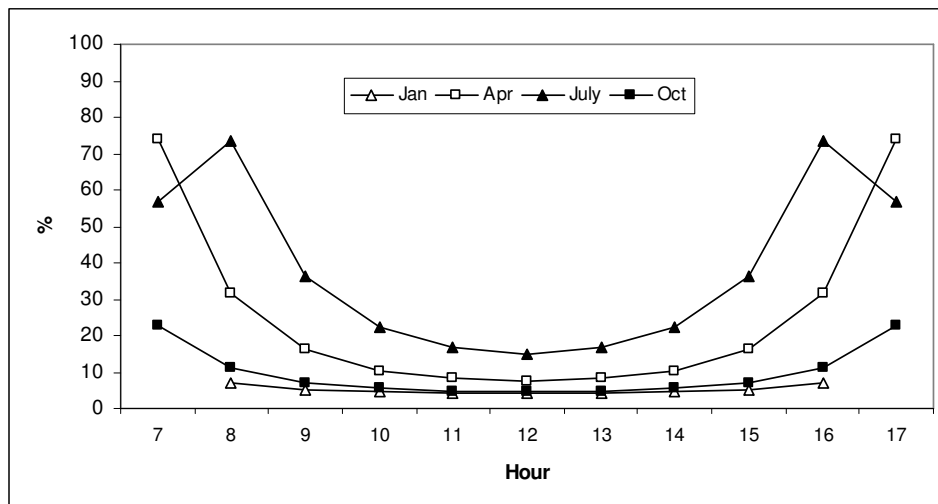


Fig.14 Hourly reflectance (%) of beam solar radiation for a N-S oriented vertical GWP (Florence: 43°48'N-12°11'E). Refractive index of LDPE =1.54

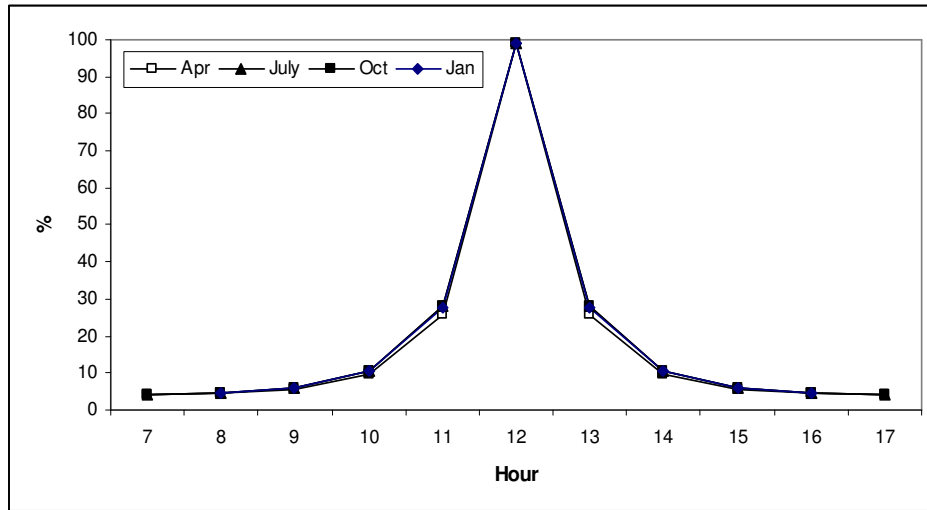


Fig. 15 Hourly reflectance (%) of beam solar radiation for a E-W oriented vertical GWP at Florence latitude 43°48'N-12°11'E). Refractive index LDPE =1.54

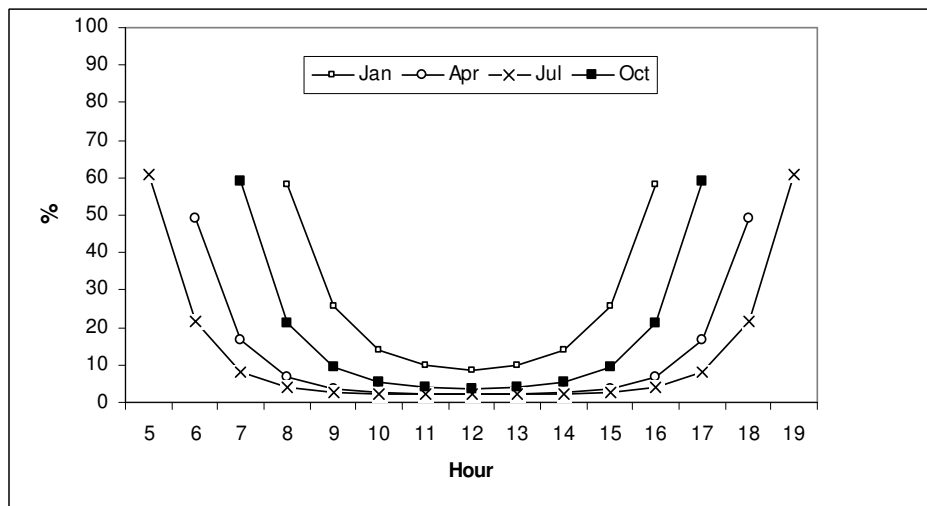


Fig. 16 Hourly reflectance (%) of beam solar radiation for an horizontal water surface (Florence: 43°48'N-12°11'E). Refractive index water: 1.33

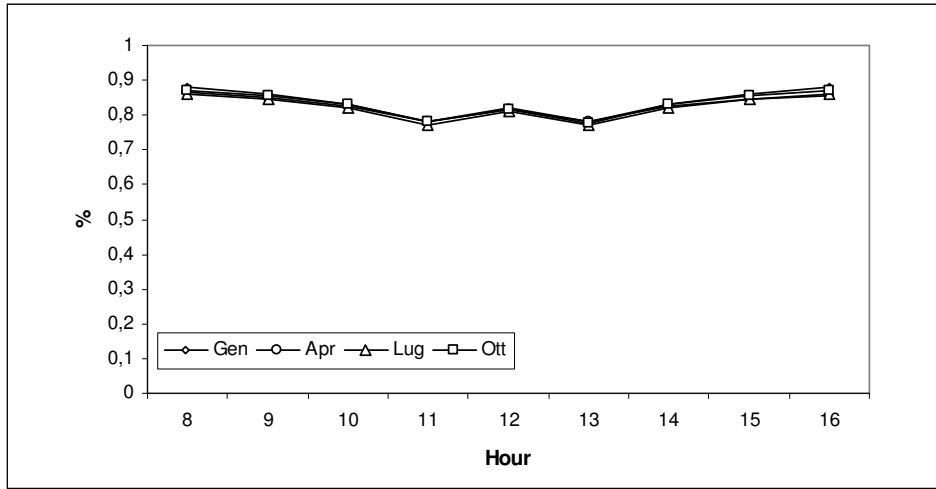


Fig.17 Evolution of hourly transmittance (% of the incident solar radiation) for E-W facing GWP

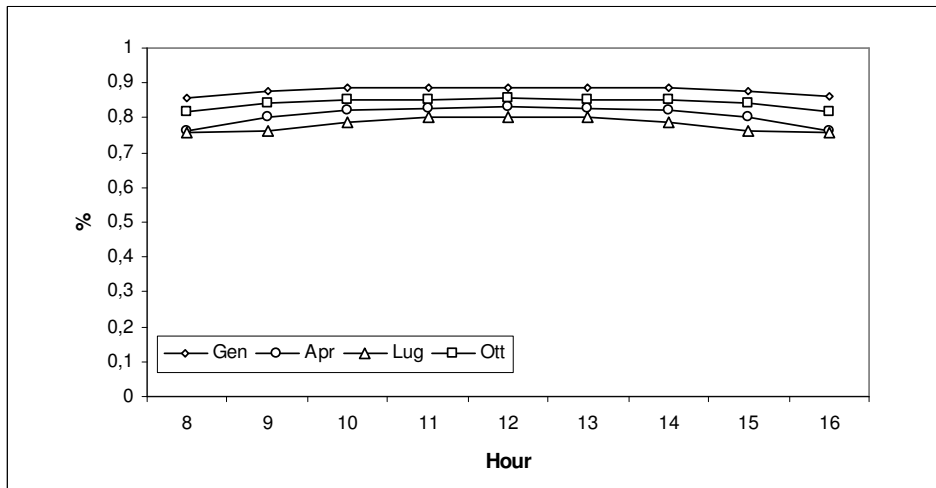


Fig.18 Evolution of hourly transmittance (% of incident solar radiation) for N-S (only south face considered) oriented GWP.

Tab. 4 Monthly average global transmittance through LDPE culture chamber for vertical GWP.

	January	April	July	October
	%			
E-W facing	83,5	82,7	82,2	83,2
N-S facing	87,7	80	77,9	84,2

2.4 Influence of GWP orientation on *Nannochloropsis* F&M-M24 areal productivity.

In order to confirm numerical simulations performed by the model, the influence of reactor's orientation on *Nannochloropsis* F&M-M24 areal productivity ($\text{g m}^{-2} \text{ground d}^{-1}$) in E-W and N-S full-scale (distance between rows: 1m) vertical GWP was studied. The period of experimentation was August 2009. At Florence latitude ($43^{\circ} 48' N- 11^{\circ} 12' E$) this period of the year is characterized by high solar irradiance available. As consequence of the greater solar radiation intercepted (+23%), E-W oriented GWP resulted as the more productive configuration. An average areal productivity of 13.41 and 11.5 $\text{g m}^{-2} \text{groud} \text{d}^{-1}$ was respectively obtained for E-W and N-S facing GWPs. The experimentation confirmed the importance of solar radiation captured per unit of occupied land to increase areal productivity. E-W oriented GWP, beside to result the best arrangement in terms of solar radiation intercepted (fig. 9 and tab.3), also presents a further advantage. This configuration make it possible to reduce incidence of solar radiation in the middle of the day, especially on summer months, when sun is high on the horizon and high solar intensity, well above saturation level, are common (fig.5 and 6). Photo saturation and photo inhibition can be so avoided respect to N-S oriented reactors that receive high levels of radiation at midday. Cooling is also improved in E-W arranged reactors where the lower level of radiation received during central hours makes easier and less expensive to keep the culture close to optimal temperature.

2.5 Conclusions

A detailed profile of solar radiation intercepted and of the actual amount of light penetrating the GWP reactor available thanks to the procedure here described.

Independently from the orientation, inclination and relative distance, reactors should be closely spaced in order to intercept as much as possible radiation. On the other hand this brings to high operative and cost effective problems and a compromise is necessary. Closely

spaced reactors in fact means higher capital costs, greater amount of water handled, lower volumetric productivities and culture's concentration and so higher harvesting costs.

It is difficult to determine which is the optimum arrangement for a panel reactor as the radiation intercepted is not the only parameter to be considered. Elements of technical nature, including ease of access to the reactors for maintenance, as well as investment and energy costs per square meter of occupied surface are all factors to keep in mind.

So in commercial facilities larger distance will be adopted, but independently by the distance and the latitude, E-W arrangements should be the preferred orientation for vertical reactors. Optimal inclined GWP's would permit to collect the highest amount of solar radiation respect to all others configurations, but problems of sedimentation on reactor's back surface would represent a limitation of this arrangement.

2.6 Nomenclature

I_0 = solar constant (W m^{-2})

N = day of the year

a , b and c = constants assuming values reported in tab.I

K_t = atmospheric transparent index

m = month

L = latitude or optical path length (m)

δ = declination ($^\circ$)

a' , b' and c' = constant assuming values reported in tab. II

ω = hour angle ($^\circ$)

h = solar hour

θ_{beam} = incident solar angle ($^\circ$)

$\theta_{\text{refraction}}$ = refraction angle ($^\circ$)

γ = surface azimuth angle ($-180^\circ \leq \gamma \leq +180^\circ$).

β = surface tilt angle relative to horizontal ($^\circ$)

θ_h = solar incidence angle on horizontal surface ($^\circ$)

G_h = hourly global radiation on horizontal surface (W m^{-2})

D_h = diffuse hourly solar radiation on horizontal surface (W m^{-2})

ρ = albedo index

h_s = solar altitude angle ($^\circ$)

ψ = solar azimuth ($^\circ$)

ψ_s = azimuth of the surface ($^\circ$)

G_{beam}^* = beam solar irradiance for full-scale reactor (W m^{-2})

n_1 = refractive index for air

n_2 = refractive index for LDPE or water.

R_{beam} = reflected beam irradiance (%)

R_{diff} = average reflection for disperse irradiance (%)

τ_λ = monochromatic transmittance (%)

K_λ = monochromatic extinction coefficient (m^{-1})

Tab. I

Day of the year	A	b	c
1 to 93	-0.0343	1	93
94 to 277	0.0327	0.978	277
278 to 365	0.0343	0.989	277

Tab. II

Day of the year	a'	b'	c'
1 to 80	23.45	1.008	80
81 to 266	23.45	0.965	80
267 to 365	-23.45	0.975	266

**HYDRODYNAMICS CHARACTERIZATION OF A DISPOSABLE FLAT PANEL
REACTOR: The “Green Wall Panel” (WO 2004/074423)**

3.1 Introduction

The design of a photobioreactor includes a series of decisions on matters ranging from basic microbiology and biochemistry to process engineering (Asenjo and Merchuk, 1994). A first classification of the existing designs includes mechanical and pneumatic reactors. The former are generally characterized by a solid (cells) and a liquid phase and are usually mixed by stirrers. The latter are instead characterized by three phases: solid, liquid and gaseous. Here the basic principles and the most important parameters influencing the fluid dynamics and biological performances of a pneumatically mixed reactor, the “Green Wall Panel” (GWP-WO 2004/074423) will be discussed.

Pneumatically mixed reactors are simply vessels in which cells, liquid and gas phases coexist. All the energy needed for mixing solid particles and gas-liquid mass transfer is provided by the gas sparged into the reactor, usually air. This type of reactor is extensively used industrially both in biotechnological applications and in wastewater treatment processes (Asenjo and Merchuk, 1994).

The hydrodynamics describing the mixing behavior of a pneumatically mixed reactor is a fundamental parameter affecting:

- The uniformity of the culture medium composition. As far as possible we should avoid the occurrence of concentration gradients such as nutrients, pH, dissolved O₂ and CO₂ and temperature.
- The light regime experienced by a single cell. This in turn affects the photosynthetic efficiency, the volumetric productivity and the composition of cultured cells.

Each type of photobioreactor is in fact characterized by its typical light regime that makes microalgae cells continuously exposed to a complex highly fluctuating light field (Tredici, 2010). Light regime is a direct function of the *light gradient* along the culture path and a *light/dark frequency* at which single cells are exposed.

Light gradient is function of reactor's geometry and biomass concentration inside the reactor, which causes an exponential attenuation of penetrating light according to Lambert-Beer's law.

The frequency of light/dark fluctuation is instead function of both reactor geometry, biomass concentration and the average cell travel-time required for cells to move back and forth between the light zone and the dark parts of the reactor (Molina Grima et al., 1999, Brindley Alias et al., 2004).

To obtain high biomass productivities, both light gradients and the L-D cycle of cells through the reactor's path must be optimized, by setting biomass concentration at the optimal density and turbulence degree at the level at which travel times begin to approach the turnover of the photosynthetic unit (Richmond 2004). The study of reactor's fluid dynamics, together with the relationship between reactor's geometry and solar radiation, is the starting point to understand the true potential and the limitations of a given photobioreactor.

In pneumatically agitated reactors several parameters have been found to be relevant to productivity, photosynthetic efficiency and energetic performances of the reactor itself (Janssen 2002, Chisti . 1999).

Air bubbled reactors (bubble columns and airlift reactors) have been deeply studied and described by many authors during the years (Asenjo and Merchuk, 1994, Chisti, 1999, Shah and Deckwer, 1983), but literature on hydrodynamic characterization of *disposable panels* for photosynthetic biomass production is still scarce (Rodolfi et al., 2009; Sierra et al., 2008).

Disposable flat panel reactors thanks to their simplicity, low construction cost and ease of operation have been proposed as a feasible solution for mass production of different algal strains and as possible technology to match with ponds in microalgae based bio-fuels production (Rodolfi et al., 2009, Tredici, 2010a., Sierra et al., 2008). The "Green Wall Panel" (GWP) is the first of such kind of reactors, but a specific characterization of its main hydrodynamics parameters has never been made.

Currently two versions of such kind of reactor exist. The first generation GWP (GWPI-WO 2004/074423) was developed and patented in 2004 (Tredici & Rodolfi, 2004a).

The GWP design has been recently improved in order to reduce its cost (GWPII-9325 PTWO). This new model has been tested with *T. suecica*, *Cylindrotheca* sp. and *Scenedesmus* sp. Here only the first version of the "Green Wall Panel", the GWPI, has been characterized.

Following the classification given by Chisti (1989) the "Green Wall Panel" reactor can be studied and described as a common *bubble column* reactor.

The gas hold-up, bubble dimensions and their rise velocity, the overall volumetric oxygen/carbon dioxide mass transfer coefficients, flow regimes, superficial gas velocity, mixing time and axial-dispersion have been determined in order to characterize the reactor. Most of these parameters are strongly influenced by the power supply (Sierra *et al.* 2008).

3.2 Materials and Methods

3.2.1 Experimental systems

GWPs of different size were employed for their hydrodynamic characterization. Axial dispersion coefficient, D_z , was determined in a 157 L GWP (2.66 x 0.059 x 1 m,) while for gas hold-up, bubble dimension, bubbles rise velocity and $(K_L a)_{O_2/CO_2}$ a 20 L GWP (0.5 x 0.04x 1m) was instead used. The mixing time, t_m , was determined for both types of reactors. Compressed air was sparged at the bottom of the reactor, for both the systems, through a perforated (\varnothing 1 mm) plastic pipe.

3.2.2 Gas hold-up

Gas hold-up was determined for tap water (1‰ salinity) at three different air flow rates (0.05-0.15-0.45 L air L⁻¹ min⁻¹), by comparing the culture volume in the GWP when the air flow was switched on to that with the air flow off. Experimental measurements were compared with calculated values using eq.(1) (Sierra *et al.*, 2008):

$$\varepsilon = 3.32 \times 10^{-4} \left(\frac{P_G}{V_L} \right)^{0.97} \quad (1)$$

In analogy with a liquid flowing into a pipe, the superficial gas velocity (U_g , m s⁻¹) for a bubble column reactor was determined from the air flow rate (L air L⁻¹ min⁻¹), by multiplying this last for the volume of the culture (L) and dividing by the cross-sectional area (m²).

3.2.3 Bubble dimensions and their rise velocity

Bubble dimensions and their rise velocities were both experimentally determined and analytically calculated for five different air flow rates ranging from 0.05 to 0.6 L air L⁻¹ min⁻¹.

Air bubbles were photographed in the GWP using a white background. Pictures were taken using a Nikon D300s digital camera (Nital S.p.a). A ruler was placed on the outside wall of the GWP for the measurement of bubbles size.

Analytically determined bubble diameter was instead calculated by Calderbank's equation (eq.2) and the expression proposed by Talbot (eq.3) (Calderbank, 1958, Poulsen et al., 1990):

$$d_b = 4.15 \left(\frac{\sigma^{0.6}}{(P_G / V_L)^{0.4} \rho_L^{0.2}} \right) \epsilon^{0.5} + 0.0009 \quad (2)$$

$$d_b = 0,0278 (d_o)^{0.5} (\text{Re}_o)^{0.33} \quad (3)$$

Bubble rise velocity was determined by means of bubbles visualisation technique. Frame by frame analysis of the video made possible to determine bubbles position at different times and by means of a ruler placed on the GWP's wall, rise velocity was determined.

3.2.4 Mixing time

Mixing time, t_m (s), was determined as described by Sierra et al. (2008). A pulse-response experiment was conducted with no water flow through the GWP (batch mode). A pulse of acid solution, 250 ml of HCl 35% (v/v), was injected at one side of the GWP. pH values were detected at inlet and at the opposite side of the reactor every five seconds. Tracer concentration $[\text{H}^+]$ was calculated from pH registered values. Mixing time was calculated for three different air flow rates: 0.05-0.15 and 0.45 L air $\text{L}^{-1} \text{min}^{-1}$ in tap water and determined as the time required to obtain 95% of homogeneity inside the GWP.

3.2.5 Axial dispersion coefficient and dispersion number.

Mean residence time ($t_{\Delta c,}$) (eq.4) and the variance of a tracer response curve ($\sigma_{\Delta c}^2$) (eq.5) were used to determine the axial dispersion coefficient, D_z , and the dispersion number, N_d . A pulse tracer response method, using an acid tracer as described above, was the technique used.

Differently from the determination of mixing time (t_m) here a continuous flow of water (tap water was used) through the GWP was applied. $[\text{H}^+]$ concentration was determined by means of pH measurements at the inlet and outlet of the reactor. Axial dispersion was determined for three different air flow rates (0.1-0.3 and 0.6 L air $\text{L}^{-1} \text{min}^{-1}$) applying a continuous water flow of 90 L (tap water) min^{-1} . Concentration tracer response curve, called "C" curves, were so obtained. All the procedures adopted are described by Metcalf and Eddy (2003).

Characterization of the “C” curves were made by the determination of the *mean residence time* (t_{Δ}) and the *variance of the distribution* obtained (σ_{Δ}^2), this last representing the amplitude of the response curve.

$$\bar{t}_{\Delta_c} = \frac{\sum t_i \cdot C_i \cdot \Delta t_i}{\sum C_i \cdot \Delta t_i} \quad (4)$$

$$\sigma_{\Delta_c}^2 = \frac{\sum t_i^2 \cdot C_i \cdot \Delta t_i}{\sum C_i \cdot \Delta t_i} - (\bar{t}_{\Delta_c})^2 \quad (5)$$

Dispersion coefficient, D_z , which quantifies the mixing as diffusion-like process was calculated from the variance value, $\sigma_{\Delta_c}^2$, of the response tracer curve (“C” curve), by the following relationship:

$$\sigma_{\theta}^2 = \frac{\sigma_{\Delta_c}^2}{\tau^2} = 2 \frac{D_z}{uL} \quad (6)$$

More frequently the axial dispersion is quantified by means of the dispersion number, Nd :

$$Nd = \frac{1}{2} \frac{\sigma_{\Delta_c}^2}{\tau^2} \quad (7)$$

Calculation of Nd is a practical method to quantify axial dispersion in industrial reactors.

Tab.1 Typical dispersion number (N_d) for industrial reactors (MetCalf & Eddy 2003).

Nd	Flow regime
0	Ideal plug flow reactor
0.05	
0.05-0.25	
0.25	
>0.25	Completely stirred reactor

3.2.6 The overall oxygen volumetric mass transfer coefficient

The overall volumetric mass transfer coefficient for oxygen $(K_L a)_{O_2}$ was measured at six different air flow rates (0.05-0.1-0.15-0.3-0.45-0.6 L L⁻¹min⁻¹). Pure oxygen was bubbled into the reactor until a concentration of 300% (corresponding to 28.35 mg L⁻¹ of dissolved oxygen at 18 °C and 1‰ salinity) of air saturation was reached. After that air was bubbled instead of pure oxygen. Oxygen concentration was measured by means of an OXY 323 oxygen meter equipped with a CelOX 325 polarographic Clark-type electrode (WTW, Germany). Saturation and stripping curves were in this way obtained and $(K_L a)_{O_2}$ was determined at constant temperature of 18 °C according to Babcock et al. (2002):

$$(K_L a)_0 = Ln \left(\frac{C_t - C_s}{C_0 - C_s} \right) \quad (8)$$

The term $K_L a$ express the overall gas transfer characteristics of an aeration process, including the contribution of the liquid film resistance, K_L , and the effect of the gas-liquid interfacial area, a .

3.2.7 Power supply

Power consumption for bubbling was calculated as the power supply in adiabatic compression. The relation applied is commonly used for the calculation of power consumption for blowers in wastewater treatment plants (Metcalf and Eddy 2003):

$$P_w = \frac{w \cdot R \cdot T_1}{29,7 \cdot n \cdot \eta} \cdot \left[\left(\frac{p_2}{p_1} \right)^{0,283} - 1 \right] \quad (9)$$

3.3 Result and Discussion

3.3.1 Gas hold-up.

In pneumatically mixed reactors the gas hold-up represents the volume fraction of gas in the gas-liquid dispersion. This parameter strongly influence on the performance of pneumatically mixed reactors (Chisti and Moo-Young, 1988).

In the case of Newtonian fluids the gas hold-up can be theoretically determined as the ratio (Joshi and Sharma, 1979):

$$\varepsilon = \frac{U_g}{U_t} \quad (10)$$

where U_g and U_t represents respectively the superficial gas velocity ($m\ s^{-1}$) and the mean terminal bubbles rise velocity ($m\ s^{-1}$). This last can be experimentally determined or theoretically calculated (Chisti and Moo-Young, 1988).

Empiric methods to determine the gas hold-up are based on comparing the level of the gas liquid and the ungasged liquid in the calibrated reactor, but numerous mathematical correlation has been also proposed for bubble column reactors (Chisti 1999, Deckwer 1992, Sierra et al. 2008):

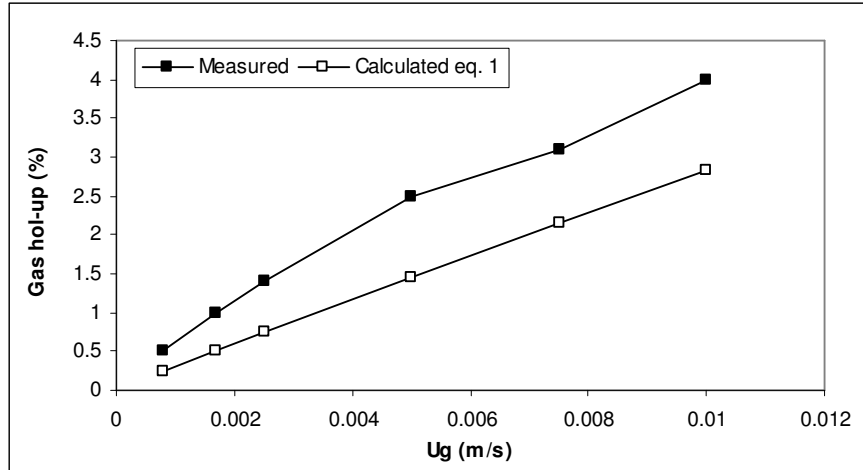


Fig.1 Gas hold-up as function of superficial gas velocity U_g ($m\ s^{-1}$). Empty "squares" correspond to calculated values by means of eq. 1.

Several literature data exists on the dependence of gas hold-up on superficial gas velocity for bubble column reactors, showing as the gas hold-up follows a potential relationship with the superficial gas velocity (Chisti and Moo-Young, 1988). The same behaviour was also confirmed for flat panel reactors by Sierra et al. (2008), where in a disposable panel similar to the GWP a potential relationship between gas hold-up and power supply was found (Sierra *et al.*, 2008). In fig.1 a similar relation between U_g and ε was also found for the GWP, showing as gas-hold up increases by increasing the gas flow rate sparged into the reactor. Calculated gas hold-up, by means of eq. 1, reported in fig. 1, is strongly dependent from the P_G/V_L ($W m^{-3}$) applied. Reported values have been calculated estimating the power requirement with eq. 13. As there is a difference in power supply determined with eq.13 and with that calculated with eq. 9, parameters as gas-hold up, $(K_L a)_{CO_2/O_2}$, depending by P_G/V_L ratio, can strongly differ if one.

3.3.2 Bubble dimension and their rise velocity

The influence of air flow rate on bubbles characteristics was also determined. Bubble's dimension is important in determining, together with the gas hold-up, the overall specific interfacial area (a_L) between the gas and liquid phase (Brindley *et al.* 2004). This in turn affects the overall volumetric mass transfer coefficient $K_L a$ which is a fundamental parameter determining the oxygen and carbon dioxide balance into the culture.

If bubbles are small (< 1 mm), their residence time into the reactor is quite long and allow to exhaust their CO_2 content or saturate their O_2 content, so mass exchange between the gas and liquid phases is sufficient to prevent stressful conditions to the culture due to over oxygen accumulation or carbon dioxide scarcity. On the other hand larger bubbles rising faster than small ones, have shorter residence times usually not sufficient to ensure proper gas exchange. High interfacial areas have also been found responsible for bubble-cell associated damage (Brindley *et al.* 2004)

In fig. 2 the influence of the air flow rate on bubble diameter for a 20 L GWP is reported. Measured and calculated values, these last by means of equations (2) and (3), are compared. Measured bubble diameters first increase by increasing the air flow rate and then, at high air rates, smaller bubbles are formed. This can be explained with the high turbulence present inside the GWP when high air flow rates are used. This causes bubble coalescence but also bubbles breakage due to mutual crashes, reducing the average bubble diameter measured.

Bubble's size is influenced by liquid phase properties as viscosity, density, temperature and superficial tension of water or culture medium. Bubble size decreases by decreasing both liquid viscosity and the interfacial tension (Brindley *et al.* 2004).

Sparger pore size can also affect bubble diameter. Bubble dimension decreases with a reduction of the sparger pore size. Here a constant temperature of 18° C and a pore size of 1 mm were used.

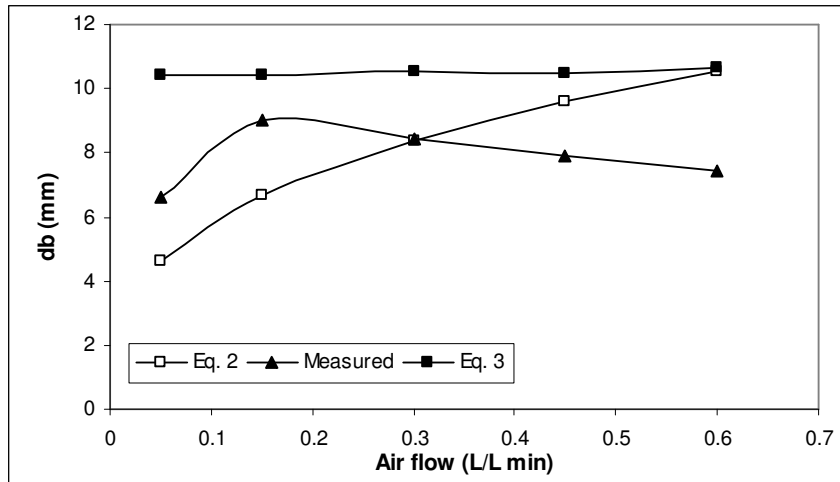


Fig. 2 Bubble dimension (mm) as function of air flow rate ($L L^{-1} min^{-1}$) in a 20 L GWP. Comparison between measured and calculated values by means of eq. 2 and 3.

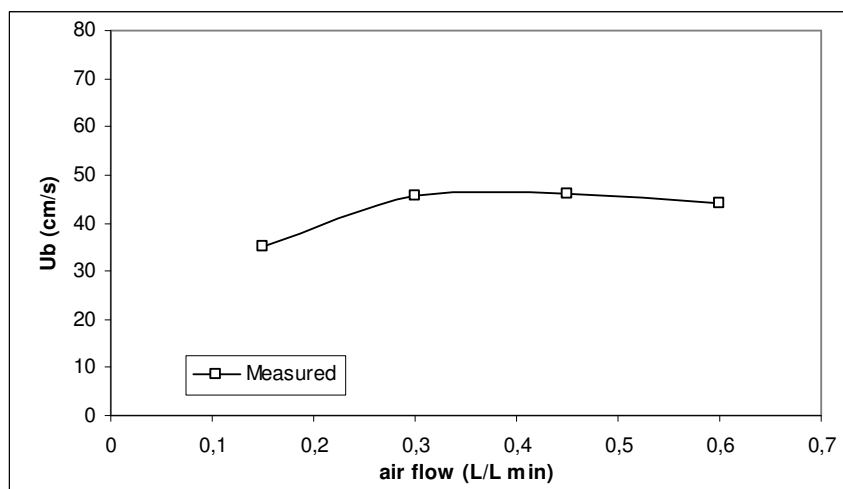


Fig. 3 Measured bubble rise velocity (cm s^{-1}) as function of the air flow rates in a 20 L GWP.

In fig.3 the influence of air flow rates on bubble rise velocity is reported. The trend is similar to that of measured bubble dimension (fig.2). After a first increase, at rates higher than $0.3 \text{ L L}^{-1}\text{min}^{-1}$, flow rates seem not to affect bubble velocity. This is probably due to a decrease in average bubble diameter at high air flow rates due to bubble breakage as consequence of the mutual crashing caused by intensive mixing. It can also be caused by excessive turbulence obtained at high air flows which slows the ascent of bubbles.

Bubbles characteristics (dimension and velocity) can responsible of cells damages in air bubbled cultures (Briendly et al. 2004). The *sheare rate*, γ , function of bubble rise velocity and bubble diameter, together with liquid microeddies formed by the high liquid turbulence, can contribute to cells stressful conditions.

Phaeodactylum tricornutum cultures were stressed at *sheare rate* greater than 30 s^{-1} (Brindley et al., 2004). At the air flows here tested in a 20 L GWP, *sheare rate* was always lower than 20 s^{-1} and microeddies length resulted always higher than average cell size. This means that liquid turbulence induced by air energy dissipation is not high enough to cause stress condition in strains commonly cultured in such kind of reactor like *Nannochloropsis* and *Tetraselmis* (Rodolfi et al., 2009, ChiniZitelli et al., 2006) that present average cell diameter lower than the microeddies formed. Microeddies length were calculated as the ratio between bubble rise velocity (U_b) and bubble diameter (d_b): $2U_b/d_b$ (Briendly et al., 2004).

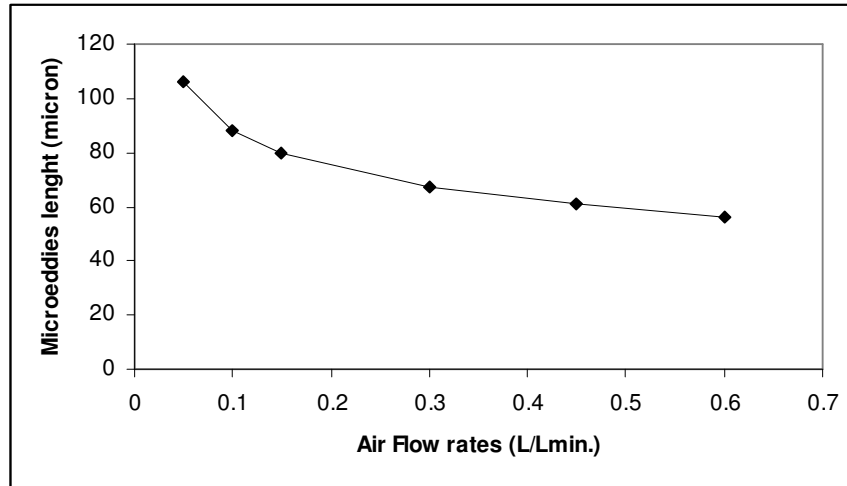


Fig.4 Influence of the air flow rate on microeddies length scale in a 20 L GWP.

3.3. 3 Mixing rate and fluid dynamics

Mixing represents one of the most important parameters determining biomass productivity of microalgae cultures influencing light regime inside the photobioreactors and gas-liquid mass transfer between phases (Tredici, 2010c, Jansenn, 2002, Camacho Rubio et al., 2004).

The mixing time, i.e the time required by a mixed liquid to reach a specified degree of homogeneity (95%) after a tracer pulse has been injected, is a common parameter used in biotechnology to represent the extension of turbulence (Kawase and Moo-Young 1989, Camacho Rubio *et al.* 2004). Mixing time is a direct indicator of the turbulence and mixing capacity of a reactor and it also gives useful information regarding heat and mass transfer, allowing the comparison with characteristic times of biological process taking place inside reactors (Kawase and Moo-Young, 1989, Sierra *et al.*, 2008).

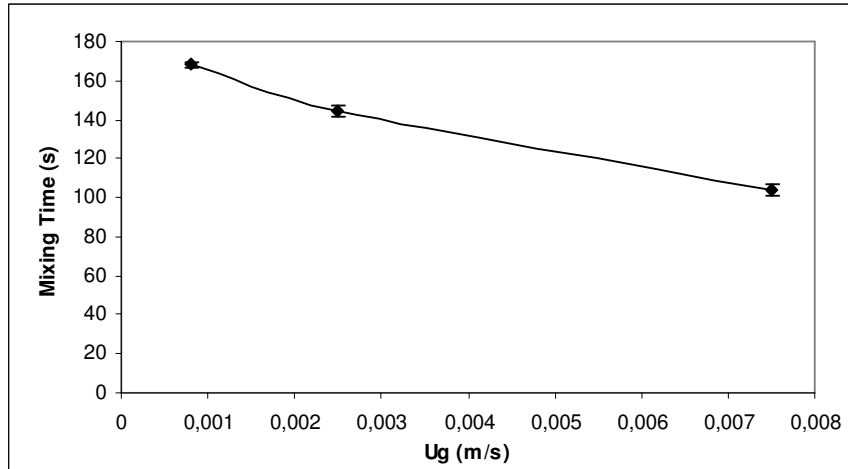


Fig.5 Characteristic mixing time in a 20 L GWP calculated by the pH pulse response method.

Mixing time in a 20 L GWP resulted almost linearly dependent with the superficial gas velocity (Fig. 5). This behaviour agrees with that reported by other authors where at homogeneous bubbly flow regimes, as those observed for the air flows tested, mixing time is inversely proportional to the superficial gas velocity (Kawase and Moo-Young, 1989, Sierra et al., 2008, Camacho Rubio et al., 2004). As the flow regime changes in heterogeneous churn-turbulent flow ($U_g > 0.05$), the influence of superficial gas velocity on mixing time is reduced and so the time required to obtain 95% of homogeneity inside the reactor can also slightly increase (Kawase and Moo-Young, 1989, Sierra et al., 2008, Camacho Rubio et al., 2004). Here, in a 20 L GWP, at the air flows tested, U_g , derived from the total air flow rate divided by the cross-sectional areal of the aerated zone, was always maintained lower than 0.05 m s^{-1} which is typical of *homogeneous bubbly flow regimes*.

Together with mixing time the axial dispersion coefficient (D_z) is another useful parameter to quantify the extension of dispersion and the mixing state occurring inside a reactor. D_z is a global coefficient representing dispersion as a complex phenomenon generated by velocity gradients inside the reactor, turbulence, bubble coalescence and breck-up, and molecular diffusion (Metcalf and Eddy, 2003, Camacho Rubio et al., 2004).

The overall hydraulic behaviour of an *ideal reactor* is represented by two borderline cases:

- Plug-flow reactors (PFR): characterized by low or any axial dispersion of the fluid elements.

- Continuous stirred tank reactors (CSTR): the fluid elements inside the reactor are instantly homogeneously dispersed. The liquid inside the reactor is so perfectly mixed at any time.

Dispersion process in *real systems* are usually different from the ideal hydraulic behaviour of a PFR or CSTR. To study and optimize real reactors is fundamental to determine the dispersion process occurring in real cases. In the case of PFR or CSTR a non-ideal hydraulic behaviour occurs when the mean residence time of fluid elements (t_m, s^{-1}) differs from the theoretical residence time (τ, s^{-1}) determined as the ratio of reactor's volume (m^3) on liquid flow rate ($m^3 s^{-1}$) (Metcalf and Eddy 2003).

The use of non-reactive tracers is a common practice for the analysis of dispersion process in bioreactors. Different types of tracers can be used (alkaline, acids and dyes) for this purpose and their main characteristics has been resumed by Denbigh and Turner (1985). Tracers are usually injected at one side of the reactor and their concentration is detected and registered, at different time steps, in the outflow and fitted with time.

Tab.2 Influence of air flow rate on fluid dynamic characteristics in a 125 L GWP. Dz , σ_{Ac}^2 and N_d were calculated by eq. 5,6 and 7.

	Air Flow Rate (L L⁻¹ min⁻¹)			
	0	0.1	0.3	0.6
Nd	0.022	0.0427	0.0411	0.0368
Dz (m²s⁻¹)	0.0014	0.0029	0.00279	0.0025
σ_{Ac}^2 (s²)	0.14	0.28	0.27	0.24
U_g (m s⁻¹)		0.0016	0.005	0.01
Tm (s)	167.5	76	85	105

In tab.2 factors used to describe the fluid dynamics occurring in real reactors are presented for the 125 L GWP.

The axial dispersion number, N_d , that quantifies the axial dispersion phenomena inside the reactors resulted inversely related with t_m (fig.6) and always lower than 0.05. Liquid dispersion at the experimental condition was so typical of a *plug flow* reactor.

The same trend for both t_m and N_d was also reported by Sierra et al. (2008), where at air flow rates higher than $0.1 \text{ L L}^{-1}\text{min}^{-1}$ axial dispersion and mixing time decreased and increased respectively, indicating a reduction in reactor mixing capacity (fig.6). This is exactly the behaviour described above where the influence of superficial gas velocity on mixing time is reduced and so the time required to obtain 95% of homogeneity increase.

Two different types of dispersion exists: radial and axial dispersion. When the length/column diameter ratio (L/d) is higher than 4, dispersion process can be described only by the use of axial dispersion coefficient D_z , radial dispersion is in fact negligible in such kind of reactors (Riquarts 1981). This is the case of GWP where L/d is higher than 100 (hydraulic diameter was considered) and mono-dimensional dispersion occurs.

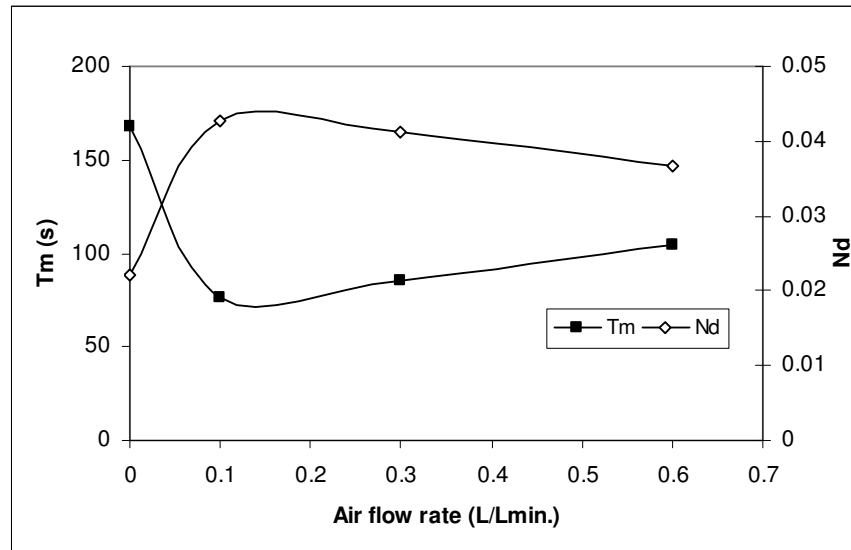


Fig. 6 Dispersion number, N_d and mixing time for the 125 L GWP as function of air flow rate. 90 L min^{-1} water flow applied

3.3.4 Gas-liquid mass transfer in GWP reactors.

Gas-liquid mass transfer can represent the limiting step in photobioreactors where oxygen produced by photosynthesis can over-accumulate up to inhibitory concentrations and carbon dioxide can not be rapidly dissolved.

Numerous theories have been proposed during the years to explain the mechanism of mass transfer occurring at gas/liquid interface. The easiest and widely accepted is that proposed by Lewis and Whitman, where liquid and gaseous boundary layers present at the liquid/gas interface represent the two major obstacles to the gas-liquid mass transfer process (Metcalf and Eddy, 2003).

The gas-liquid mass transfer velocity, r ($\text{mg L}^{-1} \text{s}^{-1}$), can be determined by means of the following relation:

$$r = K_L a (C_s - C_t) \quad (11)$$

The overall mass transfer coefficient for oxygen $(K_L a)_{\text{O}_2}$ and carbon dioxide $(K_L a)_{\text{CO}_2}$ are usually determined experimentally and their values are different if sea water, tap water or if culture medium are considered (Metcalf and Eddy, 2003, Malda, 1999, Babcock *et al.*, 2002).

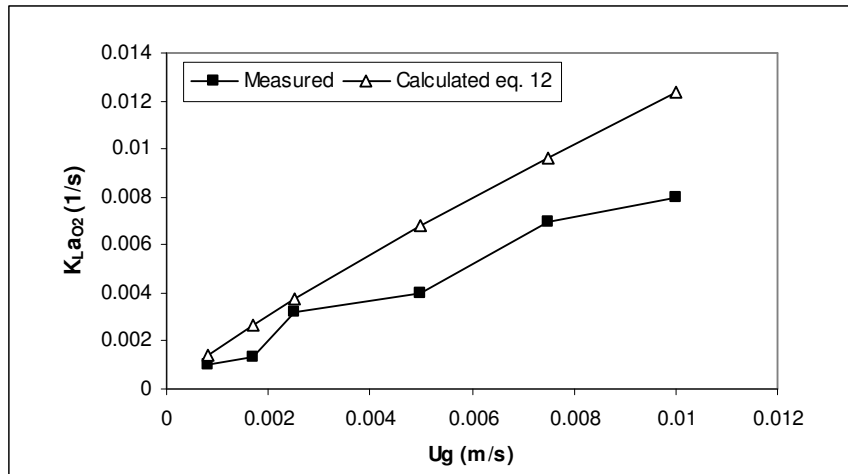


Fig.7 Overall oxygen volumetric mass transfer coefficient for a 20 L GWP . Tap water used

The overall volumetric mass transfer coefficient for oxygen in the GWP was measured at different air flow rates ranging from 0.05 to 0.6 $\text{L L}^{-1} \text{min}^{-1}$ corresponding to superficial gas

velocities from 0.0008 to 0.01 s⁻¹. When the U_g increased from 0.0008 to 0.01 s⁻¹, the (K_La)_{O₂} increased linearly from 0.001 to 0.0077 (fig. 7). Calculated K_La values were estimated with the relation reported by Sierra et al. (2008) commonly used to predict K_La in bubble column reactors:

$$K_L a_L = 2.39 \times 10^{-4} \left(\frac{P_G}{V_L} \right)^{0.86} \quad (12)$$

Daily evolution of dissolved oxygen in *Nannochloropsis* F&M-M24 outdoor cultures for the 20 L GWP showed as a (K_La)_{O₂} of 0.0032 s⁻¹, corresponding to 0.15 L air L⁻¹ min⁻¹, was not sufficient to keep the dissolved O₂ concentration at air saturation level during sunny days. At noon time, measured values of dissolved oxygen resulted in a 272% of air saturation, corresponding to 21.6 mg/L. Whether air flow rates was increase to 0.45 L L⁻¹, corresponding to U_g of 0.007, over-accumulation of dissolved oxygen was prevented.

Comparing measured and calculated values, following the equation proposed by Chisti (1989) where (K_La)_{O₂} increases potentially with power supply, good correlation resulted at low air flow rates. As the air rate increase, increasing U_g, greater difference occurred (fig.7). Others empirical correlations relating (K_La)_{O₂} to superficial gas velocity for bubble columns has been also proposed by Sierra et al. (2008) report comparable values for (K_La)_{O₂} for a flat panel reactor similar to GWP.

Comparing the measured values for GWP with that of a NHTR (*Near Horizontal Tubular Reactor*), developed at Florence University by Prof. Tredici research group (Chini Zittelli et al. 1999), it is clear how the low residence time of bubbles in GWP reactors, as for most bubble column reactors, avoids problems of oxygen oversaturation, differently to tubular reactors, where longer path and residence time can cause oxygen related damages to the cells. (K_La)_{CO₂} can be obtained from calculated values of (K_La)_{O₂} using the relationship proposed by Fair and reported by Babcock et al., (2002):

$$(K_L a)_C = (K_L a)_O \left(\frac{D_c}{D_o} \right)^{\frac{1}{2}} \quad (13)$$

where D_c and D_o represents respectively diffusivity coefficient in water of the two gasses considered (Metcalf & Eddy 2003).

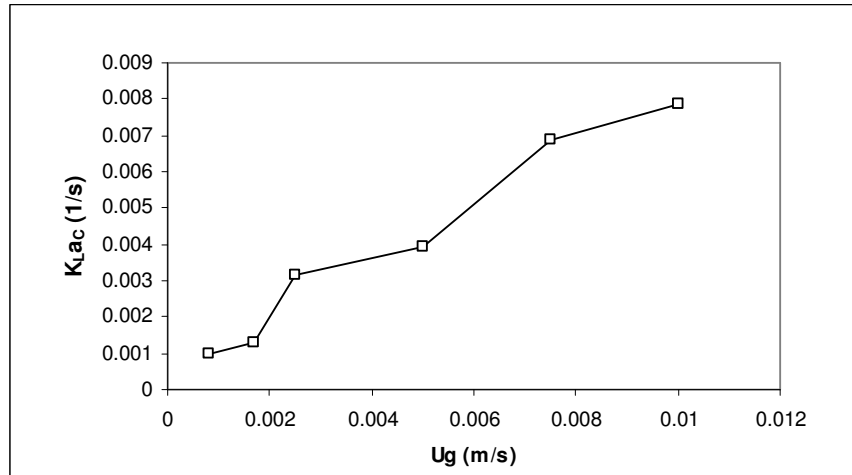


Fig.8 $(K_L a)_{CO_2}$ values calculated by means of eq. 12 for a 20 L GWP (Babcock et al . 2002)

Overall volumetric carbon dioxide mass transfer coefficient presents the same trend of $(K_L a)_{O_2}$, but with values slightly higher due to the higher molecular diffusivity coefficient of CO_2 with respect to that of O_2 .

3.3.5 Power supply

Power supply as a function of air flow rate was determined by means of equation (9), power requirement for adiabatic compression (Metcalf & Eddy, 2003). This was preferred to the more usual relation reported for bubble reactors (Chisti, 1999):

$$\frac{P_G}{V_L} = \rho_L U_g g \quad (14)$$

because able to offer more realistic values by considering the efficiency of compression machine and head losses of the sparger (perforated pipe) placed at the bottom of the reactor as function of the air flow rate.

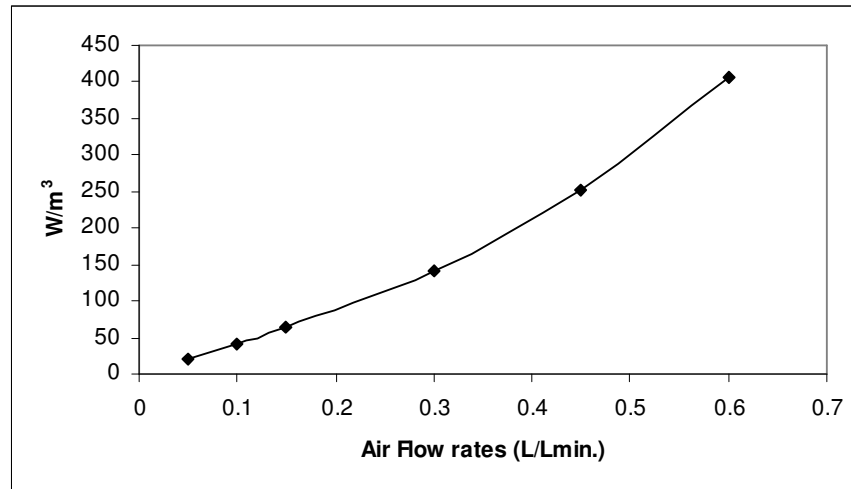


Fig.9 Influence of air flow rate on power supply ($W m^{-3}$) in GWP reactor.

Comparing the value of fig.9 with that reported by Sierra et al. (2008), where power supply for a disposable flat panel reactor is also reported, evident differences exist in terms of power consumption per m^3 of bubbled culture.

$53 W m^{-3}$ are reported by the same author to obtain a $(K_L a)_{O_2}$ of $0.006 s^{-1}$ corresponding to $0.25 L air L^{-1} min^{-1}$. Similar mass transfer capacity in GWP is obtained at $0.45 L L^{-1} min^{-1}$ corresponding to a power consumption four times higher: $250 W m^{-3}$. As previously said this difference is due to the two different equations used to calculate compression power. Similar values, of that reported by Sierra et al. (2008) for power supply, are in fact obtained if an overall efficiency of 0.98 and no friction losses in the sparger are considered for the GWP.

By considering the ratio of energy content of biomass produced ($MJ kg^{-1}$ of biomass produced) on energy expenditure for mixing, we realize that a large proportion, ranging from 16 up to 100% of caloric content of biomass ($23 MJ Kg^{-1}$, was here considered as average caloric content) is consumed only for this operation (fig.10).

In fig. 11 energy consumption per m^2 of occupied land for a *full-scale* GWP facility and reactors 1 m spaced, is reported. If this is compared with the consumption of a classical raceway ponds, $0.25 W m^{-2}$ at $20 cm s^{-1}$ (Weissman et al., 1987), it is clear as mixing in flat panels reactors, even considering the more “optimistic” values reported by Sierra et al. (2008), represents the limiting factor in the final energy balance.

For an air flow rate of $0.3 \text{ L L}^{-1}\text{min}^{-1}$, the energy consumption is equal to the energy stored into the biomass, reducing to zero the energy gain. It is so clear how pneumatically induced mixing represents a major expenditure in the management of GWP.

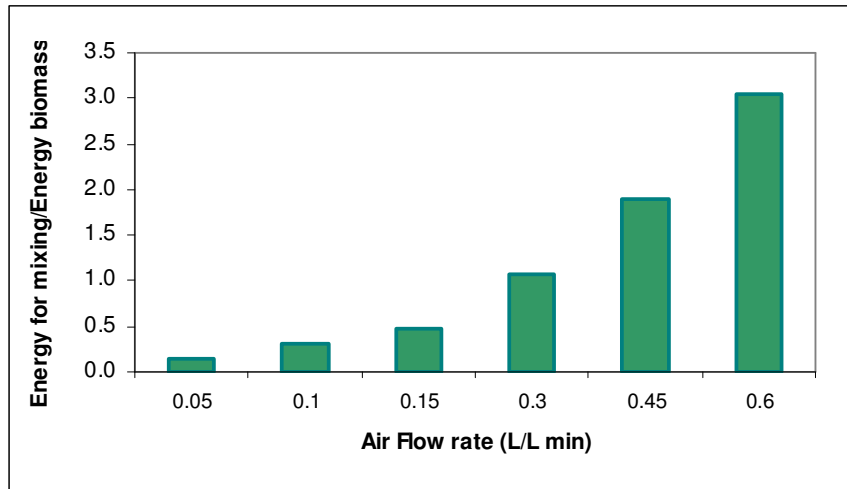


Fig. 10 Energy requirement for mixing to Energy content of biomass. An energy content of 23 MJ kg^{-1} and an average areal productivity of $20 \text{ g m}^{-2} \text{ d}^{-1}$ were considered.

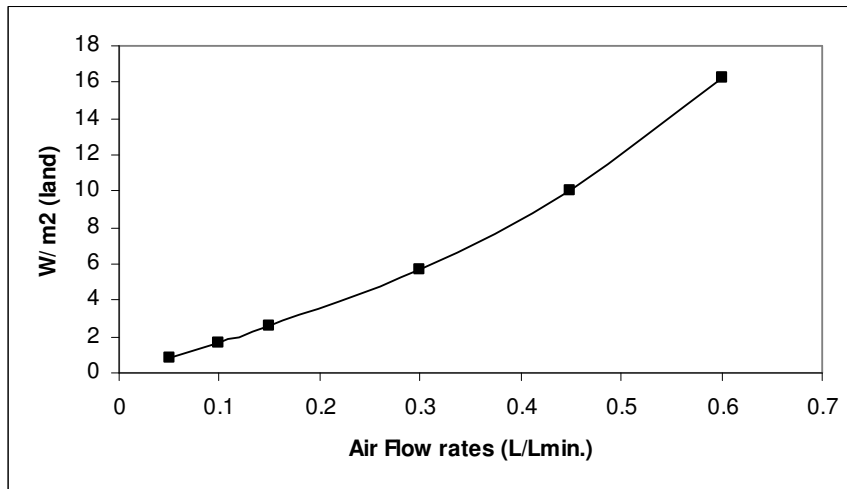


Fig.11 Power requirements (W m^{-2} of occupied area) for 1 m spaced GWP as a function of air flow rates.

3.4 Conclusions

The GWP has been characterized for its main hydrodynamic parameters. Many of the examined parameters showed a comparable trend to those found in similar reactors (Sierra et al. 2008). As we expected gas hold-up, O_2 and CO_2 overall volumetric mass transfer coefficient and mixing time showed a linear dependence with the air flow rate.

Fluid dynamic analysis showed as the GWP reactor is characterized by a modest axial dispersion ($N_d < 0.005$) even at high air flow rate $0.6 \text{ L L}^{-1} \text{ min}^{-1}$, showing a typical plug flow behaviour when a water flow of 90 L min^{-1} , was applied.

Sheare rate and microeddies length scale, calculated for the air flow rates tested, were not sufficient to cause possible stress conditions on the strains commonly cultured in this kind of reactor.

Power requirement for air bubbling resulted comparable to that of other bubble column reactors, even if slightly higher value were obtained for GWP due to a different approach in the power supply calculation. The high energy consumption associated with high mixing rates represents the limiting factor for energetic sustainable biomass production in the GWP.

3.5 Nomenclature

ε = gas hold-up (%)

P_G/V_L = energy dissipation rate per unit of volume ($W\ m^{-3}$)

d_0 = diffuser's pore diameter (m)

Re_0 = Reynold's number at the diffuser's pore.

ρ_L = medium density ($kg\ m^{-3}$)

σ = surface tension xxx

d_b = bubble diameter (m)

t_m = mixing time (s)

$t_{\Delta c}$ = average residence time (s)

$\sigma_{\Delta c}^2$ = variance of response curve "C"

$\sigma_{\theta c}^2$ = normalized variance of response curve "C" (s^2)

D_z = axial dispersion coefficient ($m^2\ s^{-1}$) (s^2)

L = reactor's length (m)

u = liquid velocity ($m\ s^{-1}$)

τ = theoretical mean residence time, V_L/Q (s)

V_L = reactor's volume

Q = liquid flow ($m^3\ s^{-1}$)

N_d = dispersion number

$(K_L a)_{O_2}$ = overall oxygen volumetric mass transfer coefficient (s^{-1})

C_t = dissolved oxygen at time t ($mg\ l^{-1}$)

C_0 = dissolved oxygen concentration at saturation ($mg\ l^{-1}$)

C_s = dissolved oxygen concentration at saturation with air ($mg\ l^{-1}$)

$(K_L a)_{CO_2}$ = overall carbon dioxide volumetric mass transfer coefficient (s^{-1})

D_c = molecular diffusivity of O_2 in water (cm^2/h)

D_o = molecular diffusivity of CO_2 in water (cm^2/h)

U_g = superficial gas velocity ($m\ s^{-1}$)

U_t = mean terminal bubble rise velocity ($m\ s^{-1}$)

INFLUENCE OF THE MIXING RATE ON THE PRODUCTIVITY OF *Nannochloropsis* *sp.* GROWN OUTDOORS IN GWP REACTORS

4.1 Introduction

Microalgae, like higher plants, are characterized by a theoretical maximum photosynthetic efficiency of 27.4% on photosynthetically active radiation (PAR) and of 12.4% if the whole solar radiation spectrum is considered. The great expectations placed upon microalgae, as highly efficient solar converters for the production of second generation bio-fuels, have raised in recent years much uncertainty about the true productive potential of these microorganisms (Tredici, 2010c).

Light represents the growth limiting “substrate” if optimal culture conditions like nutrients concentration, dissolved oxygen and carbon dioxide, pH, temperature and competitor’s control are guaranteed. Maximization of light harvesting capacity and of the efficiency with which the absorbed light is used by cells, is so the main objective in the mass cultivation of these microorganisms, because it allows to obtain maximum biomass productivity per unit of occupied land. If the maximal theoretical photosynthetic efficiencies (MPE) could be achieved in outdoor microalgae cultivation systems, the cultivation of microalgae would not have competitors in terms of biomass productivity, reaching areal productivities of hundreds of tons $\text{ha}^{-1} \text{yr}^{-1}$.

Unfortunately the maximum PE under full sunlight for outdoor microalgae mass culture rarely reaches the 12.4% but, depending on environmental and cultivation’s conditions, it is usually from 1 to 3% of the incident global radiation (Tredici, 2010c). Even under low intensity most photosynthetic microorganism intercept much more light than they are able to process. That part of the absorbed radiation not used by the photosystems is disposed as heat and fluorescence (Backer 2008).

What is the cause of the strong reduction from theoretically expected values and real outdoor efficiency ? Reflection, photorespiration, respiration, photo-saturation and photo-inhibition are the major causes of this reduction.

Reflection losses have already been dealt in Chapter 1 and depend on the geometry, arrangements and the type of material which forms the culture system used. Photorespiration can be ignored in well managed algae culture, where O_2/CO_2 ratio is low enough to prevent such kind of phenomenon. Respiration losses can not be eliminated and contribute to the loss of a substantial proportion of carbon fixed (Tredici, 2010c).

The major factors limiting solar conversion efficiency in outdoor microalgae culture are represented by photo-saturation and photo-inhibition. The P/I curve, representing the response of photosynthetically cells to light (Vonshak and Torzillo, 2004), shows that at low irradiances, the photosynthetic rate (mol. O₂/mol. phot. absorbed) linearly increases with light intensity. The rate of photosynthesis levels off at light intensities much lower than the levels found in a typical sunny day. The excess of photons absorbed by light harvesting complex can not be further used and it is wasted as heat and fluorescence (Tredici, 2010c, Vonshak and Torzillo, 2004, Janssen, 2002). If the level of light radiation further increases, beyond the level of photo-saturation, the photosynthetic process can also be inhibited and light became injurious (photoinhibition).

In order to minimize these phenomena it is useful to expose individual cells at low light levels through a process of "light dilution". Different approaches have been propose during the years (Lundquist et al., 2010, Tredici 2010c, Richmond 2004, Janssen, 2002, Tredici and Chini Zittelli, 2000).

The concentration levels at which culture systems, reactors or ponds, are usually managed do not allow homogeneous distribution of light radiation along the culture depth. Light is in fact exponentially attenuated according to Lambert-Beer's law. We are thus creating zones with different light intensities, depending on the concentration of the culture and pigment content of the biomass. Two areas can be identified: the "photic zone" and the "dark zone". The photic volume is considered that portion of the volume of the reactor where the intensity of light is sufficient to allow net photosynthetic activity (Tredici, 2010c).

High light intensity can be used efficiently by the cells if these are induced to move between the "photic zone" and the "dark zone" at high frequency. Ideally, cells should be exposed to high light intensities for short time fractions, in order to avoid photo-saturation, then moved back to the "dark zone" and kept there for a period of time 10 times greater than the time spent in the photic zone (Janssen, 2002, Molina et al., 2001).

An improvement of the efficiency of photosynthesis can so be achieved through optimization of the mixing rate inside the reactor. An increase of the air flow rate inside the reactor results in an increase in fluid velocities and L/D frequencies and therefore in a higher photosynthetic efficiency (Richmond and Wu, 2001, Richmond, 2004, Hu et al., 1996a). The same effect is achieved in mechanically stirred reactors by increasing the rotational speed of the impeller (Richmond 2004).

This increase, however, is possible only if individual cells are exposed to high levels of light intensity for a very short period of time: 1 to 100 milliseconds. This means that such a light

regime can be generated only at high liquid flows, corresponding at high superficial gas velocities in bubbled reactors. These millisecond intervals are too short for practical application in outdoor photobioreactors and above all they require, to be generated, a very large amount of energy thus leading to an increase in operating energy costs (Lundquist et al. 2010, Janssen, 2002).

High mixing rates are suitable method to dilute the incident light, but it is not energetically and economically feasible. A simpler method to dilute the light is to orient the photobioreactors vertically, instead of horizontally, or at some large angle to sunrays. This allows distribution of the available radiation on a higher surface area reducing the problems of photosaturation and photoinhibition. At this scope culture “lamination“ has been proposed as a possible solution (Wijffels and Barbosa, 2010, Tredici, 2010c). Disposing reactors in vertical arrangements, very close to each others, can be an effective way to efficiently use the available radiation and therefore maximize the productivity per unit of occupied land. But usually, the reactor unit costs more than the unit of land, represents the real limit in photobioreactor application in large scale facilities (Tredici, 2010a). This leads to an excessive investment cost, usually not compensated by the higher areal productivities eventually achieved by light lamination (Lunquist et al., 2010, Tredici, 2010a).

This problem could partly be reduced through the use of low-cost photobioreactors. Tredici et al. (2010b) have recently developed a new version of the GWP where the design of the reactor has been greatly simplified, thereby reducing costs to € 15 per meter of reactor (Tredici et al., 2010b patent: 9325 PTWO).

In order to study the power consumption for mixing, representing a consistent proportion of the energy stored into the biomass (Chapter 3), the effect of three different air flow rates (0.05-0.15-0.45 L L⁻¹ min⁻¹) on volumetric productivity of *Nannochloropsis* F&M-M24 was evaluated in vertical first generation GWPs in outdoor culture conditions at Florence (Italy) latitude. The algal strain is of particular interest for the production of oil to transform in biodiesel (Rodolfi et al., 2009). The test was carried out during three different months: February, April and October. It was also of interest to evaluate the productivity of *Nannochloropsis* F&M-M24 during the month of February, taken as representative months of winter (low temperatures and reduced photoperiod) to evaluate the possibility to extend, at least at our latitudes, the production of biomass on an annual basis.

Influence of air flow rates on volumetric productivity was also evaluated for a GWP of second generation (GWPII), patent: 9325 PTWO, during summer season.

4.2 Materials and Methods

4.2.1 Cultivation systems

The “Green Wall Panel” (GWP I - patent: WO 2004/074423):

Three 20 L GWP were used for the evaluation of the influence of mixing rate on *Nannochloropsis* F&M-M24 productivity. Modules used were 1 m high, 0.5 m long and, on average, 4 cm thick. Reactors were placed vertically in a N-S facing orientation. Compressed air was bubbled at the bottom of the reactors through a perforated (\varnothing 1 mm) plastic pipe. CO₂, used as carbon source, was injected through a small bubble gas diffuser. A control unit provided regulation of the culture’s temperature and pH by automatically activating valves. The cultures were maintained in a pH range of 7 to 7.7 by means of automatic distribution of CO₂. It was also carried out a control of the low temperatures, preventing the culture temperature to fall below 8 °C. The cultures were heated by means of electrical resistances (50 W) placed inside the reactor. High temperature, above 25 °C, were controlled by means of water spraying on the reactor’s surface.

The second generation “Green Wall Panel” (GWPII – patent: 9325 PTWO):

A new model of the “Green Wall Panel” reactor was used for the evaluation of mixing intensity on *Nannochloropsis* F&M-M24 productivity in the case of a inclined configuration. A detailed description of the reactor is given in the patent assigned to *Fotosintetica & Microbiologica* s.r.l (9325 PTWO). Reactors were, on average, 0.8 m long, 0.62 m high, 3.3 cm thick for a total culture volume of 20 L. Compressed air was bubbled at the bottom of the reactors through a perforated (\varnothing 1 mm) plastic pipe. CO₂, used as carbon source, was injected through a small bubble gas diffuser. A control unit provided regulation of the culture’s temperature and pH by activating automatic valves. Temperature control (cooling) was obtained by means of an internal heat exchanger where cold water (10 °C) was circulated.

4.2.2 Culture media and analytical procedures

The “f” medium (Guillard and Ryther, 1962) was used for the cultivation of *Nannochloropsis* F&M-M24. The medium was prepared with artificial sea water (Adriatic Sea Aquarium & Equipment, Rimini, Italy) at 30 g L⁻¹ salinity, which was filtered through 80-10-1 μ m, melt blown polypropylene cartridges (Everblue, Parma, Italy).

Culture growth was estimated by measurement of cell number, using a *Thoma* haemocytometer chamber, and dry biomass concentration. Dry weight was determined daily according to ChiniZittelli et al., (2000). Hourly and daily global and diffuse solar radiation on the horizontal surface and air temperature values were obtained from LaMMA Agrometeorological Station (CNR-IBIMET, Florence, Italy). Caloric content of biomass expressed by the Low Heating Value (LHV) of *Nannochloropsis* F&M-M24, was calculated from its average biomass composition (Rodolfi et al., 2009). A caloric content of 39 kJ g⁻¹ for lipid, 17.6 kJ g⁻¹ for carbohydrate and 23.8 kJ g⁻¹ for proteins was used (Chini Zittelli *et al.* 2006). The mean caloric content of *Nannochloropsis* F&M-M24 was used together with daily solar radiation collected by the GWP to calculate the photosynthetic efficiency (PE), g dry biomass MJ⁻¹, of the cultures.

The dissolved oxygen concentration was measured by means of an OXY 323 oxygen meter equipped with a CelloX 325 polarographic Clark-type electrode (WTW, Germany). The measurement of dissolved oxygen content was made on typical days in order to determine the time evolution of the dissolved oxygen content (% O₂ solubility in water exposed to air), depending on the degree of mixing provided.

4.2.3 Experimental plan and culture conditions

Outdoor cultivation of Nannochloropsis F&M-M24 in vertical GWPI:

The experiments were carried out during three different seasons: winter (February 13th – March 1st 2009), spring (April 21st - May 8th 2009) and autumn (October 19th - 30th 2009) at the experimental station of ISE-CNR (Istituto per lo Studio degli Ecosistemi, Sesto Fiorentino, 43° 49'N-11° 12' E). A semi-continuous daily harvesting regime was adopted. Every day a variable fraction of culture volume was withdrawn and replaced with the same volume of fresh medium. Culture's concentration for all three GWPs was at the same starting value (0.7 g L⁻¹ on average) each morning: This allowed to bring the three cultures, at least at the start, under an equal amount of photons per unit volume (μmol photons L⁻¹s⁻¹) and biomass (μmol. photons g⁻¹s⁻¹).

Outdoor cultivation of Nannochloropsis F&M-M24 in inclined GWPII:

The experiments were carried out in summer period (9-28 August 2010) at the experimental station of *Fotosintetica & Microbiologica* S.r.l. The influence of different mixing rates (0.05-0.15

and $0.45 \text{ L air L}^{-1} \text{ min.}^{-1}$) was studied in 45° tilted GWPs. A semi-continuous harvesting regime was adopted as reported above. Variable dilution was applied every morning in order to bring cultures to the same starting concentration: 0.9 g L^{-1} on average. The amount of light per unit of biomass at the start was thus the same in the three reactors.

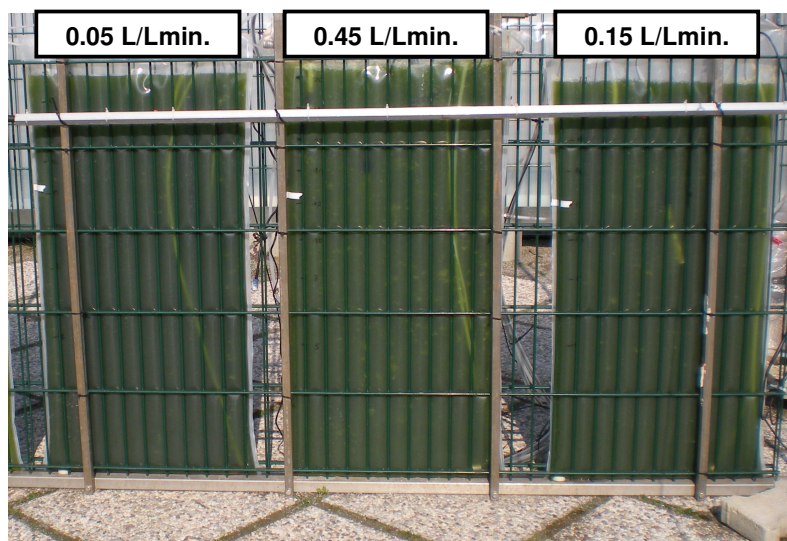


Fig.1 20 L vertical GWPI (WO 2004/074423). Reactors were North-South oriented.

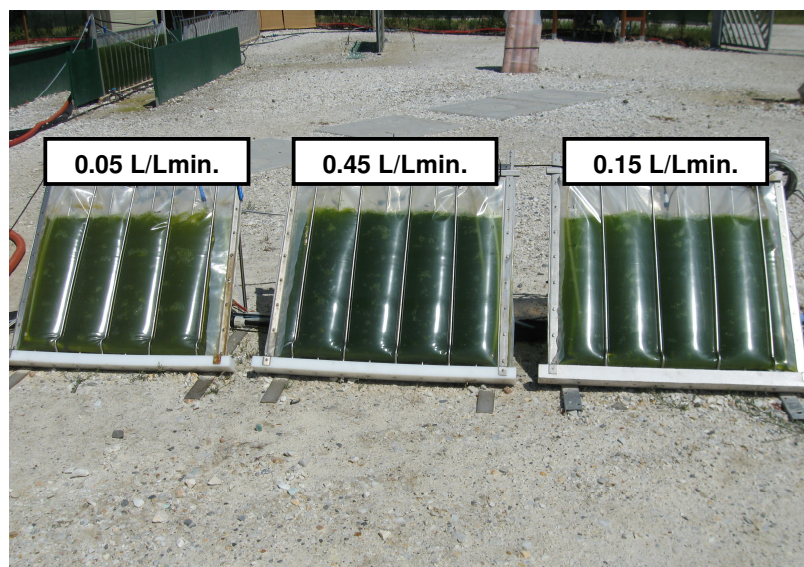


Fig.2 20 L GWPII (9325 PTWO). Reactors were 45° inclined and North-South oriented.

4.2 Results and Discussion

Already in the 50's it was clear that the increase of mixing degree (turbulence) could contribute in a positive way to increase the productivity of photosynthetic cultures (Richmond 2004). It was also clear that this effect was related to the creation of a more favorable light regime inside the reactors. As a general principle the higher the intensity of the light source, in this case the solar radiation impinging on to reactor surface, the higher becomes the optimal population density (OPD) and the greater will be the effect that mixing has on productivity. This was well elucidated by Hu & Richmond (1996a) who investigated the photosynthetic efficiency of *Spirulina* cultures as function of light intensity, mixing degree and culture concentration.

Tab.1 shows the average productivity obtained from the three tests carried out in the different seasons for vertical GWP.

Taking in account the average volumetric productivities of the period examined we should conclude that the higher mixing rates lead to a small increase in the average volumetric productivity (tab.1) and that air flow rates above $0.15 \text{ L L}^{-1} \text{ min.}^{-1}$ are just a waste of energy no leading to any further increase in productivity.

Tab. 1 Average volumetric productivity ($\text{g L}^{-1} \text{d}^{-1}$) for different mixing rates in three 20 L vertical GWP (WO 2004/074423). Reactor were N-S oriented and a semi-continues dilution regime was adopted.

	Air Flow Rate ($\text{L L}^{-1} \text{min.}^{-1}$)		
	0.45	0.15	0.05
February (n.16)	0.172±0.09	0.178±0.08	0.128±0.1
March (n.17)	0.182±0.07	0.171±0.09	0.145±0.08
October (n.10)	0.16±0.072	0.16±0.052	0.17±0.057
Average	0.171±0.018	0.169±0.014	0.147±0.014

However analyzing the data obtained in more detail and not considering the average values of productivity, but productivity as a function of intercepted radiation ($\text{MJ m}^{-2} \text{ reactor day}^{-1}$) for the three different levels of mixing applied, it is evident that increasing turbulence increases

volumetric productivity when high level of radiation are intercepted (fig. 4, 5 and 6). In other words the effect of high flow rates is evident when higher levels of solar radiation are available. This could be explained by the fact that increasing the air flow bubbled inside the reactor results in an increase in fluid velocities and L/D frequency and therefore higher photosynthetic efficiency (Richmond and Zhang, 2001, Richmond, 2004, Hu et al., 1996). Higher PE together with higher solar radiation available is translated in higher productivities.

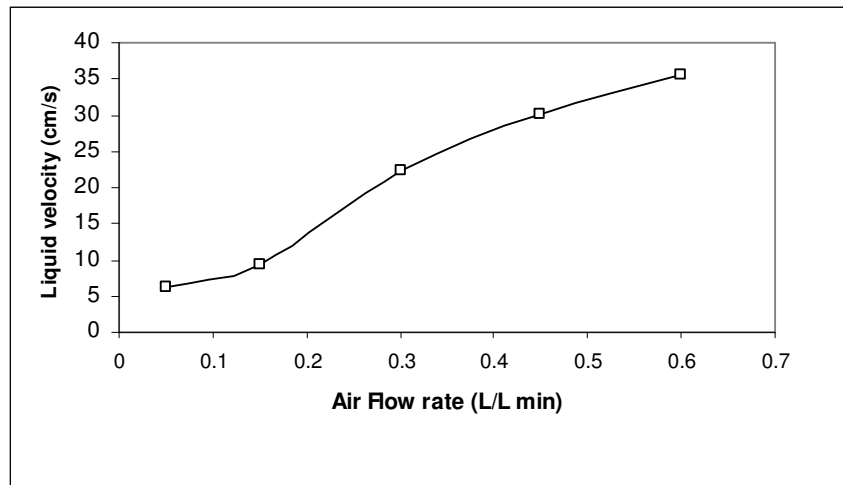


Fig. 3 Liquid velocity as function of the air flow rate in 20 L GWP. Velocity profile was measured as the rate of dispersion on a dye inside the reactor.

It's also true, as reported by Richmond (2004), that the effect of mixing on productivity much depends on the type of strain used. *Nannochloropsis* F&M-M24, unlike filamentous algae like *Arthrospira*, shows a much smaller effect of mixing on productivity due to its small dimension. This could have mitigated the increase in productivity when the airflow was increased from 0.15 to 0.45 L L⁻¹min⁻¹.

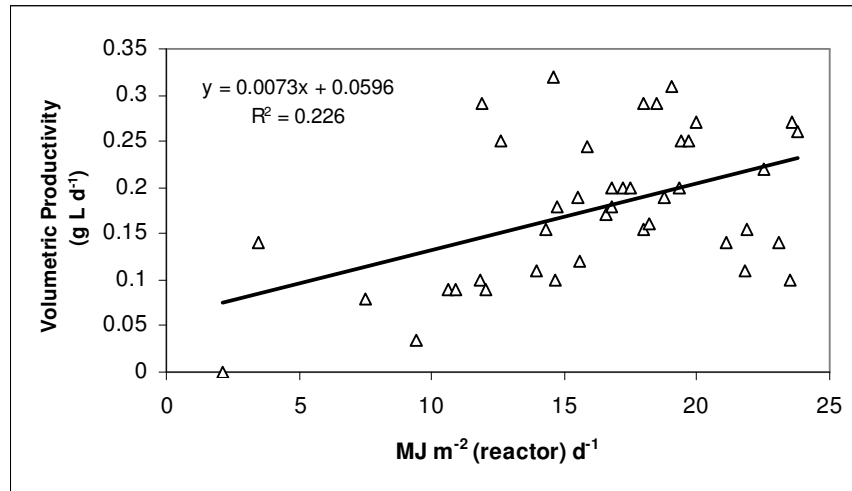


Fig.4 Volumetric productivity as a function of solar radiation intercepted in a vertical GWP.
Air flow rate: 0.45 LL⁻¹min.⁻¹

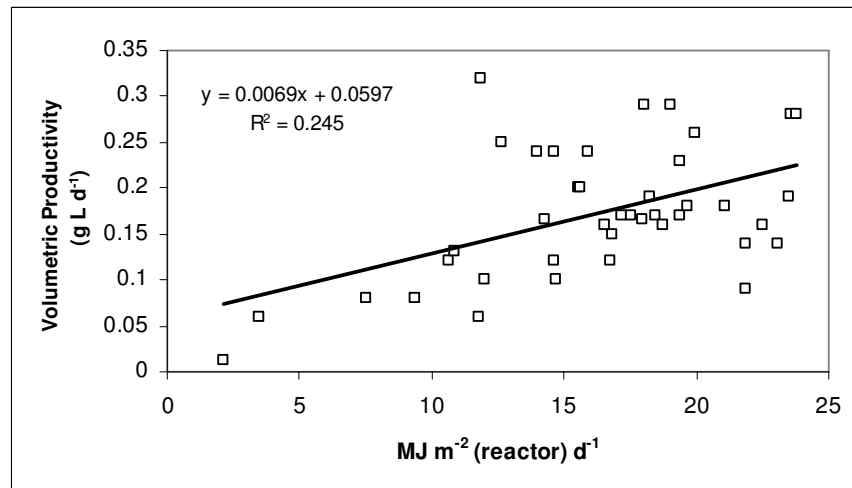


Fig.5 Volumetric productivity as a function of solar radiation intercepted in a vertical GWP.
Air flow rate: 0.15 LL⁻¹min.⁻¹

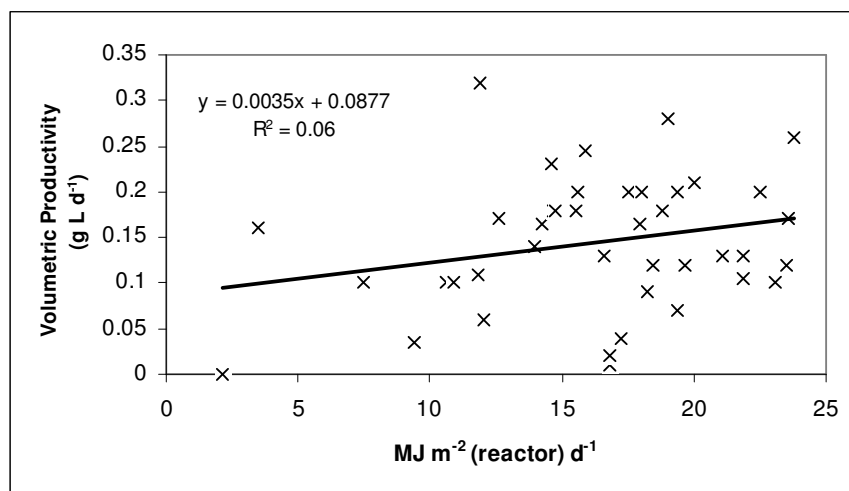


Fig.6 Volumetric productivity as a function of solar radiation intercepted in a vertical GWP.
Air flow rate: $0.05 \text{ LL}^{-1} \text{ min}^{-1}$

Tab.2 shows the average volumetric productivity obtained at the three different air flow rates for different levels of radiation intercepted. At low and medium irradiance levels (0-8 and 6-16 $\text{MJ m}^{-2} \text{ reactor d}^{-1}$) there were no significant differences between the volumetric productivities of the three reactors. While for radiation levels above $16 \text{ MJ m}^{-2} \text{ day}^{-1}$, culture subjected to the highest level of mixing ($0.45 \text{ L L}^{-1} \text{ min}^{-1}$.) provided the highest volumetric productivity. At $0.45 \text{ L L}^{-1} \text{ min}^{-1}$ productivity was increased by 10% and 45% if compared to reactors bubbled with 0.15 and $0.05 \text{ L L}^{-1} \text{ min}^{-1}$. This confirms the positive effect of mixing rate on the productivity of algal cultures. Of course, this effect is significant only if other conditions such as culture's concentration are optimized, in fact, for low concentrations, that means the culture is homogeneously illuminated, an increase in mixing rate does not lead to any positive effect on productivity (Richmond 2004).

Tab. 2 Influence of different air flow rates and solar radiation on average volumetric productivity ($g L^{-1}d^{-1}$) in *Nannochloropsis* F&M-M24 cultured in isolated N-S facing GWPs (1 m x 1 m).

Solar radiation range (MJ m ⁻² day ⁻¹)	Air Flow rate		
	0.45 L L ⁻¹ min ⁻¹	0.15 L L ⁻¹ min ⁻¹	0.05 L L ⁻¹ min ⁻¹
0-8	0.073±0.07	0.051±0.034	0.087±0.081
8-16	0.159±0.06	0.171±0.077	0.161±0.074
16-24	0.205±0.085	0.188±0.056	0.141±0.071

The effect of different levels of turbulence on the volumetric productivity of *Nannochloropsis* F&M-M24 was also tested in 45° tilted second generation “Green Wall Panels” (GWPII). The test was carried out during the summer. Inclined reactors permit to intercept a greater amount of solar radiation respect to vertical ones: 22.18 MJ m⁻² reactor day⁻¹ on average for the period of experimentation considered. The test confirmed the results obtained with the vertical reactors (fig.6). Culture subjected to the highest mixing rate (0.45 L L⁻¹min⁻¹.) increased volumetric productivity from 62 to 86% if compared to reactors where the air flow rate was reduced (0.15 and 0.05 L L⁻¹min), but only at high levels of irradiance (> 16 MJ m⁻²day⁻¹) a stimulating effect of mixing on volumetric productivity of *Nannochloropsis* F&M-M24 exists.

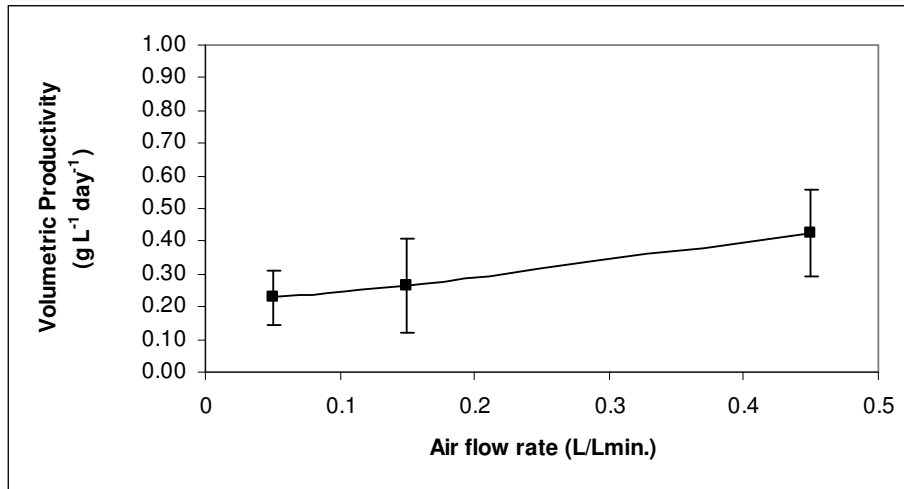


Fig. 7 Evolution of productivity as a function of different air flow rates in a 45° tilted GWPII (9325 PTWO). Average solar irradiance intercepted 22.18 MJ m⁻² reactor day⁻¹.

It is however difficult to establish with certainty whether the increase in productivity measured at high levels of radiation is due to an improved light regime (short L-D cycles) related to increased turbulence or to a combination of factors. High air flow rates reduce dissolved O₂ thanks to an increased O₂ outgassing. This avoids high levels of dissolved oxygen that could reduce the efficiency of solar radiation's conversion into biomass, increasing losses due to photorespiration (Tredici, 2010c). Dissolved oxygen concentrations reached, in fact, 250% of air saturation in 0.05 and 0.15 L L⁻¹ min⁻¹ bubbled GWPs with respect to 132% in 0.45 bubbled reactor (fig.8).

As seen in the chapter devoted to the hydrodynamic characterization of the GWP the power energy for air bubbling represents a high percentage of the energy stored in the biomass produced. For an air flow rate of 0.3 L L⁻¹ min⁻¹, the energy consumption is equal to the energy stored into the biomass, reducing to zero the energy gain. It is so clear how pneumatically induced mixing represents a major expenditure in the management of GWP.

As we observed that a reduction of three times in the air flow, from 0.45 to 0.15 L L⁻¹ min⁻¹, does not negatively affect the average volumetric productivity of *Nannochloropsis* F&M-M24 when solar irradiance is lower than 16 MJ m⁻² reactor d⁻¹, this means that in autumn-winter or on cloudy days, we can reduce the mixing degree inside the GWP saving more than 70% of energy consumed, improving the final energy balance of the system.

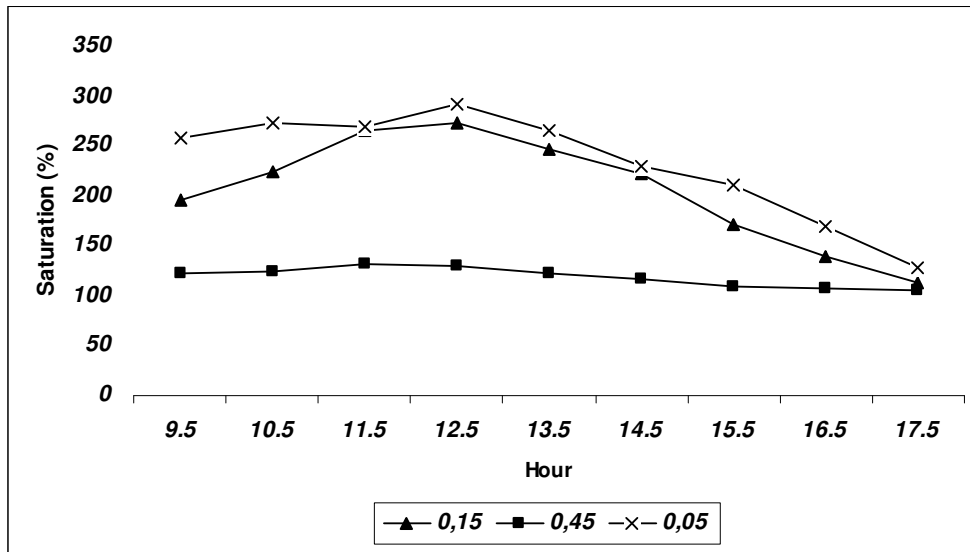


Fig. 8 Diurnal variation of dissolved oxygen in *Nannochloropsis* F&M-M24 cultures growth in isolated vertical GWPI at three different air flow rates. Values measured in a typical sunny day: $19 \text{ MJ m}^{-2} \text{ reactor day}$ (January 28th 2010).

ECONOMIC AND ENERGETIC ASSESMENT OF MICROALGAE BIOMASS PRODUCTION IN THE DISPOSANEL “GREEN WALL PANEL” REACTOR

5.1 Introduction

Microalgae dominate the bodies of both fresh and salty waters. Together with macroalgae and cyanobacteria, microalgae are responsible for 50-60% of primary production on land. The cultivation of microalgae biomass is not new; their cultivation was seen in the 1940 as a possible solution to meet the increasing demand of protein sources for human nutrition (Burlew, 1953). Nowadays, microalgae are cultivated for the production of many commercially important products including: bio-pesticides and agricultural fertilizers, food supplements, cosmetics, dyes, preservatives, antioxidants, probiotics, and are extensively used in aquaculture (Pulz et al., 2004, Tredici et al., 2009). The annual production of algal biomass in the world, mainly for human and animal nutrition, is estimated between 8,000 and 10,000 tons, 90% of which is made in open culture systems (Leher and Posten, 2009). However, they can also cause serious environmental and public health problems like eutrophication, mucilage and toxic blooms.

In recent years the interest in these photosynthetic microorganisms has exploded, especially in the field of renewable energy. The main reasons for such recognition, after years of relative disregard, are that microalgae are considered far more productive than traditional crops used for the production of first generation bio-fuels (sunflower, sugarcane, rapeseed, oil palm etc.) and by the fact that some strains can accumulate up to 60% of lipids, mainly triglycerides (TAG), the fraction suitable for the production of biodiesel after trans-esterification (Williams and Laurens, 2010, Rodolfi et., al 2009, Borowitzka, 1988). The enormous expectations placed upon microalgae generated uncertainty about the true productive potential of these microorganisms. Their real potential has been often overestimated, because they are considered to possess higher photosynthetic efficiencies than traditional land crops (Tredici, 2010c).

On the other hand, we should recognize that the reasons behind the interest in microalgae as a source of *second generation* bio-fuels are also supported by facts. Compared with crops used for the production of *first generation* bio-diesel (soybean, sunflower, rapeseed, oil palm) these microorganisms achieve much higher lipid productivities. For example, one hectare of sunflower or rapeseed can attain 700-1000 kg of oil per year, while a well managed algal culture

in regions characterized by a high and constant availability of solar radiation along the year and stable climate conditions, is able to provide well over 15 tons of lipid per hectare per year (Rodolfi et al., 2009). What makes this biomass extremely interesting and competitive with traditional oil crops is the fact that algal cultures do not compete for fertile soils, they require no pesticides and can be made on seawater or on agricultural, industrial or domestic wastewaters. Besides, algal cultures consume large amounts of CO₂ (about two kilograms of CO₂ per kg of algal biomass produced) and can be efficiently grown using the flue gas of power plant stations (Kadam, 2001).

Despite the high interest generated by these microorganisms in recent years, to date there is no commercial companies that produce significant quantities of bio-fuels from algae (Lardon et al., 2009).

Despite the advantages in the use of bio-fuels, it is not yet clear what could be their real impact on the environment. The production of algal biomass, as well as the cultivation of all other energy crops, requires inputs such as electricity, fertilizer, water and many raw materials. Which means a more or less direct consumption of energy and water and a release of substances with a potential pollution impact (CO₂, NO_x, SO_x etc.). It is therefore important to quantify the possible environmental benefit and energy consumption associated with the production and usage of any bio-fuel. Life-Cycle Assessment (LCA) is used as an objective method for the evaluation of the energy and environmental impacts associated with a product, process or activity from the production of raw materials to the disposal of waste and products at the “end of life” (Stephenson et al., 2010). Among the tools created for the analysis of industrial systems the LCA has assumed a prominent role and is rapidly expanding. Energy assessments of first generation bio-fuels have been carried out during the last years, showing as in some cases that the negative environmental impacts associated with them are greater than the benefits obtained from their production and use (Clarens et al., 2009).

LCA is not simple to perform, requiring a detailed inventory of all materials and energy fluxes characterizing the examined process and an evaluation of their environmental footprint. Target of our work was so shifted to identify those limitations that currently represent the main obstacles to an energetic sustainable microalgae production facility. We limited our analysis to the evaluation of the Net Energy Ratio (NER) for the production of 1 kg of *Nannochloropsis* F&M-M24 biomass, produced in a virtual commercial plant, of one hectare, where the system of cultivation employed is the “Green Wall Panel” (GWP-WO 2004/074423).

Net Energy Ratio is commonly used as a monetary-independent index to evaluate the efficiency of any energy generation process, and represents “*the ratio of the total energy production to the primary non-renewable energy requirements associated with the system life cycle*” (Burgess and Fernandez-Velasco, 2007).

Two possible different scenarios are here considered: the production of biomass under nutrient sufficient conditions (*base case*) and the production of biomass rich in lipids according to a “*two-phase*” strategy proposed by Rodolfi et al., (2009).

In addition to the evaluation of the energy balance we have also carried out an economic assessment to evaluate the production cost of 1 kg of *Nannochloropsis* F&M-M24 biomass, under the same scenarios mentioned above.

The assessments, both energetic and economic, relied on the availability of data acquired through the experience gained over the last five years by the research group of Prof. Tredici on the GWP reactor and on the existing data in the literature for similar analysis (Benemann & Oswald, 1996; Weissmann & Goebel, 1987, Lundquist et al., 2010, Stephenson et al., 2010, Lardon et al., 2010, Clarence et al., 2010). Although most of the existing literature data refer to open systems like raceway ponds, these have been adapted to our specific case and can be safely used in an analysis that involves the use of different systems. Finally, some of the data used come from suppliers contacted directly by the authors.

5.2 Materials and Methods

Evaluation of all energy inputs, represented by the embodied energy of materials employed and by the operational energy consumed annually by the plant, is a complex work requiring a detailed design in order to include all materials, components and utilities necessary for the ordinary operations. At present not many works have evaluated the energy balance of a commercial scale microalgae plant and in the most of the cases extrapolation from laboratory or small pilot scale plants were the routine (Lardon et al., 2009). In the following paragraphs criteria adopted for the plant design will be explained and a plant’s description will be made.

5.2.1 System boundaries and the functional unit

The comparison of different systems, process or products can be achieved if they perform the same function (Kadam, 2001). So it is first necessary to define a *function unit* in order to compare different systems on the same quantitative basis.

The *functional unit* is here represented by the kilogram (dry weight) of wet biomass (not dried) produced in one hectare GWP plant.

5.2.2 The Net Energy Ratio

The net energy ratio (NER) of a system represents “*the ratio of the total energy production to the primary non-renewable energy requirements associated with the system life cycle*” (Burgess and Fernandez-Velasco, 2007) and is given by eq. 1:

$$NER = \sum \frac{OutputEnergy}{InputEnergy} \quad (1)$$

5.2.3 Input energies

The overall energy input considered was the sum of the *Embodied Energy* (E.E), MJ kg⁻¹, of all materials and components employed (reactors, fertilizers, pumps, pipes, centrifuges, blowers, constructions etc.) and the electrical energy required for all daily operations (medium supply, harvesting, mixing, CO₂ supply, cooling and biomass concentration.). Drying was not considered.

The Embodied Energy (E.E):

E.E is defined as “*the total primary energy consumed during the whole life time of the product*” (Hammond and Johns, 2006). The embodied energy values change according to the boundaries conditions defined for each material. Values used in this work were collected from the existing literature and refers to “Cradle to Gate” or “Cradle to Site” boundary conditions. For materials with high E.E and high density, the difference between the two boundaries condition is negligible (Hammond and Jones, 2006).

The caloric value of organic feedstock like timber, if present, has been also considered, because it represents a real use of energy (Boustead, 2005).

For machinery (blowers, pumps and centrifuges) beside the E.E associated with the machine itself, the Total Accumulated Repair (TAR) energy was also determined. The latter was calculated as a percentage (15%) of the E.E (Doering, 1980).

Operative electrical energy:

Auxiliary energy, representing the total electricity supplied and used by the plant for daily operations and expressed as $\text{MJ ha}^{-1}\text{y}^{-1}$, has been directly quantified by determining the power supply and the working hours necessary for all daily operations (water, nutrients and CO_2 supply, mixing, cooling, harvesting and biomass concentration.). An overall efficiency of 70% was assumed for all electrical machines.

For a detailed explanation of the procedures adopted for piping dimension and power supply calculation see Appendix I and II.

A productive season of 360 days was considered. Cooling was considered to be necessary for 8 hours per day for 5 months per year.

Nutrients:

The total amount of nutrients required ($\text{Kg ha}^{-1} \text{yr}^{-1}$) was calculated from the total annual biomass production assuming the relative content of nutrients into the biomass as reported by Grobbelar (2004). Their energy contribution to the overall energy input was evaluated from the annual consumption of N, P and K multiplied by the average energy cost (MJ kg^{-1}) to produce one kg of that element (Riello, 2006).

5.2.4 Output Energy

The output energy considered was the mean caloric content (23 MJ Kg^{-1}) of the biomass of *Nannochloropsis* F&M M-24. It was calculated from its biochemical composition assuming the values reported by Chini Zittelli et al., (2004). In the “two phase “ strategy lipid content increased to 60% after 3 days of nitrogen starvation and the average caloric content of 1 kg of dry biomass increased from 23 to 27.7 MJ kg^{-1} (Rodolfi et al., 2009).

5.2.5 Life Span

Life span data, the period during which the material-component is functional, were collected from the existing literature (Burgess and Fernandez-Velasco 2007) and adjusted considering the specific operative and environmental conditions of the plant. For all those materials where references were not available, lifespan values were gathered by personal communications from producers.

5.2.6 Data source

In energy or economic analyses, like those here proposed, different type of data sources can be used: primary and secondary (Kadam, 2001). Here both of them have been used. Primary data come directly from production plants, suppliers and companies directly contacted. Primary data have been used for the harvesting-concentration step (centrifuges and sedimentation pond's costs), GWP reactor's materials, HDPE pipes, pumps and blowers; especially in the economic assessment.

Secondary data, instead, are all the published sources such publications, journals, books and database. Secondary data have been used primarily to determine the energy cost of materials (E.E) and for some items during the economic analysis such as the costs for site preparation, the cost of CO₂ and nutrients (Benemann & Oswald, 1996; Weissmann & Goebel, 1987, Ben Amotz, 2007, Lundquist et al., 2010, Pimentel, 1980.; Hammond and Jones, 2006.; Burgess and Fernandez-Velasco, 2007).

In order to reduce the variability of the existing data values only one reference for E.E was considered: ICE V1.6a database (Hammond and Jones, 2006).

5.3 Cultivation System's Description

5.3.1 Base case

The reactor used in the analysis the first generation "Green Wall Panels" (GWP- patent: WO 2004/074423), a vertical disposable flat panel reactor (Tredici & Rodolfi, 2004). For the present analysis a 50 m long, 1 m high and 0.04 m thick GWP was considered. The volume of each panel was therefore equal to 2 m³, corresponding to 40 L m⁻² of reactor. Reactors were arranged in parallel rows spaced of 1 m and E-W oriented in order to maximize solar radiation capture on annual basis (see Chapter 2). The entire system consists of 8 modules, each made up of 25 panels 50 m long. Each panel therefore occupies an area of 50 m² and each module covers an area of 1.250 m².

A continuous daily dilution of the culture was here considered. Daily, 33% of the volume of each module (16.5 m³ mod⁻¹ d⁻¹) is collected and *fresh* medium (sea water + nutrients) replenished. The chosen value of dilution ensures a volumetric productivity of about 0.35 g L⁻¹ d⁻¹ with *Nannochloropsis* F&M-M24 in outdoor culture condition (Rodolfi et al., 2009). We considered a 100% nutrient up-take efficiency, so that the clarified medium obtained from harvesting and culture concentration is completely devoid of nutrients and disposed as waste. This is possible if nutrients are dosed daily according to the daily production of biomass.

Seawater for daily dilution is directly pumped from the sea by means of a submersible pump and distributed by an HDPE pipeline (PE 80 Ø 50 mm) to the individual modules. We assumed that the plant is placed next to the sea shore.

Water losses by evaporation have been determined from field experience and evaluated in the order of 3 mm, equivalent to $1.2 \text{ m}^3 \text{ ha}^{-1} \text{ d}^{-1}$. Water lost by evaporation is replenished by sea water. This leads to a slightly increase of medium salinity from 30‰ to 30.3‰ at the equilibrium. The salinity value will be reached at equilibrium, S_E , is function of dilution rate (D) adopted and the level of evaporation (E_v), according to the equation (2) (Tredici et al., 1987):

$$S_E = S \left(1 + \frac{E_v}{D} \right) \quad (2)$$

The evaporated water is replenished through the same line used for daily dilution.

Flue gas with a content of CO_2 of 12.5% vol. would be used as the carbon source (Kadam 2001). We assumed that only 10% of CO_2 in the flue gas will be transferred to the culture. This value might seem too low, but is reasonable if one considers that efficiency values just above 20% were obtained with pure CO_2 and small bubble diffuser in GWP reactors (personal data). The same blowers used for air bubbling are also used for the flue-gas delivery to the GWPs. The 1 ha facility is assumed to be next to the flue-gas generator (anaerobic digester or coal power plant). The auxiliary energy for CO_2 pumping was estimated in $22.2 \text{ kWh ton}^{-1} \text{ CO}_2$ (Kadam, 2001).

Mixing, necessary to avoid culture sedimentation and to ensure a desired L-D cycle and gas-liquid mass transfer, is provided by means of blowers. Different air flow rates are employed for daytime and night. During the night, in fact, no photosynthetic activity occurs and air flow rate can so be much reduced, reducing the energy consumption. An air flow rate of $0.15 \text{ L L}^{-1} \text{ min}^{-1}$ is applied for 12 daylight hours and $0.05 \text{ L L}^{-1} \text{ min}^{-1}$ for the remaining period. Results obtained in outdoor experimentation, show that reducing the air flow rate (from 0.45 to $0.15 \text{ L L}^{-1} \text{ min}^{-1}$.) no significant differences in the average volumetric productivity occurred with *Nannochloropsis* F&M-M24 at low irradiance (see Chapter 4). This was translated in a 70% energy saving and so in a better energetic performance of the reactor. Power consumption during the day was 2.54 W m^{-2} of occupied land and was reduced to 0.81 W m^{-2} during the night.

Every day $132 \text{ m}^3 \text{ ha}^{-1}$ of culture, with an average concentration of 1.06 g L^{-1} , will be harvested. This concentration is more than reasonable considering a dilution rate of 33% and with an average solar irradiance of $20 \text{ MJ m}^{-2} \text{ d}^{-1}$ on the horizontal as annual average value. Culture is continuously (10 hours) harvested by means of two centrifugal pumps (0.5 kW) to the harvesting station and is then concentrated (100x) by means of one disk-stack clarifier (model: MACFUGE 710 CHPT C5) with an hydraulic capacity of $22 \text{ m}^3 \text{ h}^{-1}$. For high harvesting efficiency (< 10% of harvested cultures lost into the out flow) an operative flow rate of $13.2 \text{ m}^3 \text{ h}^{-1}$ is necessary. Electrical consumption for centrifugation was estimated in 1 kWh m^{-3} . Cooling is done through the use of heat exchanger inserted inside the GWPs. It is assumed to cool the reactor through the use of sea water at 18° C which is pumped ($460 \text{ m}^3 \text{ h}^{-1}$) directly from the sea. A 26 kW submersible pump is used. Cooling will be necessary for 8 hours a day per 5 months. Fresh medium is continuously supplied by means of two 0.5 kW centrifugal pumps, working 10 hours day.

5.3.2 Nitrogen starvation: the “two phase” strategy

In the previous section we described one of the many possible scenarios. Compared to the base case, there are alternative scenarios that in part modify the cultivation system described above. We have evaluated also the NER and the production cost of one alternative scenario, where nitrogen starvation is used to increase lipid synthesis by means of a “two-phase” strategy. The “two-phase” strategy was successfully experimented with *Nannochloropsis* F&M-M-24 (Rodolfi et al., 2009) in a outdoor GWP pilot plant. The strain was able to respond to nitrogen deficiency with a significant increase of lipid synthesis. A lipid productivity of $90 \text{ Kg ha}^{-1} \text{ d}^{-1}$ (10 and $80 \text{ Kg ha}^{-1} \text{ d}^{-1}$ for the first and the second phase respectively) was attained employing the former strategy. The lipid accumulation phase takes 3 days. On the morning of 4th day the culture is harvested from four of the eight modules making up the plant (see fig.3). Unlike the base case, a continuous daily dilution of 50% vol. ($20 \text{ m}^3 \text{ h}^{-1}$) is applied. This does not cause however any changes to the base case plant design, especially in pipes dimension. The culture is diluted with only seawater during the three days of starvation. During the starvation period no nutrients are applied. Nutrients will be used only for 12.5% of the 10.000 m^2 plant, corresponding to 1 of the 8 modules made of 25 GWP (fig.3). Here the inoculum that will be transferred to the next phase of starvation is daily produced.

A two steps harvesting procedure, similar to that reported by Stephenson et al., (2010), is here adopted. Culture is first flocculated through the use of aluminum sulphate flocculant and the concentrated slurry will be sent to a sedimentation pond. This allows to concentrate the harvested culture of a factor of 25, reducing the volume of culture to be processed by centrifugation. The energy cost for the flocculation, using a paddle mixer, was estimated in 4.85 Wh m^{-3} of treated culture and calculated following the procedure described by Metcalf & Eddy (2003). Flocculation is then followed by a sedimentation in a circular settling pond as described by Stephenson et al., (2010), where a power supply of 0.8 W m^{-2} of sedimentation was considered.

The reactor's cooling is carried out as described for the base case (see above). Mixing and flue-gas delivery procedures are the same described above for the base case. The amount of CO_2 consumed annually, however, is different due to different productivity considered for the *base case* and for the *two phase strategy*. Considering both the amount of biomass produced in the first phase ($6.3 \text{ ton ha}^{-1} \text{ yr}^{-1}$) and for the starvation phase ($38 \text{ ton ha}^{-1} \text{ yr}^{-1}$) the amount of CO_2 delivered (overall efficiency 10%) is equal to $797 \text{ ton ha}^{-1} \text{ yr}^{-1}$ (tab.2).

Tab.1 Design parameters for the “Green Wall Panel” reactor

GWP Parameters	Unit	Value
<i>Height</i>	m	1
<i>Length</i>	m	50
<i>Thickness</i>	m	0.04
<i>Volume</i>	L m^{-1}	40
<i>Distance between rows</i>	m	1
<i>Orientation</i>	E-W	E-W
<i>Meters of GWP in 1 ha</i>	m	10,000

Tab.2 Design parameters for the 1 ha facility. Base case and nitrogen starvation in the “two phase” strategy.

Facility Parameters	Unit	Base Case	Two phase strategy
<i>Facility size</i>	m ²	10,000	10,000
<i>Module size</i>	m ²	1,250	1,250
<i>Number of modules</i>	n.	8	8
<i>Number GWP per module</i>	n.	25	25
<i>Facility Volume</i>	m ³	400	400
<i>Module Volume</i>	m ³	50	50
<i>Daily dilution</i>	%	33	50
<i>CO₂ content in Flue-Gas</i>	%	12.5	12.5
<i>Total CO₂ supplied</i>	Ton yr ⁻¹	907	797
<i>Electricity</i> ³	kWh ton. CO ₂	22.2	22.2
Operating Parameters			
<i>Operating period</i>	Day	360	360
<i>Average solar radiation (horizontal)</i>	MJ m ⁻² d ⁻¹	20	20
<i>Concentration factor: centrifuges</i>	-	100	8
<i>Concentration factor: Flocc.- Sedimentation</i>	-	-	25
<i>Concentration at harvest</i>	(g L ⁻¹)	1.06	0.5
<i>Concentration after Flocculation-sedimentation</i>	(g L ⁻¹)	-	12.5
<i>Harvest efficiency</i>	%	90	90
<i>CO₂ solubilization efficiency</i>	%	10	10

³ Kadam 2001.

Tab.3 Biomass composition and culture parameters for *Nannochloropsis F&M-M24*. *Rodolfi et al. 2009. **Reboloso-Fuentes et al., 2001. ***Grobbelar (2004).

Parameter	Unit	Base Case	Two phase strategy
Productivity **	(g m ⁻² d ⁻¹)	14	-
Productivity first phase	(g m ⁻² d ⁻¹)	-	14
Productivity second phase	(g m ⁻² d ⁻¹)	-	12
Average caloric content	(MJ kg ⁻¹)	23	27.7
Lipid *	(g kg ⁻¹)	300	600
Protein **	(g kg ⁻¹)	288	Nd
Carbohydrates **	(g kg ⁻¹)	270	Nd
Ash **	(g kg ⁻¹)	94	Nd
Fiber **	(g kg ⁻¹)	2.41	Nd
RNA/DNA **	(g kg ⁻¹)	2.35	Nd
C ***	(% dw)	50	Nd
N ***	(% dw)	7	Nd
P ***	(% dw)	1	Nd
K ***	(% dw)	0.5	Nd

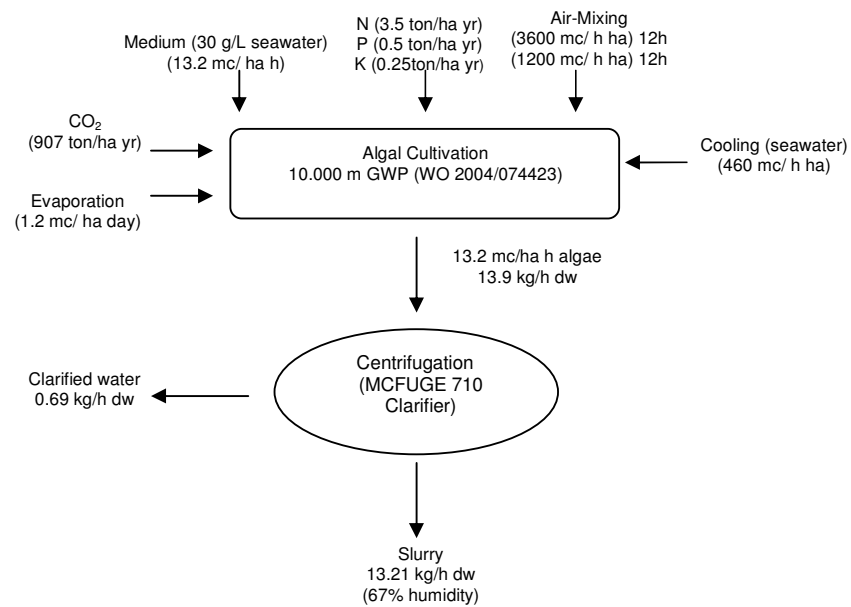


Fig. 1 Base case: Process chain and mass flows for the production of *Nannochloropsis F&M-M24* biomass in a 1 ha facility.

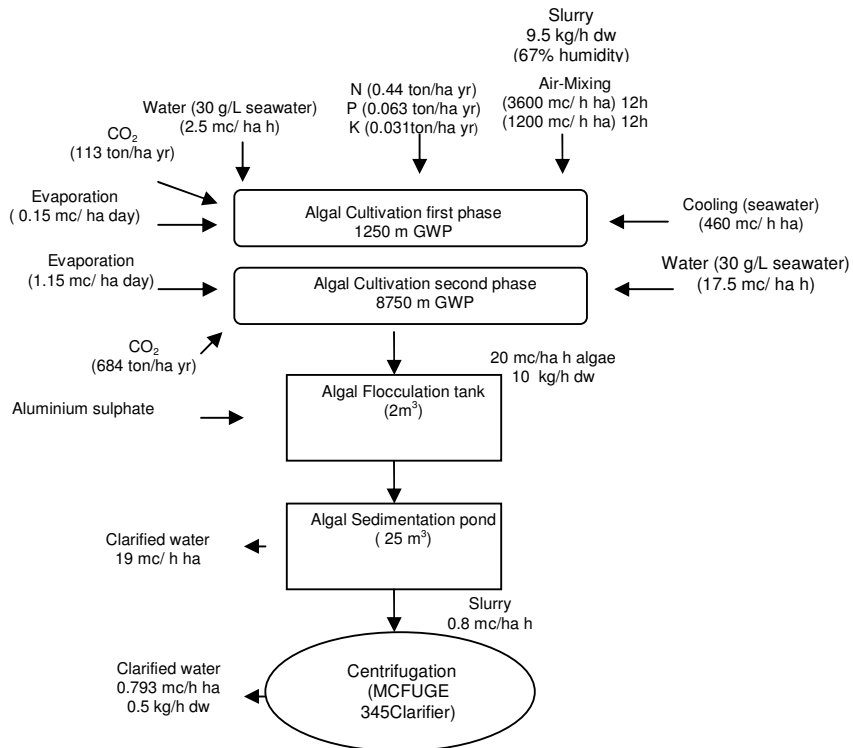


Fig. 2 Nitrogen starvation through the “two phase “ strategy: Process chain and mass flows for the production of *Nannochloropsis F&M-M24* biomass in a 1 ha facility

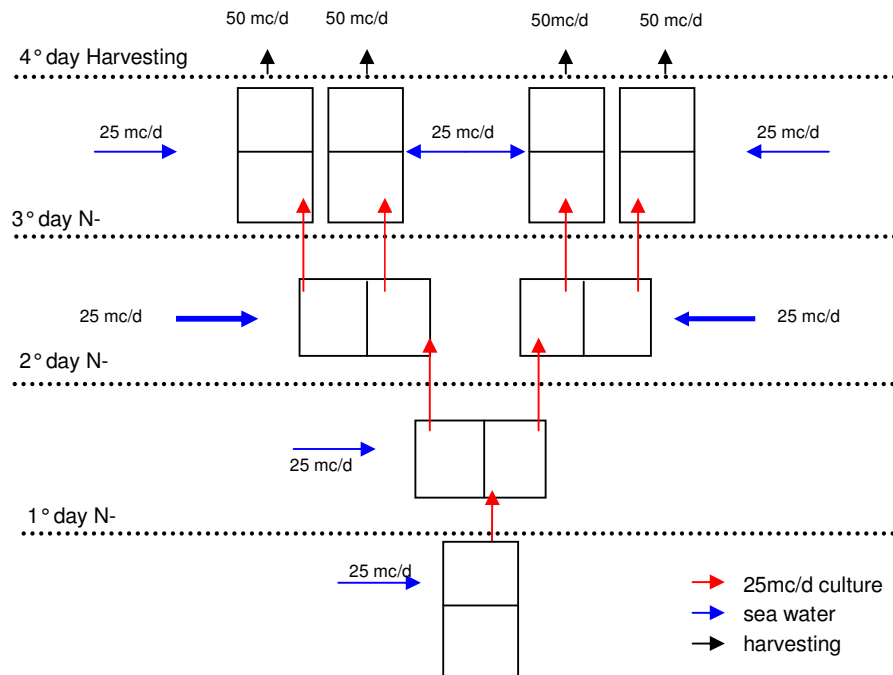


Fig.3 Scheme of a "two-phase" strategy applied to a plant consisting of 10,000 m of GWP photobioreactor. The facility, as in the base case, is divided into eight modules of 25 GWP 50 m long.

5.4 Results and Discussion

5.4.1 Energy balance of *Nannochloropsis* F&M-M24 biomass production in 1 ha GWP plant

Objective of this study was to evaluate the energy performance of one hectare facility, through the determination of an index able to express the ratio between the energy produced and energy consumed, for the production of algae biomass as a new feedstock of second generation bio-fuels. This work should not be confused with an LCA analysis, that would require a far more complex assessment of possible environmental effects related to the process considered.

Currently there are no industrial plants that produce microalgae biomass for exclusive energy use. The technology presented here, the photobioreactor GWPI (WO 2004/074423), however is currently used in commercial (ArchimedeRicerche s.r.l.- Imperia) and research (Eni spa-Rage s.p.a (CT), Enel s.p.a -Brindisi) facilities.

Much of the data used for this analysis come from the experience thus gained on these plants, which although not yet at industrial scale, are concrete applications of this technology.

In recent years several research groups have begun to carry out energy performance analysis of algae derived bio-fuels production in order to verify the sustainability of the process (Clarence et al, 2009, Lardon et al., 2009, Stephenson et al., 2010, Jorquera et al., 2010, Burges and Fernandez-Velasco, 2007, Lher and Posten, 2009). Most of these works are focused on the analysis of scenarios in which the culture system used is composed exclusively of open raceway ponds (Clarence et al. 2009, Lardon et al. 2009). Others have compared the energy performance of ponds with respect to closed systems such as tubular and flat panel reactors (Stephenson et al, 2010, Jorquera et al., 2010). Most of these works, correct in the method of analysis, show their main limitations in the chosen biological aspects.

Many of the proposed analysis has been in fact based on scenarios involving the use of freshwater strains such as *Chlorella*., a situation not sustainable in our view, because of the high consumption of fresh water that would require the production of tons of biomass in plants of hundreds of hectares. This problem could be partially solved with the use of wastewaters, but it is difficult to think of a large scale system in which the only source of water is represented by waters not characterized by a homogeneous composition and not stable over time. There could be problems of contamination which will adversely affect the maintenance of the selected strain. It was therefore considered that the choice of a marine strain such *Nannochloropsis* F&M-M24, widely studied and tested in outdoor culture (Rodolfi et al. 2009, Rodolfi et al., 2003, ChiniZitelli et al., 2000) would increase the significance of the analysis.

Here as follow, results for both the base case and nitrogen starvation through a "two phase" strategy are summarized.

Base case:

the analysis of the energy balance for the base case shows that the 52% of the annual energy costs is due to E.E of materials employed (tab.4). The determination of this value took into account the different lifespan for each type of materials used. The remaining 48% of the input energy is shared between nutrients for a 12%, mainly nitrogen $261 \text{ GJ ha}^{-1} \text{ yr}^{-1}$, while the remaining 36% is given by the electricity consumed annually for the overall daily operations like medium supply, harvesting, biomass concentration and cooling. Similar results were also

obtained by Burgess & Fernandez-Velasco (2007) who evaluated the NER of a tubular system for the production of hydrogen from algae. Also their analysis shows that the cost associated with reactors material dominate the overall energy consumption balance.

With an annual average productivity of $50.4 \text{ ton} \cdot \text{ha}^{-1} \cdot \text{yr}^{-1}$, equivalent to $1160 \text{ GJ} \cdot \text{ha}^{-1} \cdot \text{yr}^{-1}$ of stored energy into the biomass (tab.4), the final NER of the plant resulted: 0.5. This means that for the examined conditions, the amount of energy consumed annually is twice what it is "produced" through photosynthesis. This value is much lower than those reported by Jorquera et al. (2010) where a compared energy analysis for raceway ponds, tubular reactor and a reactor similar to the GWP is made. The same authors reports a NER of 4.51 for the production of $100 \text{ ton} \cdot \text{ha}^{-1} \cdot \text{yr}^{-1}$ of biomass produced in a plant of comparable size to that proposed here. This value is 9 times greater than the value reported here for the base case. One of the possible reasons for such high NER is probably due to the fact that many of the energy inputs have been neglected in the analysis of Jorquera et al., (2010). The energy consumption term, in fact, only takes into account the energy expenditure for the agitation of the culture (mixing) and energy costs of LDPE for manufacturing the photobioreactor. Other important energy inputs like harvesting, nutrients and E.E of all others materials were omitted. An areal productivity of $27 \text{ g} \cdot \text{m}^{-2} \cdot \text{d}^{-1}$ was also considered by Jorquera et al. (2010), but this value seem too optimistic for *Nannochloropsis*, especially in vertical flat panel reactors similar to GWP. Even considering in our analysis such an high value of productivity and excluding energy costs for nutrients, the energy balance would be only slightly higher than 1.

From a detailed analysis of the E.E of materials and components we can see as almost all the E.E is represented by the GWP photobioreactor (fig. 5). The reactor is in fact composed of a complex and heavy stainless-steel structure (grids and up-rights) accounting for a significant value of the input energy and representing 95% of the energy stored into the biomass (tab.5). The GWP design has been recently improved in order to reduce its cost and energy contribution (Tredici et al., 2010b). In the new design (GWPII- patent: 9325 PTWO) the grids have been eliminated and the culture chamber is contained within a simpler structure made by a base and a number of vertical uprights driven directly into the base or into the ground. This allowed to reduce significantly the structure by reducing the use of materials such stainless steel and LDPE. By this way we have not only reduced the reactor's cost at about $15 \text{ €} \cdot \text{m}^{-1}$, making it competitive with open systems such as ponds, but we have also substantially

decreased the energy demand associated with it. A fully implementation of the plant with the new model, GWPII, would rise the final NER to 0.6, much reducing the relative weight of E.E materials and energy costs of operation.

Operating energy costs are more evenly distributed than E.E of materials (fig. 6). Mixing, together with culture concentration represent 73% of operative energy demand, confirming as the air bubbling represents an energetically expensive method for culture mixing.

The 11.5% of the overall energy demand is instead due to the use of chemical fertilizers (tab.4). The use of wastewaters would eliminate the need to use chemical fertilizers, improving the energy balance to a final NER of 0.56. Clarence et al. (2009) analyzed how the use of different wastewaters would improve the environmental and energetic performance of the cultivation of algae (strain not specified) in open raceway ponds, showing as there is a great difference in terms of energy saved, depending on the type of wastewater used.

The energy cost for biomass concentration depends on the type of culture system adopted, the method of culture management (continuous, batch or semi-continuous) and of course the rate of growth. For the base case scenario, where the concentration of biomass is carried out entirely by means of centrifuges for 10 hours per day, the overall energy (E.E plus operative energy) for biomass concentration accounted for 15.1% of energy into the biomass (tab.5).

Nitrogen Starvation case: the “two phase strategy”:

The “two-phase” strategy presented here was successfully experimented by Rodolfi et al. (2009) during summer season in outdoor GWPs. *Nannochloropsis* F&M-M24 was able to respond to nitrogen stress conditions with a significant increase of lipid synthesis. A lipid productivity of 90 Kg ha⁻¹ d⁻¹ (10 and 80 Kg ha⁻¹ d⁻¹ for the first and the second phase respectively) was obtained. We hypothesized to maintain the same biomass productivity reported by Rodolfi et al., (2009) both for the first phase (nitrogen sufficiency) and for the next phase of starvation, even if the dilution rate was increased to 50%, respect to 40% reported by the author.

Thanks to the high lipid content, 60% of the biomass after 3 days of starvation (Rodolfi et al., 2009), the average caloric content of 1 kg of dry biomass was increased to 27.7 MJ kg⁻¹. We considered 14 MJ kg⁻¹ for the remaining 40% of the biomass. Despite the increased lipid content, and therefore the higher caloric content of biomass, the output energy does not increase compared to the base case (tab.4). This is due to a decrease in the areal productivity from 14.6 to 12 g m⁻² d⁻¹ as consequence of nitrogen starvation. The amount of energy

produced by the plant each year is equal to that contained in 38 tons $\text{ha}^{-1} \text{yr}^{-1}$ of harvested biomass (fig.3), with an average caloric content of 27.7 MJ kg^{-1} .

Despite a reduction in the amount of input energy required respect to the base case scenario (tab.4), the increased lipid content of biomass is not sufficient to compensate the decline in productivity due to the stress condition. This translates in an increase of NER of only 8%: from 0.5 to 0.54 (tab.4).

Compared to the base case scenario there is a reduction of the energy requirement for those components related to the culture concentration: E.E of centrifuges and operating costs for biomass concentration (tab.5). Thanks to the pre-concentration step by means of flocculation-sedimentation process, the overall energy for harvesting represent less than 1% of the energy stored into the biomass (tab.5). A reduction in the use of centrifuges did not seem to cause any significant advantages when only closed reactors are used as culture system, due to the relative small culture's volumes collected. A significant contribution it could instead be obtained in the case of raceway ponds were used as cultivation system. Here the amount of culture to be processed on a daily basis is much higher than in GWP.

As for the base case if we compare the final NER obtained for this scenario with those reported by Jorquera et al., (2010), for the high lipid content scenario, a great difference is evident. Jorquera et. al., (2010) reports a final NER of 6.21 when the lipid content of biomass increase to 60%. These values seem too optimistic. Even considering only the energy for mixing and an output of 30 tons ha^{-1} per year of lipids, equivalent to 50 tons of biomass, a NER of 2.56 would result in our analysis.

The GWP reactor does not seem a sustainable energetic solution if used as exclusive culture system for biomass production for energy use. Both the scenario here examined showed a too much high energy consumption respect to the biomass produced. Even the high lipid content scenario, although an increase in the final NER was obtained, does not allow to produce more energy than that consumed. The energy cost of materials, especially the E.E of GWP reactor, together with modest areal productivity ($14 \text{ g m}^{-2} \text{d}^{-1}$) of *Nannochloropsis* F&M-M24 seems the two main reasons of such low NER values. Higher productivities than those here used will results in better performance. In fig.9 and fig.10 a sensitivity analysis of the final NER for different areal productivities is reported. As we can see positive energy balance ($\text{NER} > 1$) are obtained only at average areal productivities greater than $30 \text{ g m}^{-2} \text{d}^{-1}$ for the base case scenario and $22.5 \text{ g m}^{-2} \text{d}^{-1}$ if a 60% lipid rich biomass is considered. These productivities are quite difficult, although impossible, to obtain for long periods with *Nannochloropsis*, especially

under nitrogen starvation, unless very favorable climatic conditions and very productive strain are available.

Tab.4 Net Energy Ratio for the production of 1Kg of *Nannochloropsis F&M-M24* biomass (dry weight) in 1 ha GWP facility. Base case and nitrogen starvation scenarios.

	Unit	Base Case	Nitrogen Starvation
E.E materials	GJ ha ⁻¹ yr ⁻¹	1210	1206
Operative Energy	GJ ha ⁻¹ yr ⁻¹	853	703
Nutrients	GJ ha ⁻¹ yr ⁻¹	270.5	33.8
Energy into the biomass	GJ ha ⁻¹ yr ⁻¹	1160	1052
NER		0.50	0.54

Tab.5 Energy inputs (GJ ton⁻¹ biomass yr⁻¹) for the production of 1 ton (dry weight) of *Nannochloropsis F&M-M24* wet biomass and % of the energy stored into the biomass.

	Base Case		Nitrogen Starvation	
	Input/Output GJ ton. ⁻¹ yr ⁻¹ (23 GJ ton ⁻¹)	Input/Output %	Input/Output GJ ton. ⁻¹ yr ⁻¹ (27.7 GJ ton ⁻¹)	Input/Output %
Embodied Energy				
<i>GWP I</i>	21.91	95	29	105
<i>Centrifuge</i>	0.101	0.44	0.016	0.06
<i>Pumps</i>	0.071	0.31	0.094	0.34
<i>Blowers</i>	0.196	0.85	0.259	0.94
<i>Piping</i>	1.747	7.5	2.32	8.36
Operative Energy				
<i>Mixing and flue gas</i>	10.731	45	14.23	51.38
<i>Flocc-Sedimentation</i>	-	-	0.037	0.13
<i>Centrifugation</i>	3.394	14.76	0.273	0.98
<i>Cooling</i>	2.229	10	2.95	10.67
<i>Medium supply</i>	0.180	0.78	0.36	1.3
<i>Culture Harvesting</i>	0.180	0.78	0.36	1.3
<i>Labour</i>	0.214	0.93	0.284	1.03
Nutrients	5.367	23.3	0.89	3.21

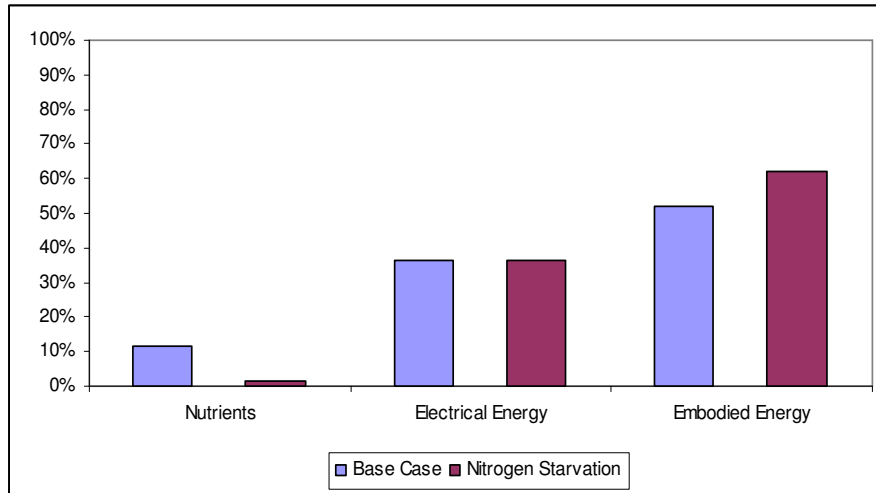


Fig.4 Relative contribution of nutrients, operative energy and embodied energy of materials to the overall energy demand for the production of *Nannochloropsis F&M-M24* biomass (dry weight) in 1 ha GWP plant.

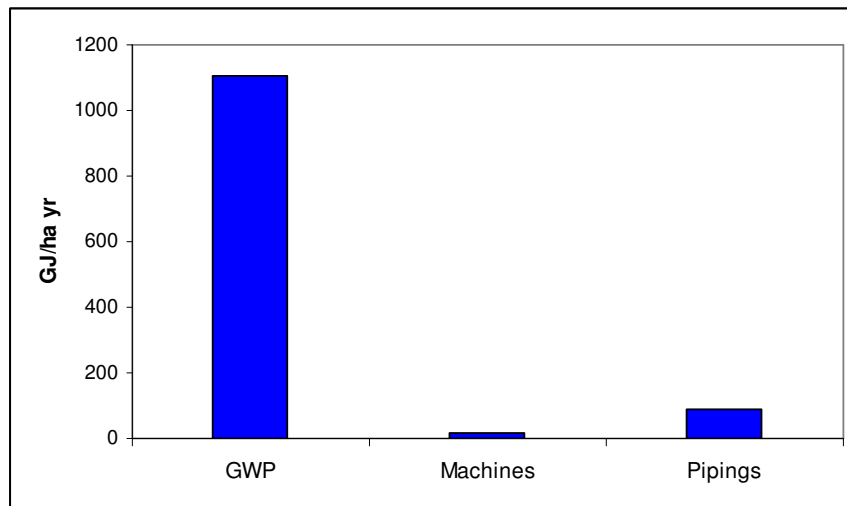


Fig.5 Base case. Main contributions to the total Embodied Energy of materials ($\text{GJ ha}^{-1}\text{yr}^{-1}$) in 1 ha GWP facility for the production of *Nannochloropsis F&M-M24* biomass.

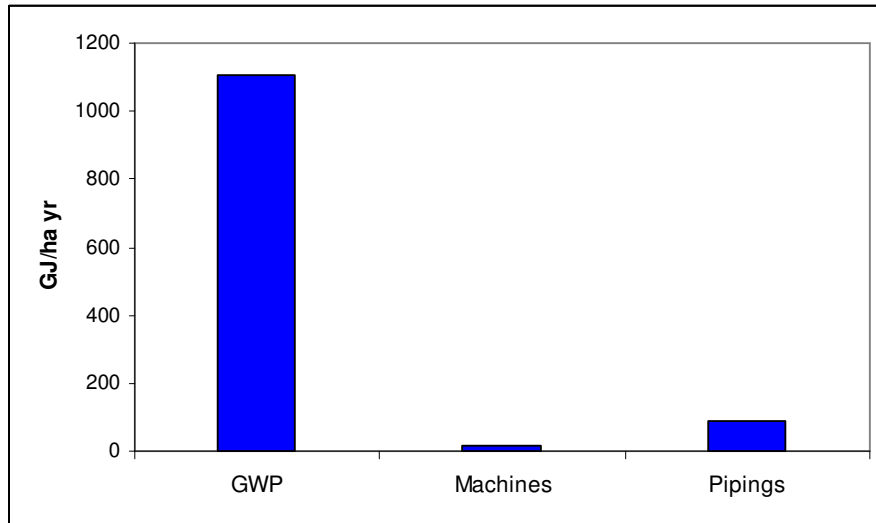


Fig.6 Nitrogen starvation: total Embodied Energy of materials ($GJ ha^{-1}yr^{-1}$) in 1 ha GWP facility for the production of *Nannochloropsis F&M-M24*(dry weight) wet biomass.

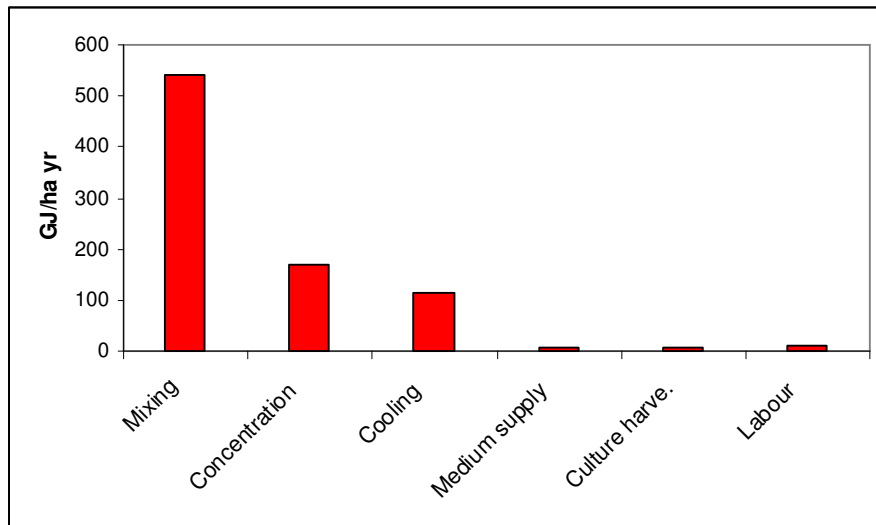


Fig. 7 Base case: annual operative electrical energy consumption ($GJ ha^{-1}yr^{-1}$) in 1 ha facility for the production of *Nannochloropsis F&M-M24* wet biomass.

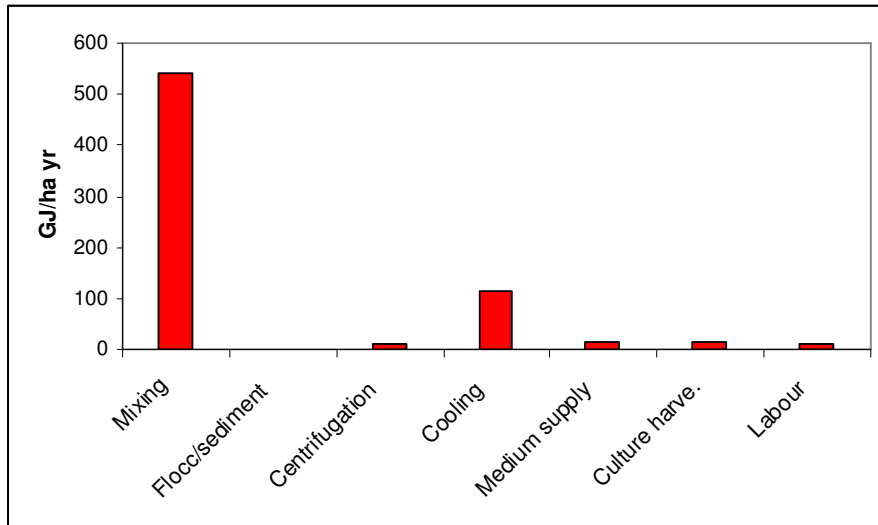


Fig.8 Nitrogen starvation: annual operative electrical energy consumption ($GJ\ ha^{-1}\ yr^{-1}$) in 1 ha facility for the production of *Nannochloropsis* F&M-M24 wet biomass .

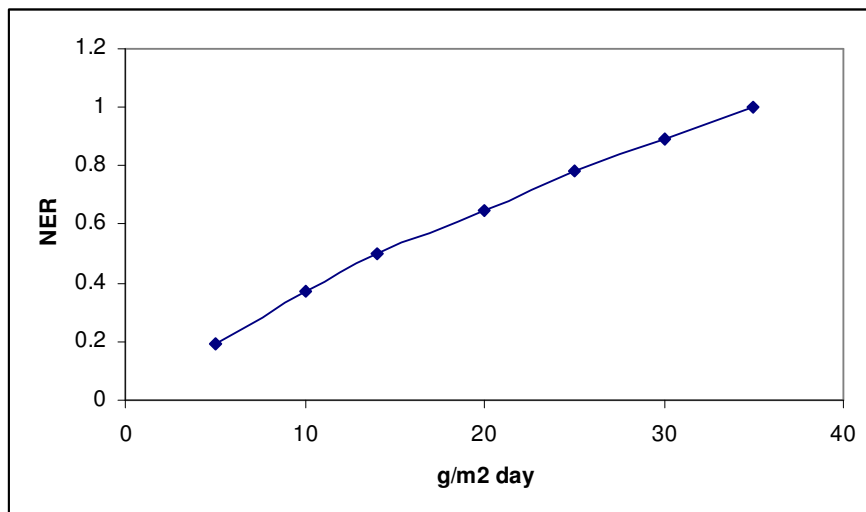


Fig.9 Influence of areal productivity on the Net Energy Ratio in *Nannochloropsis* F&M-M24 biomass production in a 1 ha GWP plant. Base case scenario

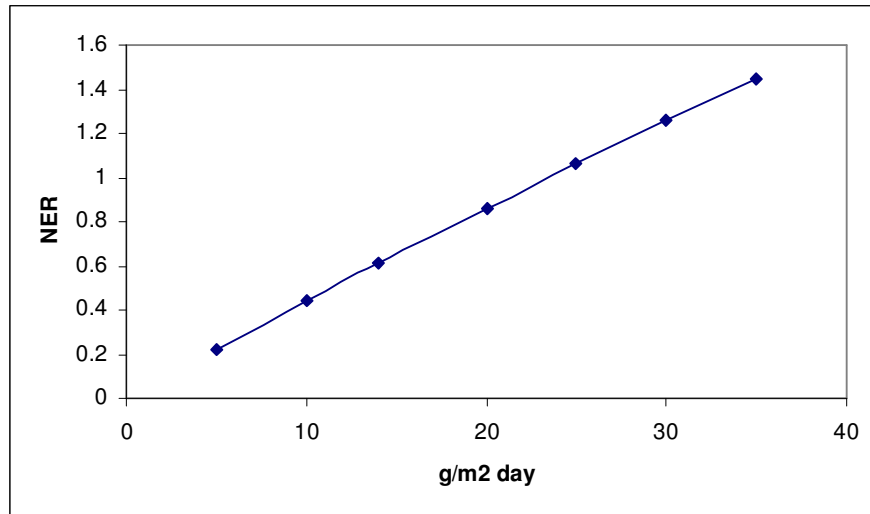


Fig.10 Influence of areal productivity on Net Energy Ratio of *Nannochloropsis* F&M-M24 biomass production in a 1 ha GWP plant. Nitrogen starvation through the “two phase strategy”.

5.4.2 Economic evaluation of *Nannochloropsis* F&M-M24 biomass production in a 1 ha GWP plant

An economic assessment for the production of *Nannochloropsis* F&M-M24 biomass in a 1 ha facility was carried out. The plant has the same characteristics described above for the energy analysis and reported in tab.1, 2 and 3 and also in materials and methods.

The analysis presented here takes into account a relatively small facility, even if only few plants entirely realized with photobioreactors of this size are present today (Tredici 2010a). This choice was driven by the need to reduce the size of the plant at a scale that would allow us to minimize extrapolations and base the analysis on costs that could be easily scaled without excessive margins of error from the pilot and small commercial GWP’s plants currently operating.

The analysis used as input data, to estimate capital and operating costs, available values from the literature (Weissman & Goebel 1987, Benemann & Oswald 1996, Becker 1994, Lundquist et al., 2010, Ben-Amotz 2008) and primary sources such as those from industrial plants or suppliers specifically contacted. The analysis also is drawn on the experience gained over the last few years by the research group of Prof. Tredici on the GWP reactors and the cultivation of *Nannochloropsis* F&M-M24 in outdoor pilot plants.

Some of the data used do not refer to recent works (Benemann & Oswald, 1996, Weissman & Goebel, 1987, Becker 1994). In order to enhance the effectiveness of the analysis, capital costs referred to those components for which there has been no substantial improvement in technology over the last years, have been updated. The costs were discounted with the formula of compound interest, assuming an average annual rate of inflation equal to 2.78%.

A useful life was assigned for each piece of equipment included and the depreciation of assets is thus based on the useful life assigned to each equipment. For the majority of the equipment (reactors, blowers, piping) it was assumed a useful life of 15 or 10 years. 20 years of useful life time was instead assigned to the harvesting system: centrifuges and settling pond. Pumps and the LDPE culture chamber have instead a shorter life span, 5 and 1 year respectively.

Depreciation spreads the initial cost of fixed assets on the useful life of the capital itself. The annual depreciation was here calculated as the ratio of the of the initial capital cost divided by the number of years of useful life, considering the possible value of recover at the end of the useful life equal to zero.

A growing season of 360 days was considered. This is plausible if we consider the plant located in regions where annual average solar radiation is about $20 \text{ MJ m}^{-2} \text{ day}^{-1}$ (<http://re.jrc.ec.europa.eu>). The same assumption was also made for the evaluation of NER (see above).

Compared to the energy balance discussed above, where the *base case* and the “*two phase*” *strategy* were analyzed from an energetic point of view, in the economic assessment we have included additional variables for each scenario:

1. Purchase of major nutrients (N-P-Fe) and pure CO_2 .
2. Purchase of major nutrients (N-P-Fe) and use of Flue-gas (12.5% CO_2) as carbon source.
3. Use of wastewaters as source of macro-nutrients and flue gas (12.5% CO_2) as carbon source.

In case 1 and 2 nitrogen was supplied as NaNO_3 , phosphorus as NaH_2PO_4 and iron as Fe-EDTA. A total cost of 403 € ton^{-1} of biomass was considered.

During the last years, due to the growing emphasis on microalgae as new biomass for the production of second-generation bio-fuels, numerous economic estimates of the production cost of biomass or biodiesel derived from microalgae have been published. Most of these

studies refers to open systems such as raceway ponds or integrated system where only the inoculum is produced in photobioreactors, mainly tubular reactors, while the bulk production is still carried out in ponds (Williams & Laurence, 2010). It is therefore difficult to make comparisons with the analysis carried out here, where vertical disposable reactors are exclusively employed as culture system.

Among the available economic assessments designed to estimate the production cost of biomass in several hectare plants, the facility size we decided to consider for algal biomass for bio-fuels, there are those carried out by Benemann & Oswald (1996), Weissman & Goebel (1987), Kadam (2001) and more recently Lundquist et al., (2010). All these, however, as most of the economic analyses carried out, refer to raceway ponds.

Taking into account the most recent estimates made, biomass's cost vary depending on the assumptions made and the strain used: from 0.21 to \$15 kg⁻¹ for raceway pond and from 0.47 to 30.4 \$ kg⁻¹ for photobioreactors (Williams & Laurence, 2010).

Our analysis shows a cost of biomass production ranging between 7.5 and 14.2 € kg⁻¹ of wet biomass, depending on the scenario considered (tab.8). Comparing these values with the cost of production reported by Williams & Laurence (2010) for other photobioreactors, the cost resulting from our analysis is midway between the maximum and the minimum values reported.

Leher & Posten (2009) reported an investment cost of 12 € m⁻² as threshold for the annual biomass production costs for energy use. The costs of our analysis are far beyond that threshold. A reduction in production costs could result from the employment of the second generation GWP (GWPII - 9325 PTWO), where the reactor's cost was reduced to 15 € m⁻¹ with respect to the 80 € m⁻¹ of the first generation GWPI (patent: WO 2004/074423) taken in consideration for the present analysis. This would reduce the investment cost of about three times, reducing the cost of production of biomass of € 2 per kg⁻¹.

In the following tables capital and operative costs for the *base case* and for the *"two phase" strategy* for the three different cases considered are reported.

Investment costs are different between the base case and the "two phase" strategy (tab.6). The investment costs of this last are, in fact, about 10% lower compared to the base case. This is due to the different system of biomass concentration adopted. In the base case the culture is completely concentrated by centrifugation unlike the "two phase" strategy where the culture is first pre-concentrate by flocculation-sedimentation, before being processed by centrifuge. Anyway, for both scenario considered, the 80% of the investment costs is represented by the

GWP reactor and the harvesting concentration system (tab.6). The remaining 20% is shared between engineering, piping and machines.

Tab.6 Capital Cost assessment for 1 ha GWP facility for the production of Nannochloropsis F&M-M24 biomass. Capital costs are the same for case1, case 2 and case 3.

	Base Case (€ ha⁻¹)	Nitrogen Starvation (€ ha⁻¹)
Site preparation and enclosure	28,000	28,000
GWP reactors		
External metal frame	800,000	800,000
Grids	320,000	320,000
Valves and fittings	50,000	50,000
Internal heat exchanger	70,000	70,000
Piping		
Cooling	26,000	26,000
Medium supply and Harvesting	1116	1116
Air and CO ₂	5000	5000
Machines		
Blowers	40,000	40,000
Pumps	5,400	5,400
Others	9,040	9,040
Biomass Concentration		
Flocculation and Settling pond ⁴	-	17,000
Centrifuges	175,000	33,800
Building and Roads	10,000	10,000
Service	5,000	5,000
Remote control & Instrum.	28,000	28,000
Laboratory	15,000	15,000
Subtotal	1,587,556	1,463,356
Eng. & Contingencies	158,755	146,335

⁴ 85 € m⁻³ of harvested culture (personal evaluation).

(10% subtotal)		
TOTAL INVESTEMENT	1,746,312	1,609,692

The operating costs are different depending on the specific case considered (tab.7). For case 1 (pure CO₂ and nutrients from fertilizers) 75 and 78%, for the *base case* and the *nitrogen starvation* respectively, of the operating cost are represented by manpower and CO₂ purchased. Labor can, instead, account for up to 70% of operating costs in the case that nutrients are not purchased and the CO₂ comes from flue gas (case 3) (tab.7).

Electrical energy accounts from 5 to 9 % of the operating costs , where the energy required for mixing and distribution of CO₂ is the main contributor: 150,000 kWh ha⁻¹ yr⁻¹ on a total of about 183,942 kWh ha⁻¹ yr⁻¹.

Labor greatly contributes to the final production costs, because of the small size of the plant. In larger installations, tens of hectares, the labor costs would decrease significantly. Weissman & Goebel (1987) reported the use of 23 people for a facility of 400 ha entirely made with raceway ponds, equivalent to a cost of € 1800 ha⁻¹ yr⁻¹ (€/ U.S\$: 1.38). Introducing this value in our analysis the cost of biomass production will decline as shown in fig.13 and fig.14

As for the energy assessment the exclusively use of this kind of photobioreactor does not appear a feasible solution to the production of biomass for low cost application.

Tab.7 Summary of the Operating Costs for the production of *Nannochloropsis F&M-M24* biomass in 1 ha GWP facility. Scenarios 1 (purchased nutrients and pure CO₂). Scenario 2 (Nutrients purchased and CO₂ from flue-gas). Scenario 3 (Nutrients from wastewaters and CO₂ from flue-gas.)

	Base Case			Nitrogen Starvation		
	(€ ha ⁻¹)			(€ ha ⁻¹)		
	1	2	3	1	2	3
Electricity ⁵						
Mixing	15,023	15,023	15,023	15,023	15,023	15,023
Cooling	3,120	3,120	3,120	3,120	3,120	3,120
Water supply and Harvesting	251	251	251	381	381	381
Flocculation-Sedimentation	-	-	-	386	386	386
Centrifugation ⁶	4752	4742	4752	288	288	288
Nutrients (N-P-Fe)	20,348	20,348	-	2,374	2,374	-
Pure CO₂ ⁷	181,000	-	-	159,000	-	-
Flocculant ⁸	-	-	-	1020	1020	1020
Labour ⁹	166,200	166,200	166,200	166,200	166,200	166,200
Filtration System	2400	2400	2400	2400	2400	2400
Others	1500	1500	1500	1500	1500	1500
Subtotal	394,994	213,584	193,246	351,692	192,692	190,318
Maintenance (2% Subtotal Capital)	31751	31751	31751	29,267	29,267	29,267
General Overheads (10% Subtotal above)	39,499	21,358	19,324	35,169	19,269	19,031
Operating Cost	466,245	266,694	244,322	416,128	241,228	238,617

⁵ 0.1 € kWh⁻¹.

⁶ 1 kWh/m³ of treated culture.

⁷ € 400 ton/CO₂

⁸ Benemann & Oswald (1996).

⁹ Adapted from Weissman & Goebel (1987)

5.5 Conclusions

Albeit from a preliminary analysis it is clear that this technology, the GWP reactor, can not be used as the only culture system for the production of biomass for energy use. Energetic and economic assessments have shown that microalgae biomass produced in GWP reactors, at least for the strain considered, is not currently a competitive process. Leher & Posten (2009) estimated in 1 € kg⁻¹ the maximum price of algae biomass for energy use. From tab.8 we can see how even in our best hypothesis, the case 3 for both the base case and the nitrogen starvation, the biomass production cost in GWP is far away from 1 € kg⁻¹. The use of less expensive reactors, such as the GWPII, although reducing the production cost of the biomass of 20-30% depending on the scenarios considered, it is not able to close the gap.

The use of an integrated system, photobioreactors and open ponds, seems so the only possible solution able to approach a competitive biomass production costs for energy use. Through the use of an integrated system, not only we would obtain a reduction in production costs, but also we improve the final NER (personal data).

From a preliminary economic evaluation of an integrated system for the production of starved biomass through the "two phase" strategy, in which the plant surface is occupied for a 5% by GWPI photobioreactors and the remaining 95% of the surface is occupied by ponds, the production cost of biomass (CO₂ is from flue-gas and nutrients from wastewaters) resulted less than 1 € kg⁻¹. However, increasing the surface occupied by reactors to 35% of total plant area, the cost rises dramatically.

We must also specify that we did not consider in this analysis any revenue from the sale of by-products that would remain after oil extraction. The exploitation of biomass residue is in fact extremely interesting due to its high content of important nutritional principles as polyunsaturated fatty acids (PUFA) (Tredici et al., 2009), but the possible market price for the residual biomass is still yet to be determined.

Tab.8 *Nannochloropsis F&M-M24* production cost in 1 ha GWP plant for the base case and the “Two-phase” strategy. Case 1 (purchased nutrients and pure CO₂). case 2 (Nutrients purchased and CO₂ from flue-gas). Case 3 (Nutrients from wastewaters and CO₂ from flue-gas.).

		Base Case			“Two Phase” Strategy		
		1	2	3	1	2	3
Depreciation	€ ha ⁻¹ yr ⁻¹	134,331	134,331	134,331	123,822	123,822	123,822
Operating Costs	€ ha ⁻¹ yr ⁻¹	466,245	266,694	244,322	416,128	241,228	238,617
Total Annual Costs	€ ha ⁻¹ yr ⁻¹	600,576	401,025	378,653	539,951	365,051	362,439
Biomass Production	Ton. ha⁻¹ yr⁻¹	50.4	50.4	50.4	38	38	38
Biomass Production Costs	€ kg⁻¹	11.9	7.95	7.51	14.20	9.60	9.53

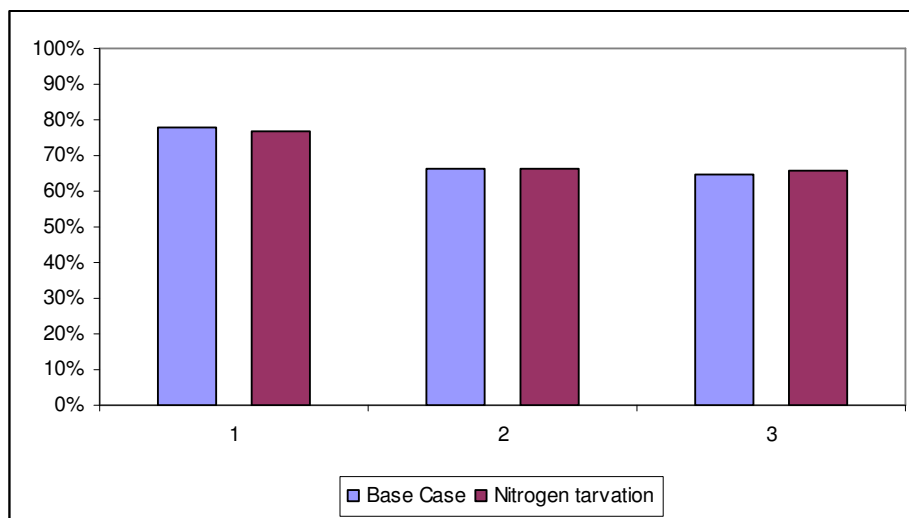


Fig.11 Relative contribution of the operating costs on overall annual production costs for different cases. 1 (purchased nutrients and pure CO₂), 2(Nutrients purchased and CO₂ from flue-gas) and 3 (Nutrients from wastewaters and CO₂ from flue-gas.).

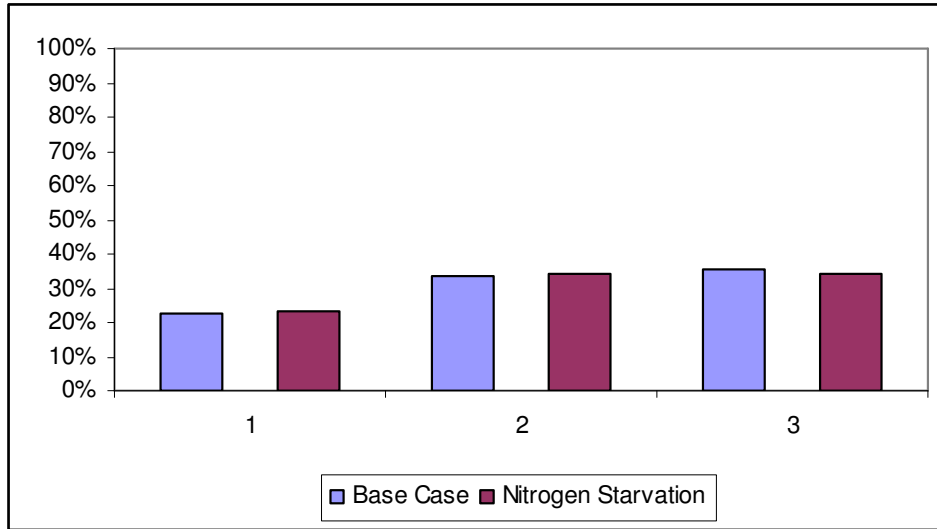


Fig.12 Relative contribution of depreciation on overall annual production costs for different cases. 1 (purchased nutrients and pure CO₂), 2(Nutrients purchased and CO₂ from flue-gas) and 3 (nutrients from wastewaters and CO₂ from flue-gas.)

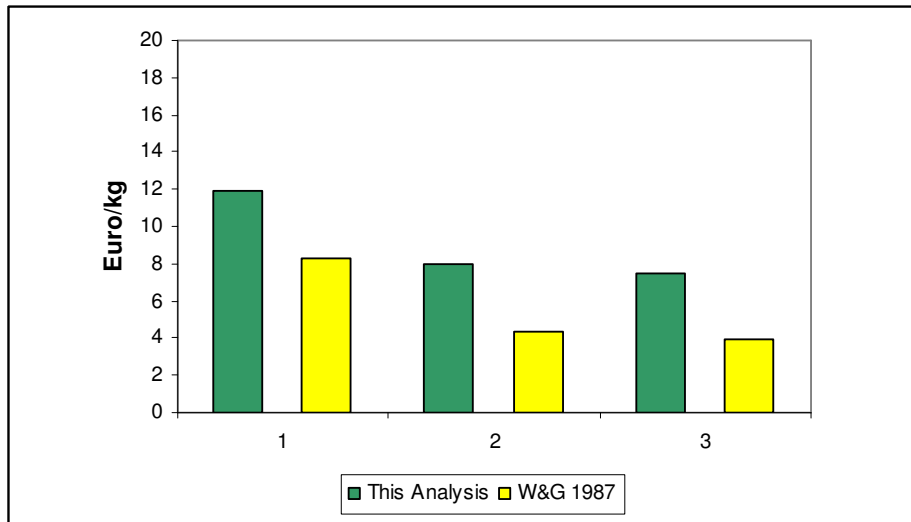


Fig.13 Base case: *Nannochloropsis* F&M-M24 biomass production cost as function of labour's cost for different cases. 1 (purchased nutrients and pure CO₂), 2 (nutrients purchased and CO₂ from flue-gas) and 3 (nutrients from wastewaters and CO₂ from flue-gas.).

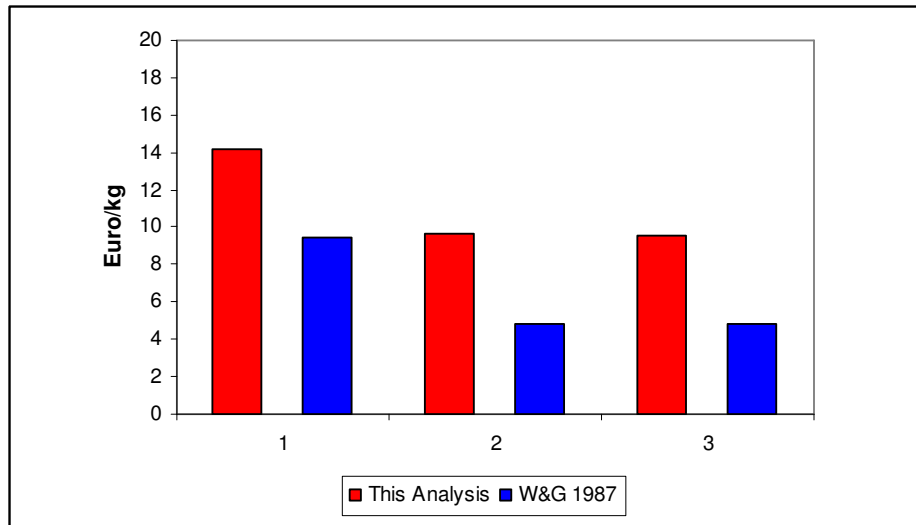


Fig.14 Nitrogen starvation: *Nannochloropsis F&M-M24* biomass production cost as function of labour's cost for different cases: 1 (purchased nutrients and pure CO₂), 2 (nutrients purchased and CO₂ from flue-gas) and 3 (nutrients from wastewaters and CO₂ from flue-gas.).

6.

SUMMARY

The main purpose of this work was the characterization of a disposable flat panel photobioreactor: the “Green Wall Panel” (GWP, patent: WO 2004/074423). The reactor has been developed and patented at the Agricultural Biotechnology Department of the University of Florence (Tredici & Rodolfi, 2004).

The high investment, operative and energy costs of many of the existing photobioreactors, make microalgae biomass production still too expensive for low-cost applications. In addition, most conventional photobioreactor designs still present technical limitations, making difficult their scaling-up at industrial scale. The characterization of any photobioreactor at large scale is therefore the fundamental starting point to fully evaluate the real potential and limitations of a given technology. It is only through a complete characterization that is possible to detect the existing limitations and optimize the system, creating the conditions for better productivities and lower costs.

The GWP reactor, thanks to its structural simplicity and low cost, if compared to other commercial available photobioreactors, has gained during last years an increased consideration. Currently the GWP reactor is operating at ENI S.p.A. refinery of Gela (Italy), at ENEL Ingegneria e Innovazione S.p.A. (Brindisi, Italy), at Bioscan S.A. (Antofagasta, Chile) for research purposes. Commercial facilities are operating at Archimede Ricerche S.r.l. (Camporosso, Italy) and Necton S.A. (Olhão, Portugal). Despite its diffusion, a detailed characterization of the reactor has never been made. Aim of this work was therefore to carry out a characterization and an evaluation of the most important aspects influencing GWP.

The work was divided in four chapters, each of which explores a particular aspect of the GWP. Chapter 2 was devoted to the study of how different arrangements, including orientation, inclination and mutual spacing between reactors, influence the amount of solar radiation intercepted per unit of reactor surface or occupied land (MJ m^{-2} reactor/ground, day^{-1}). As biomass productivity is strongly influenced by solar radiation intercepted, disposition of reactors on the field needs to be studied in detail to decide which is the arrangement able to maximize solar radiation intercepted. As is it impossible to intercept more solar radiation than that falling, on a horizontal surface, all possible GWP arrangements (except the horizontal) lead to a loss of solar radiation captured. A numerical model was so developed to predict solar radiation impinging on the reactor surfaces and to estimate the transmittance across the

transparent GWP's walls. This model provides a tool that allows to determine with relatively good precision the actual amount of solar radiation available for the photosynthetic process.

Model's simulations and field measurements for incident and transmitted irradiance, were performed for both *isolated* and *full scale* configurations using vertical and inclined GWPs in order to validate the methodology used. Simulations of the average daily solar radiation impinging on GWP reactors with different orientation, inclination and distance were performed. Closely spaced reactors ($d = 0.1$ m) resulted in the best arrangement in terms of solar radiation intercepted per unit of occupied surface ($\text{MJ m}^{-2} \text{ ground d}^{-1}$), independently the latitude and inclination considered. We concluded that E-W orientation should be adopted in commercial scale plants regardless of the latitude and the distance between reactors because able to intercept more solar radiation than N-S facing reactors. Although the advantage of this configuration is minimal. Beside, E-W oriented reactors allows to reduce photosaturation and photoinhibition, by reducing the solar radiation intercepted at midday, when high light intensity occurs especially on summer months.

An estimation of the transmittance through the transparent LDPE film of GWP's culture chamber, showed as an important proportion, about 20%, of the incident light is reflected off and absorbed by the plastic material. This further contributes to reduce solar radiation actually available for microalgae and thus to lower the maximal photosynthetic efficiency attainable.

In [Chapter 3](#) we have addressed the characterization of hydrodynamics of the GWP reactor. Mixing, and thus the turbulence, represents one of the most important parameters influencing the productivity of photosynthetic microorganism, determining, together with culture concentration, the efficiency with which solar radiation is used. The level of turbulence also affects reactor's energy performance and its running costs. Parameters such mixing time, O_2 and CO_2 volumetric mass-transfer coefficients, axial dispersion coefficient and dispersion number, bubble dimensions and the power consumption for air bubbling have been determined for different air flow rates. The results were presented at the 11th Congress of the International Society for Applied Phycology (Galway, June 21th – 30th Ireland). It was shown that the reactor was characterized by low axial dispersion even at high air flow rates and a typical plug flow behaviour when a water flow through the reactor was applied. Parameters as $(K_L a)_{\text{O}_2}$, $(K_L a)_{\text{CO}_2}$, gas hold-up, bubble dimension resulted to those reported in literature for similar disposable panel reactors (Sierra et al. 2008). Hydrodynamic characterization also confirmed the strong dependence of the former parameters from power supply and as this represents the main limitation of such kind of reactor for energy production. Power for mixing used fact, a great proportion of the energy stored into the biomass at the air flow rates commonly used.

In order to reduce the power consumption for mixing, the effect of three different air flow rates (0.05-0.15-0.45 L L⁻¹ colt. min⁻¹) on volumetric productivity of the marine Eustigmatophyte *Nannochloropsis* F&M-M24 was evaluated, both in vertical and inclined GWPs. Results obtained, discussed in [Chapter 4](#), showed as volumetric productivity is strongly influenced by turbulence only at high solar radiation levels (> 16 MJ m⁻² reactor d⁻¹). This confirmed both in vertical and inclined GWPs. On average, anyway, a reduction in the air flow rate by 3 times did not significantly affected the average volumetric productivity. This was translated in a 70% energy saving and so in a better energetic performance of the reactor. Air flow rate should be modulated in function of weather conditions, season and latitudes, employing higher air flow rates in typical sunny days and lower rates when solar radiation impinging on reactors surfaces results lower than 16 MJ m⁻² reactor day⁻¹.

Finally in [Chapter 5](#) an energetic and economic assessment of *Nannochloropsis* F&M-M24 biomass production in 1 ha GWP “virtual” facility was performed. The Net Energy Ratio (NER), representing the energy performance of a given process, was calculated for two different scenarios: nitrogen sufficient and nitrogen starved *Nannochloropsis* F&M-M24 biomass. The final NER ranged from 0.5 to 0.54 depending on the scenario considered. Inputs of energy used for biomass production resulted so always higher than the energy stored in the biomass, showing as the use of the GWP reactor can no be a solution for the production of microalgae biomass for energy use. Two aspects mainly contributes to the low NER obtained: the high embodied energy of the reactor and the electrical energy consumed for mixing. Together these represent from 70 to 84% of the total energy requirement. An integrated system where the GWP is used for inoculum production, covering only a relative small fraction of the total plant area, while the bulk production is realized in open ponds seems the solution where a positive energy balance is required.

The evaluation of *Nannochloropsis* F&M-M24 production costs, for a nitrogen sufficient (base case) and a nitrogen starved scenario, showed that biomass cost range from 7 to 14.2 € kg⁻¹ (drying not considered) as function of different cases considered. As for the energy balance, the economic assessments showed the unfeasibility of the GWP as exclusively technology to be used for the production of low cost algae biomass. Operating costs, especially labour, constitute the major contribution to the annual production cost. The GWP material was instead the major contribution to the total investment cost. Through the use of an integrated system, not only we would get an improvement in the energy balance of the whole process, but we also will obtain a reduction in production costs. From a preliminary economic evaluation (data not shown) of an integrated system for the production of starved biomass through the "two phase"

strategy, in which the plant surface is occupied for a 5% by GWPI photobioreactors and the remaining 95% of the surface is occupied by ponds, the production cost of biomass (CO₂ is from flue-gas and nutrients from wastewaters) resulted about 1 € kg⁻¹.

The use of low cost photobioreactors, as the new version of the GWP (GWPII – patent: 9325 PTWO) (Tredici et al., 2010) could decrease the biomass's production cost of 2-3 € kg⁻¹ in comparison with a system made of GWPI.

We did not consider in this analysis any revenue from the sale of by-products that will remain after oil extraction. The exploitation the residual is in fact extremely interesting due to its high content of important nutritional principles as polyunsaturated fatty acids (PUFA) (Tredici et al., 2010), but the possible market price of the residual biomass is still to be determined.

GWP reactors are now fully characterized in their main aspects: energetic, economic and biological performances. Achievable productivities with this kind of reactors are strain dependent and economic and energetic assessments here proposed have to be considered only to the specific cases here discussed.

7.

RIASSUNTO

Le microalghe (organismi eucarioti, foto-autotrofi talvolta capaci anche di crescere in eterotrofia) grazie alla loro semplicità strutturale sono caratterizzate da un'elevata efficienza fotosintetica (EF). Il massimo teorico, così come le piante superiori, è il 27,6 % della radiazione foto sinteticamente attiva (PAR) ed il 12,4 % se si considera l'intero spettro della radiazione solare (Tredici, 2010, Richmond, 1986). In realtà l'EF di questi microorganismi, soprattutto in coltura massiva all'aperto, quasi mai arriva a tali valori ma, a seconda delle condizioni ambientali e culturali, si attesta intorno al 3% della radiazione totale incidente (Tredici 2010). E' proprio la massimizzazione dell'EF l'obiettivo principale a cui mirare nella coltura massiva di questi microorganismi, così da ottenere la massima produttività di biomassa per unità di superficie. Le enormi aspettative riposte nelle microalghe, principalmente come nuova fonte di biocombustibili, hanno generato negli ultimi anni, anche all'interno della comunità scientifica, grande confusione ed incertezza sulle reali potenzialità produttive di questi microrganismi.

Gli elevati costi di produzione della biomassa algale (3-30 €/Kg), rendono però attualmente diseconomico l'impiego delle biomassa algali per usi energetici (Chisti, 2007; Tredici, 2008).

L'obiettivo principale della ricerca di dottorato è stato quello di procedere ad una caratterizzazione ed ottimizzazione del fotobioreattore "Green Wall Panel" (GWP) (brevetto: WO 2004/074423) sviluppato presso il Dipartimento di Biotecnologie Agrarie (Tredici & Rodolfi, 2004). Il reattore, grazie alla sua semplicità strutturale e basso costo (< € 100 m⁻¹ di reattore), se paragonato ad altre tipologie di reattori oggi esistenti, ha riscontrato negli ultimi anni un interesse considerevole. Attualmente il reattore GWP è impiegato sia in impianti di ricerca: raffineria ENI di Gela SpA (Italia), ENEL Ingegneria e Innovazione SpA (Brindisi, Italia), Bioscan SA (Antofagasta, Cile), che in impianti commerciali (Archimede Ricerche Srl, Camporosso, Italia e SA Necton, Olhao, Portogallo. Nonostante la sua diffusione, una caratterizzazione dettagliata del reattore ancora non esiste. Sierra et al. (2008) hanno caratterizzato un reattore "*disposable*" molto simile al GWP.

Gli elevati costi d'investimento e di gestione di molti dei fotobioreattori esistenti, rendono il costo di produzione della biomassa algale ancora troppo elevato per applicazioni a basso valore aggiunto (es. bio-fuels). Limitazioni di natura tecnica rendono inoltre difficile lo *scaling-up* di molti degli attuali sistemi chiusi. La caratterizzazione di un reattore è quindi il punto di partenza per valutare appieno le reali potenzialità produttive ed i limiti di una determinata

tecnologia. E' solo attraverso una completa caratterizzazione che risulta possibile individuare i limiti esistenti e quindi procedere ad un'ottimizzazione delle produttività e ad una riduzione dei costi di produzione.

Il lavoro è stato suddiviso in quattro capitoli principali, ognuno dei quali analizza un particolare aspetto del reattore GWP.

Nel Capitolo 2 si è studiato l'effetto di differenti configurazioni (orientamento, inclinazione, distanza tra le file) sulla quantità di radiazione intercettata dal reattore per unità di superficie d'impianto o di reattore ($\text{MJ m}^{-2}\text{giorno}^{-1}$). Siccome la produttività areale ($\text{g m}^{-2}\text{d}^{-1}$) risulta fortemente dipendente dalla quantità di radiazione solare intercettata, la disposizione "in campo" dei reattori deve essere studiata nel dettaglio al fine di stabilire la configurazione in grado di massimizzare la radiazione solare intercettata. Non essendo possibile intercettare un quantitativo di radiazione superiore a quello intercettato da una superficie orizzontale, tutte le possibili configurazioni, portano inevitabilmente ad una perdita di radiazione solare disponibile rispetto all'orizzontale. Abbiamo quindi sviluppato un modello in grado di determinare la radiazione solare incidente (diretta, diffusa e riflessa) sul reattore e di stimare la quantità di radiazione trasmessa attraverso la parete del reattore (film di LDPE, 300 μm). Risulta così determinabile con discreta precisione ($\pm 10\%$), l'effettiva quantità di radiazione solare disponibile per il processo foto sintetico.

I valori ottenuti dal modello sono stati confrontati con misurazioni dirette in campo su reattori verticali isolati e *full-scale* al fine di validare il modello sviluppato. Stabilita la bontà dei valori calcolati dal modello, si è proceduto ad effettuare una serie di simulazioni numeriche per stabilire la disposizione ottimale in termini di radiazione intercettata per unità di superficie occupata. Reattori distanziati di 0.1 m ed orientati E-O sono risultati in grado di massimizzare la radiazione intercettata per unità di superficie di suolo ($\text{MJ m}^{-2}\text{suolo d}^{-1}$), indipendentemente dalla latitudine e dall'inclinazione considerate. L'orientamento E-O dei reattori consente inoltre di ridurre fenomeni di fotosaturazione e fotoinibizione riducendo la radiazione solare intercettata durante le ore centrali del giorno in corrispondenza di elevati livelli di intensità luminosa, soprattutto durante il periodo estivo. Tale disposizione facilita inoltre il raffreddamento delle colture minimizzando l'irraggiamento ricevuto durante le ore più calde della giornata. E' stato inoltre valutata la trasmittanza della camera di coltura del GWP (film in LDPE) alla radiazione incidente. La trasmittanza della camera di coltura, sia misurata che stimata attraverso il modello, è risultata oscillare tra un 78 ed un 83% della radiazione totale incidente, in funzione della stagione e dell'orientamento del reattore. La radiazione "persa" in conseguenza della riflessione e dell'assorbimento, che assieme determinano la trasmittanza di

un materiale, contribuisce così a ridurre la quantità di radiazione solare effettivamente disponibile, diminuendo ulteriormente l'efficienza di conversione della radiazione solare.

Nel capitolo 3 abbiamo invece affrontato la caratterizzazione degli aspetti idrodinamici del GWP. Il livello di turbolenza (mixing rate) rappresenta, insieme alla concentrazione della coltura, uno dei principali parametri determinanti l'efficienza di fotosintesi e di conseguenza la produttività delle colture microalgali. Il grado di mixing, di conseguenza la quantità di aria insufflata, influenza l' "efficienza energetica" del reattore ed i costi operativi dello stesso. Parametri quali il tempo di mixing, il coefficiente volumetrico di trasferimento di massa per l'ossigeno e l'anidride carbonica (K_{La}), i fenomeni di dispersione, la dimensione e velocità delle bolle d'aria e l'energia spesa per l'agitazione della coltura (air bubbling) sono stati determinati per differenti flussi d'aria ($L L^{-1}min^{-1}$). I risultati ottenuti, presentati all' 11th Congress of the Internatioanal Society for Applied Phycology (Galway, 21-30 Giugno 2008, Irlanda) hanno evidenziato come il reattore GWP sia caratterizzato da una modesta dispersione assiale, anche in corrispondenza di elevati flussi d'aria, mostrando un comportamento idrodinamico tipico dei reattori plug low (PFR) quando una portata di acqua di $90 L min^{-1}$ è stata applicata al reattore. ($K_{La}O_2$, ($K_{La}CO_2$, gas-hold up, tempo di mixing e coefficiente di dispersione assiale sono risultati paragonabili a quelli riportati in letteratura per un reattore simile (Sierra et al. 2008). Suddetti parametri sono inoltre risultati fortemente legati alla potenza applicata per unità di volume ($W m^{-3}$). E' proprio l'energia consumata per l'agitazione ha rappresentare il principale limite di questa tipologia di reattore, limitandone la sua applicazione come sistema per la produzione di biomasse ad uso energetico. L'energia spesa per insufflare aria e mantenere in continua agitazione la coltura rappresenta, infatti, una parte consistente (fino al 100%) dell'energia contenuta nella biomassa.

Al fine di ridurre il consumo di energia legato al mixing, è stato valutato l'effetto di tre differenti flussi d'aria (0.05-0.15-0.45 $L L^{-1}min^{-1}$) sulla produttività volumetrica di *Nannochloropsis* F&M-M24, microalga marina appartenente alla famiglia delle Eustigmatophyceae. L'effetto dei tre differenti livelli di agitazione è stato valutato sia in reattori GWP verticali che inclinati. I risultati ottenuti, discussi nel capitolo 4, hanno mostrato come la produttività volumetrica risulta essere fortemente influenzata dal grado di turbolenza solamente in corrispondenza di elevati livelli di radiazione solare ($> 16 MJ m^{-2}$ reattore giorno⁻¹). Tale effetto è stato confermato sia in reattori verticali che in reattori inclinati (45° rispetto all'orizzontale), entrambi orientati N-S. Considerando le produttività volumetriche medie ottenute, una riduzione del flusso d'aria applicato (da 0.45 a 0.15 $L L^{-1}min^{-1}$) non influenza in maniera significativa la produttività media volumetrica della coltura. Questo si traduce in un risparmio energetico pari al 70% e di conseguenza in una migliore performance energetica del

reattore. La quantità di aria fornita dovrà quindi essere modulata in funzione della stagione, della latitudine e delle condizioni meteorologiche, diminuendo il flusso d'aria in corrispondenza di valori di radiazione solare inferiore ai $16 \text{ MJ m}^{-2} \text{ giorno}^{-1}$. La turbolenza della coltura potrà invece essere aumentata in corrispondenza di valori di radiazione superiori a tale soglia, ottenendo così un incremento dell'efficienza di utilizzo della radiazione solare e quindi della produttività.

Infine nel capitolo 5 si è proceduto ad effettuare una valutazione tecnico-economica ed un'analisi energetica della produzione di biomassa di *Nannochloropsis* F&M-M24 prodotta in un impianto di superficie 1 ha interamente realizzato con reattori GWP. L'efficienza energetica dell'intero sistema è stata valutata mediante la determinazione di un indice, il Net Energy Ratio (NER), in grado di esprimere il rendimento energetico di un determinato processo/prodotto. L'analisi ha preso in considerazione due differenti scenari: produzione di biomassa in condizioni di azoto sufficienza e produzione di biomassa in azoto carenza (starvazione). Quest'ultima condizione risulta necessaria per incrementare il contenuto medio in lipidi della biomassa (Rodolfi et al., 2009). Il NER ottenuto varia da 0,5 a 0,54 a seconda dello scenario considerato. Da tali valori risulta evidente come l'impiego esclusivo del GWP non rappresenti una soluzione energeticamente sostenibile per la produzione di biomassa ad uso energetico. L'energia immagazzinata nella biomassa risulta, infatti, la metà dell'energia globalmente spesa per la produzione della stessa. Due sono gli aspetti che maggiormente determinano un $\text{NER} < 1$: l'*embodied energy* dei materiali, in particolare del reattore GWP e l'energia elettrica necessaria per il mixing della coltura. Assieme, queste due voci di input energetico, rappresentano dal 70 all' 84% del fabbisogno totale di energia. Un sistema integrato, in cui una percentuale dell'impianto (5%) è occupata dal reattore GWP, necessario per la produzione di inoculo, mentre la restante superficie (95%) è interamente dedicata alla produzione da realizzarsi in vasche, sembra una possibile soluzione in grado di rendere positivo il bilancio energetico finale.

L'analisi economica, volta a valutare il costo di produzione della biomassa di *Nannochloropsis* F&M-M24, ha messo in evidenza come il costo di produzione possa variare dai 7 ai $14,2 \text{ € kg}^{-1}$ (essiccazione della biomassa esclusa) in funzione dello scenario considerato (azoto sufficienza e azoto carenza). Sono i costi operativi (costi di gestione), in particolare il costo della manodopera, a rappresentare la maggiore voce del costo di produzione. Il costo del reattore GWP rappresenta invece il maggior contributo sul totale del costo d'investimento iniziale. Anche la valutazione economica, così come il bilancio energetico, ha evidenziato come l'utilizzo esclusivo del reattore GWP non può rappresentare l'unica soluzione tecnologica da impiegare per la produzione di biomassa algale a basso valore aggiunto. Attraverso l'uso di

un sistema integrato vasche-reattori, sarebbe possibile ottenere, oltre ad un miglioramento delle performance energetiche del sistema, anche una riduzione del costo di produzione della biomassa. Da una prima valutazione (dati non riportati) del costo di produzione di biomassa di *Nannochloropsis* in un impianto integrato vasche-reattori, è risultato un costo di produzione inferiore ai 2 € kg⁻¹.

L'utilizzo di fotobioreattori a basso costo, come la nuova versione del GWP (GWPII-brevetto:9325 PTWO) (Tredici et al., 2010) potrebbe ulteriormente diminuire il costo di produzione della biomassa di 2-3 € kg⁻¹. Dobbiamo inoltre precisare che nella presente analisi non sono stati considerati eventuali ricavi derivanti dallo sfruttamento dei sottoprodotti che rimangono nella biomassa dopo un'eventuale estrazione dell'olio in essa contenuto. Lo sfruttamento commerciale della biomassa residua è in realtà estremamente interessante per l'alto valore commerciale di molti composti presenti (es. acidi grassi polinsaturi) (Tredici et al., 2010).

Il fotobioreattore GWP è stato caratterizzato per quanto riguarda fondamentali aspetti determinati la produttività (caratteristiche idrodinamiche e radiazione intercettata), le performance energetiche ed il costo di produzione della biomassa. Tali valutazioni sono strettamente dipendenti dalla tipologia di ceppo algale considerato e risultati anche differenti da quelli qui riportati potrebbero essere ottenuti con ceppi algali diversi da *Nannochloropsis* sp.

8.

REFERENCES

- Abdulqader G., Barsanti L., Tredici M.R. (2000) Harvest of *Arthrospira platensis* from Lake Kossorom (Chad) and its house hold usage among the Kanembu. *J. Appl. Phycol.* 12: 493-498.
- Acien F.G., Garcia F.G., Sanchez J.A., Fernandez J.M., Molina E. (1997) A model for light distribution and average solar irradiance inside outdoor tubular photobioreactors for the microalgal mass culture, *Biotechnol. Bioeng.*, 1997, 55:701-714.
- Acien F.G., Garcia F.G., Sanchez J.A., Fernandez J.M., Molina E. (1998), *Modelling of biomass productivity in tubular photobioreactors for microalgal cultures: effects of dilution rate, tube diameter and solar irradiance*, *Biotechnol. Bioeng.*, 58 :605-616.
- Acien F.G., Fernandez J.M., Sanchez J.A., Molina Grima E., Chisti Y. (2001) *Airlift- driven external loop tubular photobioreactors for outdoor production of microalgae: assessment of design and performance*, *Chem. Eng. Sci.*, 56, 2721-2732.
- Apt K.E., Behrens P.W., (1999) *Commercial developments in microalgal biotechnology*, *J. Phycology*, 35, 215-226.
- Asenjo J.A., Merchuk J.C. (1995) *Bioreactor system design*. Ed.: Juan A. Asejo, Josè C. Merchuk. New York.
- Babcock R., Malda J., Radway J., (2002) *Hydrodynamics and mass transfer in a tubular airlift photobioreactor* *Journal of Applied Phycology* 14,169-184.
- Backer R.N. (2008) *Chlorophyll fluorescence: a probe of photosynthesis in vivo*. *Annual Review of Plant Biology*. 59:89-113.
- Batty JC, Keller J. *Energy requirements for irrigation*. In *Handbook of energy utilization in agriculture*. Pimentel D (ed). CRC Press, Boca Raton, Florida; 1980:35-44.

Becker E.W. (1994) *Microalgae: biotechnology and microbiology*, Cambridge University Press Cambridge, U.K.

Ben-Amotz A., (2008) *Bio-fuels and CO₂ capture by algae*. 11th Congress of the International Society for Applied Phycology. Galway, Ireland, 21-30th June.

Benemann J.R., Goebel R.P., Weissman J.R., Augenstein J.C. (1982) *Microalgae as a source of liquid fuels*. Final technical report, US DOE.

Benemann J.R., Oswald W.J. (1996) *Systems and economics analysis of microalgae ponds for conversion of CO₂ to biomass*. Final report, U.S DOE

Borjesson P.I.I. (1996) *Analysis of biomass production and transportation*. Biomass and Bioenergy 11, 305-318.

Borowitzka M.A., (1988) *Fats, Oils and Hydrocarbons*. Micro-Algal Biotechnology. Cambridge University Press, Cambridge, UK.

Boustead I., (2005) *Eco-profiles of the European Plastic industry*. Plastic Europe, Association of plastic manufacturers.

Briendly Alias C., Garia-Malea Lopez M.C, Acien Fernandez F.G., Fernandez Sevilla J.M., Garcia Sanchez J.L., Molina Grima E. (2004) *Influence of power supply in the feasibility of *Phaeodactylum tricornutum* cultures*. Biothechnology and Bioengineering , 87, 723-733.

Burgess G., Fernández-Velasco J.G., (2007) *Materials, operational energy inputs, and net energy ratio for photobiological hydrogen production*. International Journal of Hydrogen Energy, 32, 1225 – 1234.

Camacho F., Acien F.G., Sanchez J.A., Garcia F., Molina E. (1999) *Prediction of dissolved oxygen and carbon dioxide concentration profiles in tubular photobioreactors for microalgal culture*, Biotechnol. Bioeng., 62, 71–86.

Camacho Rubio F., Sánchez Mirón A., Cerón García M.C., García Camacho F., Molina E. Chisti Y., (2004) *Mixing in bubble columns: a new approach for characterizing dispersion coefficients*. Chemical Engineering Science, 59, 4369 – 4376.

Carlozzi P., (2003) *Dilution of solar radiation through “culture” lamination in photobioreactor rows facing south–north: A way to improve the efficiency of light utilization by cyanobacteria (Arthrospira platensis)*, Biotech. and Bioeng., 81, 305-315.

Chini Zittelli G., Lavista F., Bastianini A., Rodolfi L., Vincenzini M., Tredici M. (1999) *Production of eicosapentaenoic acid by Nannochloropsis sp. cultures in outdoor tubular photobioreactors*. Journal of Biotechnology, 70, 299–312.

Chini Zittelli G., Pastorelli R., Tredici M.R. (2000) *A modular flat panel photobioreactor (MFPP) for indoor mass cultivation of Nannochloropsis sp. under artificial illumination*. Journal of Applied Phycology, 12, 521–526

Chini Zittelli G., Rodolfi L., Tredici .R., (2003) *Mass cultivation of Nannochloropsis sp. in annular reactors*. J. of Applied Phycology, 15, 107-114.

Chini Zittelli G., Rodolfi L., Biondi N., Tredici M.R., (2006) *Productivity and photosynthetic efficiency of outdoor cultures of Tetraselmis suecica in annular columns*, Aquaculture, 261: 932-943.

Chisti Y., Moo-Young M. (1988) *Gas Hold-Up in Pneumatic Reactors*. Chemical Engineering Journal, 38, 149-152.

Chisti Y., *Shear sensitivity* (1999). In: Encyclopedia of Industrial Biothechnology. Flickinger M., ed John Wiley & Sons, Inc. New York.

Chisti Y. (2007) *Biodiesel from microalgae*. Biotechnology advances, 25:294-306.

Clarens A.F., Resurreccion E.P., White M.A., Colosi L.M., (2009) *Environmental Life cycle comparison of algae to other bio-energy Feedstock*. Environ. Sci. Technol., 44, 1813-1819.

Deckwer W. D., Burckhart R., Zoll G., (1974) *Mixing and mass transfer in tall bubble columns*. Chem. Eng. Sci., 29: 2177.

Deckwer W.D., (1992) *Bubble Column Reactors*. Ed: John Wiley & Sons. New York. pp.533.

Doering O. (1980) *Accounting for energy in farm machinery and building*. In Handbook of energy utilization in agriculture. Ed.: Pimentel. CRC Press LLC, Boca Raton, FL, USA, 9-14.

Grobbelar J.U. (2004) *Algal Nutrition*. In: *Microalgae Culture: Biotechnology and Applied Phycology*. Ed.: Amos Richmond. Blackwell Science Ltd, Iowa, USA.

Guschina I.A., Harwood L.J., (2006). *Lipids and lipid metabolism in eukaryotic algae*. Progress in Lipid Research, 45, 160-186.

Hammond G., Jones C. (2008) *Inventory of Carbon and Energy (ICE) 1.6*. Available from: www.bath.ac.uk/mech.eng/sert/embedded.

Hu Q., and Richmond A. (1996a) *Productivity and photosynthetic efficiency of Spirulina platensis as affected by light intensity, algal density and rate of mixing in a flat plate photobioreactor*. J. Appl. Phycol., 18, 139–145.

Hu Q., Gutterman H., Richmond A. (1996b) *A flat inclined modular photobioreactor for outdoor mass cultivation of photoautotrophs*. Biotechnol., Bioeng., 51: 51–60..

Hu Q., Fairman D., Richmond A. (1998) *Optimal tilt angles of enclosed reactors for growing photoautotrophic microorganisms outdoors.*, J. Ferment. Bioeng., 85, 230–236.

Huesemann M., Benemann J.R., (2009). *Biofuel from Microalgae: Review of Products, Process and Potential with Special Focus on Dunaliella sp.* Publisher: A. Ben-Amotz, J.E.W. Polle, and D.V. Subba Rao; Science Publishers, New Hampshire, United States(US).

Janssen M. (2002) *Cultivation of microalgae: effect of light/dark cycles on biomass yield*. Thesis Wageningen University, Wageningen, The Netherlands.

Jorquera O., Kiperstok A., Sales E., Embiruçu M., Ghirardi M.L. (2010) *Comparative energy life-cycle analyses of microalgal biomass production in open ponds and photobioreactors*. *Bioresource Technology*, 101, 1406–1413.

Joshi J.B., Sharma M.M., (1979) *A circulation cell model for bubble columns*, *Trans. Inst. Chem. Eng.*, 57, 244-249

Kadam K., (2001) *Microalgae Production from power plant flue gas: environmental implications on a Life Cycle Basis.*, NREL/TP-510-29417

Kawase Y., Moo-Young M., (1989) *Mixing time in bioreactors.*, *J. Chem. Tech. Biotech.*, 44: 63–75.

Kreith F., Kreider J.F., (1978) *Principles of solar engineering*, McGraw Hill, New York, U.S.

Lardon L., Helias A., Salve B, Stayer J.P., Bernard O. (2009) *Life-Cycle assessment of biodiesel production from microalgae*. *Environmental Science & Technology*, 43: 6475-6481.

Legros A., Tredici M., Asinari C., Collard F., Dujardin E., Sironval C., Florenzano G., Nyns E.J., Naveau H., (1983) *Pilot plant biomethanation of cultivated marine algae Tetraselmis for energy production in southern Italy*. In: *Energy from biomass, Solar Energy R&D in the European Community*, Ed.: Palz W., and Pirrwitz D., Vol. 5.

Leher F., Posten C. (2009) *Closed Photobioreactors as tools for biofuel production*. *Curr. Opin. Biotechnol.*, 20, 280-285.

Lundquist T.J., Woertz I.C., Quin N.W.T., Benemann J.R, (2010) *A realistic technology and engineering assessment of algae bio-fuel production*. Energy Biosciences Institute, University of California Berkeley, California, USA.

Masojidek J., Koblizek M., Torzillo G., (2004) *Photosynthesis in microalgae*. In: *Microalgae culture: bio-technology and Applied phycology*. Ed.: Amos Richmond. Blackwell Science Ltd, Iowa, USA.

Matthias A.D., Fimbres A., Sano E.E., Post D.F., Accioly L., Batchily A.K, Ferreira L.G, (2000) *Surface roughness effects on soil albedo*. *Soil Sci. Soc. Am. J.*, 64, 1035-1041.

Metcalf & Eddy. (2003) *Ingegneria delle acque reflue*. Ed.: McGraw-Hill, Milano, Italia.

Metting Jr. F.B. (1996) *Biodiversity and Application of Microalgae*. J. Industr. Microb., 17, 477-489.

Molina Grima E., Camacho Garcia F., Sanchez Perez J.A., Fernandez Sevilla J.M, Gomez Contreas A (1994). *A mathematical model of microalgal growth in light limited chemostat cultures*. J. Chem. Technol. Biotech., 61,167-173

Molina Grima E., Fernandez Sevilla J.M, Sanchez Perez J.A., Garcia Camacho F., (1996) *A study on simultaneous photolimitation and photoinhibition in dense microalgal cultures taking into account incident and averaged irradiances*. Journal of Biotech., 45:59-69

Molina Grima E., Acien Fernandez F.G., Garcia Camacho F.F., Chisti Y. (1999) *Photobioreactors: light regime, mass transfer and scale up*. Journal of Biotech., 70, 231-247.

Molina Grima E., Acien Fernandez J., Chisti Y., (2001) *Tubular photobioreactors design for algal cultures*, J. Biotechnol., 92: 113–131.

Mustacchi C., (1985) *Ingegneria dei processi solari*. Ed.: Liguori. Napoli, Italia.

Perez R., Seals R., Anderson J., Menicucci D., (1995) *Calculating Solar Radiation Received by Tubular Solar Energy Collectors*. Solar Engineering. Ed: Stine & Tanaka.

Pimentel D., (1980) *Handbook of energy utilization in agriculture*. CRC Press, Boca Raton, Florida

Poulsen B.R, Iversen J.J., (1998) *Characterization of gas transfer and mixing in a bubble column equipped with a rubber membrane diffuser*. Biotech. and Bioeng., 58, 633-641.

Pruvost J., Cornet J.F., Legrand J., (2008) *Hydrodynamics influence on light conversion in photobioreactor an energetically consistent analysis*. Chemical Engineering Science, 63, 3679-3694.

Pulz O., Gross W., (2004) *Valuable products for biotechnology of microalgae*. App. Microbiol. Biotechnology, 635-648.

Reboloso Fuentes M.M., Navarro Perez A., Garcia Camacho F., Ramos Miras J.J., Guil Guerrero J.L. (2001) *Biomass Nutrient Profile of the Microalga Nannochloropsis*. J. Agric. Food Chem., 49, 2966-2972.

Richmond A., Wu Z., (2001) *Optimization of a flat plate glass reactor for mass production of Nannochloropsis sp. outdoors*. Journal of Biotech., 85, 259-269.

Richmond A., (2004) *Biological principles of mass cultivation*. In: Microalgae culture: biotechnology and Applied phycology. Ed.: Amos Richmond. Blackwell Science Ltd, Iowa, USA.

Riello L.; (2006) Tesi di dottorato in agronomia Ambientale. *Analisi Ambientale della produzione di oleaginose a scopo energetico*. Padova

Riquarts H. P., (1981) *A physical model for axial mixing of the liquid phase for heterogeneous flow regime in bubble columns*., Ger. Chem. Eng., 4, 18-23.

Rodolfi L., Chini Zitelli G., Barsanti L., Rosati G., Tredici M. (2003) *Growth medium recycling in Nannochloropsis sp. mass cultivation*, Bio-molecular Engin., 20,243-248.

Rodolfi L., ChiniZitelli G., Bassi N., Padovani G., Biondi N., Bonini G, Tredici M. (2009) *Microalgae for oil: strain selection, induction of lipid synthesis and outdoor mass cultivation in a low cost photobioreactor*. Biotech. and Biongi.102,100-112.

Sheehan J., Dunahay T., Benemann J., Roessler P. (1998) *A loock back at the U.S Department of Energy's aquatic species program:biodiesel from algae*. A Joint Study sponsored by U.S Department of Agriculture and U.S Department of Energy.NREL/TP-580-24190, National Renewable Energy Laboratory.U.S Department of Energy.

Sierra E., Acien F.G., Fernandez J.M, Garcia J.L,Gonzalez C:,Molina Grima E., (2008) *Characterization of a flat plate photobioreactor for the production of microalgae*. Chemical Engineering Journal, 138, 136-147.

Singh J. & Gu S.2010. *Renewable and Sustainable Energy Review*., 14, 2596-2610.

Stephenson A.L., Kazamia E., Dennis J.S., Howe C.J., Scott S.A., Smith A.G. (2010) *Life-cycle assessment of potential algal biodiesel production in the United Kingdom: a comparison of raceways and air-lift tubular bioreactors*. Energy Fuels, 24, 4062-4077.

Tomaselli L. (2004) *The microalgal cell*. In: Microalgae culture: bio-technology and Applied phycology. Ed.: Amos Richmond. Blackwell Science Ltd, Iowa, USA.

Tredici M., Papuzzo T., Tomassello V., Milicia F., Balloni W. (1987) *La coltura di Spirulina su acqua di mare*. In: Biotecnologie per la produzione di Spirulina, Monografia n° 17 – I.P.R.A.-C.N.R.

Tredici M.R., Carlozzi P., Chini Zittelli G., Materassi R. (1991) *A vertical alveolar panel (VAP) for outdoor mass cultivation of microalgae and cyanobacteria*, Bioresource Tech., 38 153–159.

Tredici M.R., Chini Zittelli G. (1997) *Cultivation of Spirulina (Arthrospira) platensis in flat plate reactors*. In: *Spirulina platensis: physiology, cell-biology and biotechnology*. A. Vonshak (ed). Taylor & Francis, London. 117-130.

Tredici M., Chini Zittelli G., (2000) *Efficiency of sunlight utilization: tubular versus flat photobioreactors*. Biotech. and Bioeng., 57, 187-197.

Tredici M.R., Rodolfi L. (2004a) *Reactor for industrial culture of photosynthetic microorganisms*. Patent WO 2004/074423 A2 (to Università degli Studi di Firenze, Italia).

Tredici M., (2004b). *Mass Production of microalgae: Photobioreactors*. Microalgae culture: bio-technology and Applied phycology. Ed.: Amos Richmond. Blackwell Science Ltd, Iowa, USA.

Tredici M., Biondi N., Chini Zittelli G., Ponis E., Rodolfi L. (2009) *Advances in microalgal culture*. In Gavin Burnell and Geoff Allan eds, *New-technologies in Aquaculture*, Woodhead publishing, Ltd, Cambridge, UK, and CRC Press LLC, Boca Raton, FL, USA, 610-676.

Tredici M., Chini Zittelli G., Rodolfi L. (2010a) *Photobioreactors*, In: *Encyclopedia of Industrial Biotechnology*. Flickinger M., ed John Wiley & Sons, Inc. New York.

Tredici M., Rodolfi L., Sampietro G., Bassi N. (2010b) *Low-cost photobioreactor for microalgae cultivation*. Patent: 9325 PTWO (to Fotosintetica & Microbiologica S.r.l)

Tredici M. (2010c) Photobiology of microalgae mass culture: understanding the tools for the next green revolution. *Biofuels*, 1 , 143-162.

Vandajon L., Rossignol N., Jaouen P., Robert J.M., Quemeneur F. (1999) *Effects of shear on two microalgae species. Contribution of pumps and valves in tangential Flow filtration system*. *Biotech. and Bioeng.*, 63.

Varley R. (1995). *Submerged gas-liquid jets: bubble size prediction*. *Chemical Engineering Science*, 50, 901-905.

Vonshak A., Torzillo G., (2004) *Environmental stress physiology*. In: *Microalgae culture: biotechnology and Applied phycology*. Ed.: Amos Richmond. Blackwell Science Ltd, Iowa, USA

Weissman J.C, Goebel R.P.(1987) *Design and analysis of microalgal Raceway Pond Systems for the purpose of producing fuels*. SERI,Colorado.Report XK-3-03153-1.

Weissman J.C, Goebel R.P, Benemann J.R. (1988) *Photobioreactor design: mixing, carbon utilization, and oxygen accumulation*, *Biotechnology and Bioengineering*, 31, 336–344.

Wijffels R., Barbosa M., (2010) *An outlook on microalgal biofuels*. *Science*, 13, 796-799.

Williams P.J.B., Laurens M.L (2010) *Microalgae as biodiesel & biomass feedstock: review & analysis of the biochemistry ,energetic & economics*. *Energy and Environmental Science*, 3, 554-590.

Wu Z.C., Zmora O., Kopel , Richmond A.(2001) *An industrial-size flat plate glassreactor for massproduction of Nannochloropsis sp.Eustigmatophyceae*. *Aquaculture*,195,35–49.

Zhang K., Kurano N., Miyachi S., (1999) *Outdoor culture of a cyanobacterium with a vertical at-plate photobioreactor: effects on productivity of the reactor orientation, distance setting between the plates and culture temperature*. *Appl. Microbiol. Biotech.*, 52, 781-786

Zijffers J.W., Salim S., Janssen M., Tramper J., Wijffels R. (2008) *Capturing sunlight into a photobioreactor: Ray tracing simulations of the propagation of light from capture to distribution into the reactor*. Chemical Eng. Journal., 144, 316-327.